SATELLITE IMAGE ANALYSIS OF RECENT CHANGES IN GLACIER EXTENT IN THE NORTHERN MACKENZIE MOUNTAIN RANGE, NORTHWEST TERRITORIES AND YUKON, CANADA

by

Rachel A. Kendall

A thesis submitted in fulfillment of the
requirements of GEOG 4526

for the Degree of Bachelor of Science (Honours)

Department of Geography and Environmental Studies
Saint Mary's University
Halifax, Nova Scotia, Canada

April 10, 2018

Members of the Examining Committee:

Dr. Philip Giles (Supervisor)
Department of Geography and Environmental Studies
Saint Mary's University

Dr. Kevin Hamdan
Department of Geography and Environmental Studies
Saint Mary's University

ABSTRACT

Satellite image analysis of recent changes in glacier extent in the Northern Mackenzie Mountain Range, Northwest Territories and Yukon, Canada

by

Rachel A. Kendall

The state of a small assemblage of glaciers not previously reported on in the northern Mackenzie Mountains across Yukon and Northwest Territories were investigated over the past three decades. Landsat TM and OLI satellite imagery was used from 1987 to 2013/2017, with images in the years of 1987, 1994, 1999, 2004, 2013, and 2017, to determine whether there was a trend in glacier change. A semi-automated thresholded Red/SWIR band ratio method was used to delineate the glacier boundaries. Since only ~70% of the total glaciers were visible in the 2017 image due to partial cloud cover, glacier area change was analysed from 1987-2013, and from 1987-2017 in some parts of the study area. It was hypothesised that glaciers within the study area would be affected by changes in climate by decreasing in spatial extent in accordance with other glacier studies throughout the world. Glacier area decreased from 69.9 ± 1.75 km^2 in 1987 to 41.0 ± 1.03 km^2 in 2013, a loss of 41.5 ± 2.08% or 29.0 ± 1.45 km^2, with an area reduction rate of 1.59% · a^{-1}. For the 1987-2017 period, glacier area decreased from 52.8 ± 1.32 km^2 in 1987 to 24.9 ± 0.62 km^2 in 2017, a loss of 52.9 ± 2.65% or 27.9 ± 1.40 km^2, with an area reduction rate of 1.76% · a^{-1}. The smaller size glaciers ($A < 0.1$ km^2) were found to have the largest change in relative area. As glaciers reduced in size, there was an increase in area loss over the time period. Reduction rates are high compared to glacier area loss reported for other mountain ranges in the late twentieth century. This may be due to their small size and high perimeter-area ratio. By extrapolating the total glacier area values, it is predicted that the study area will be glacier-free by 2045 for the 1987-2013 sample and by 2044 for the 1987-2017 sample.

April 10, 2018

RÉSUMÉ

Satellite image analysis of recent changes in glacier extent in the Northern Mackenzie Mountain Range, Northwest Territories and Yukon, Canada

par

Rachel A. Kendall

L'état d'un petit assemblage de glaciers non déclaré antérieurement dans le nord des montagnes Mackenzie à travers du Yukon et des Territoires du Nord-Ouest a été examiné durant les trois dernières décennies. L'imagerie satellite Landsat TM et OLI a été utilisé de 1987 jusqu'à 2013/2017 incluant des images des années 1987, 1999, 2004, 2013 et 2017 pour déterminer s'il y avait une tendance en changement glacière. Les limites glacières ont été délimités en utilisant une méthode seuil semi-automatisé du rapport de bandes rouge/IRCL. Car seulement ~70% du total des glaciers était visible dans l'image de 2017 à cause d'une couverture nuageuse partielle, le changement en superficie glaciaire à été analysé pour 1987-2013 et pour 1987-2017 dans certaines portions de la zone étudiée. C'était supposé que les glaciers dans la zone étudiée soient affectés par la changement climatique en forme d'une décroissance en portée spatiale en accordance avec d'autres études de glaciers à travers du monde. La superficie des glaciers a diminué de 69.9 ± 1.6 km^2 en 1987 à 41.0 ± 1.0 km^2 en 2013, qui constitue une perte de 41.5 ± 2.08% ou de 29.0 ± 1.45 km^2 avec un taux de réduction de superficie de 1.59% · a^{-1}. Pour la période de 1987-2017, la superficie des glaciers s'est réduite de 52.8 ± 1.3 km^2 en 1987 jusqu'à 24.9 ± 0.6 km^2 en 2017 pour une perte de 52.9 ± 2.65% ou de 27.9 ± 1.40 km^2 avec un taux de réduction de superficie de 1.55% · a^{-1}. Les glaciers de plus petit taille ($A < 0.1$ km^2) ont été trouvés d'avoir le plus grand changement en superficie relatif. Il y avait une augmentation en perte de superficie à mesure que la taille des glaciers s'est réduite le long de la période. Les taux de réduction sont très élevés comparés aux taux rapportés pour d'autres chaines montagneuses à la fin du 20e siècle. Cela est possiblement à cause de leur faible superficie et le ratio élevé du périmètre à la superficie. En extrapolant les valeurs de la superficie totale des glaciers, il est prévu que la zone étudiée sera libre de glaciers par 2043 pour l'échantillon de 1987-2013 et par 2047 pour celui de 1987-2017.

le 10 avril 2018

ACKNOWLEDGEMENTS

I am very grateful to have had the opportunity to develop this thesis and the skills that I have gained from working independently from start to finish. I would like to thank Dr. Philip Giles for presenting me with the project topic of mapping glaciers back in 2016. I appreciate all of his guidance and assistance with my writing, as well as answering all my questions and concerns when they arose. I would also like to thank Dr. Kevin Hamdan for agreeing to be my second reader and for also helping me improve on my writing skills. There are many other people who I would like to thank for providing me support along the way, including my friends and peers who may have listened to my frustrations and were there for me when I needed a break and someone to talk to, and my family, especially my parents, who were always encouraging me and cheering me on every step of the way through my undergraduate degree. I would also like to thank Jenna Miller for translating my abstract to French for me. Lastly, the Department of Geography and Environmental Studies deserves acknowledgement for providing a supportive learning environment allowing for the success of their students. The interesting topics presented by our professors in the many geography courses offered by the department were what sparked my interest to want to pursue such a topic in-depth.

TABLE OF CONTENTS

LIST OF TABLES

LIST OF FIGURES

CHAPTER 1

Introduction

1.1 Research Overview

Earth's climate is continuously changing as the atmospheric concentration of carbon dioxide from anthropogenic inputs continues to rise. Throughout the world, there are trends of long-term atmospheric warming and changes in precipitation trends outside normal levels. The impacts of climate change are global in scope, but these changes may differ regionally. In northwestern Canada, climate conditions have been characterised by increasing mean annual surface air temperatures and reductions in winter snowfall since the 1950s (DeBeer et al. 2016; Derksen and Brown, 2012).

As a result of climate change, glaciers have been observed to generally be retreating. The length, thickness, area, and volume of glaciers will be balanced in response to increases or decreases in temperature and precipitation over many years. In recent decades, most alpine glaciers have been marked by decreasing extent, and these glaciers have undergone an acceleration of mass loss and terminal retreat. The changes in glacier extent are an indicator of the changes in climate regionally. Recent past studies have been conducted in the region of northwestern Canada on glacier change and found most glaciers in this region to be retreating (e.g., Barrand and Sharp, 2010; Demuth et al., 2014).

There have been recent efforts to monitor and document the area and volume loss of glaciers in northwestern Canada using methods of ground-based measurements, aerial reconnaissance, and

satellite imaging. The use of satellite imagery has been increasingly widely applied to glacier mapping, especially for remotely located glaciers. Although there have been many glacier studies conducted in northwestern Canada, none of these studies have mapped a complete inventory of the extents of a small assemblage of glaciers in the northern Mackenzie Mountains (Figure 1.1). Since there have been previous glacier mapping studies conducted in this region, this thesis is a similar study to map the extents of this small group of glaciers in the Mackenzie Mountains.

1.1.1 Purpose and Objectives of this Thesis

The purpose of this thesis is to map the changes in extent of glaciers located in the northern Mackenzie Mountains in Yukon and Northwest Territories using satellite imagery acquired over the past three decades. With glaciers changing in spatial extent globally and generally decreasing in size because of climate change, it is hypothesised that glaciers in the study area will also be affected by these changes in climate by decreasing in spatial extent. The specific objectives of this study are as follows:

1. To determine the most effective band combination, based on visual examination, for distinguishing ice from snow and other surface features;
2. To map glacier extents from Landsat 5 and 8 satellite images covering the study area between 1987 and 2013/2017, in the years of 1987, 1994, 1999, 2004, 2013, and 2017;
3. To determine whether there is a trend in glacier extents over time in the study area between 1987 and 2013/2017; and
4. To compare results with other studies in Canada and elsewhere in the world.

This thesis investigated all the glaciers within the study area in which there were 117 glaciers mapped in total.

Figure 1.1. Location of glaciers analysed in this thesis. Study area indicated by red star.

Map data: GCS North American 1983, Canada Lambert Conformal Conic. Sources: World Hillshade: ESRI, 2015. Admin 1 – States, provinces, 1:50 000 000: Natural Earth. Admin 0 – Countries, 1:50 000 000: Natural Earth.

1.2 Literature Review

With a changing global climate, glaciated areas have been affected by increases in surface air temperature and changes in precipitation, generally resulting in a retreat of glaciers worldwide. As changing glaciers alter the surrounding environment, the proximal ecosystems and landscape are affected as well. To understand how glaciers will continue to be impacted by future climate changes and how nearby ecosystems will change in conjunction with glacier retreat, various glacier mapping techniques are used to monitor the movement and changes of glacier extent. In particular, remote sensing of glaciated areas allow for time-efficient approaches to mapping glacier change by using an automated or semi-automated method of thresholded band ratios and normalised images. This method may be applied to various satellite images, including images from Landsat satellites used in this thesis.

1.2.1 Climate Change

Earth's climate is changing with levels of air temperature and precipitation increasing or decreasing outside normal levels. Although climate change is a global issue, patterns of changing precipitation and air temperature vary in different regions (DeBeer et al., 2016; Environment and Climate Change Canada (ECCC), 2016). In the northern higher latitudes, changing conditions have been especially large in which studies have shown alterations in the amount and phase of precipitation (Mekis and Vincent, 2011), diminishing seasonal snow cover (Derksen and Brown, 2012), warming and thawing of permafrost (Burn and Kokelj, 2009), shifts in timing and magnitude of river discharge (Déry and Wood, 2005), as well as the retreat and loss of glaciers.

Of all previous decades with recorded global mean surface air temperature, the past three decades have been successively warmer. This global mean surface air temperature data calculated

by a linear trend exhibits a warming of 0.85°C from 1880–2012 (Hartmann et al., 2013). In addition to this overall warming trend, Hartmann et al. (2013) stated that global mean surface air temperatures have shown considerable decadal and interannual variability.

Air temperature and precipitation are both fundamental to regions of high latitudes and high altitudes influencing cryosphere and hydrosphere systems. Across Canada, mean annual air temperature trends have been dominated by statistically significant increases of approximately 1.5°C between 1950 and 2010, with the greatest amount of warming occurring over northwestern Canada (DeBeer et al., 2016; Vincent et al., 2015; Barrand and Sharp, 2010; Zhang et al., 2000). Surface air temperature is an important climatic variable by controlling the phases of precipitation that reach the surface, in which precipitation may fall in the solid phase as snow or in the liquid phase as rain depending on the air temperature.

There is considerable variation in precipitation trends throughout northern high latitudes (ECCC, 2016), with some areas experiencing increased precipitation and others decreased precipitation. According to DeBeer et al. (2016), annual average precipitation has increased by about 14% over various areas of western Canada since 1950. However, the authors have noted a considerable variability in the magnitude and significance of local trends. Even though there may be increased levels of precipitation in some areas, the phase of precipitation is changing, impacting the depth of seasonal snow cover.

With rising winter temperatures there will be a greater proportion of winter precipitation that falls to the surface in the liquid phase as rain rather than the solid phase as snow, as well as more glacier area that will be exposed to above-freezing temperatures. Over the interior of

northwestern Canada, DeBeer et al. (2016) reported an average temperature increase of 3.9°C in the winter, with a maximum increase of up to 6°C in parts of the northern Mackenzie basin and surrounding areas. Decreasing snow depths and snow cover duration and extent have also been observed over most of Canada since the mid-1970s (DeBeer et al., 2016, Derksen and Brown, 2012). These declines are largest in western Canada and disproportionally greater during late winter and spring. Glacier formation requires an adequate amount of snow to maintain size, so with less snow cover and more precipitation falling as rain, the conditions for glaciation will not be favourable.

1.2.2 Glaciers and Glacier Change

Glaciers are a part of the hydrologic cycle and store a large proportion of Earth's freshwater. A basic requirement for glacier growth is snowfall, which should be abundant enough in the winter so that not all snow will melt in the summer. However, a glacier can still experience a negative mass balance, and thus retreat with precipitation as snow if the glacial ice losses are greater than the inputs of snow. The amount of seasonal snowfall depends on surface air temperature, and is sensitive to changes in temperature, especially during the spring when snow begins to melt (Hartmann et al., 2013). When ice has become sufficiently thick to deform under its own weight, it will begin to flow downslope until it reaches lower altitudes where environmental conditions limit further growth (Kuhn, 2010). As surface air temperatures continue to rise, many glaciers may become more susceptible to an increase in retreat. Surface air temperature during summer months and the accumulation of snow during winter largely determine the surface mass balance of glaciers (Larsen et al., 2007).

Throughout the world, many studies have found glaciers to be in a state of retreat from the Alps (Paul et al., 2007), Himalayas (Xiang et al., 2014), and the Tienshan Mountains of China (Wang et al., 2015) to the Cordillera Blanca (Durán-Alarcón et al., 2015) and the Rocky Mountains (Tennant and Menounos, 2013). Particularly in cold regions, cryospheric and hydrologic regimes are strongly influenced by variations in surface air temperature, melting of snow and ice, and the transition between snowfall and rain (DeBeer et al., 2016). With reductions in snow cover and summer warming, there will be increasingly negative mass balances of glaciers (Figure 1.2).

Using global climate models of new emission and climate scenarios for the Fifth Assessment Report of the Intergovernmental Panel on Climate Change (IPCC), Radić et al. (2014) predicted

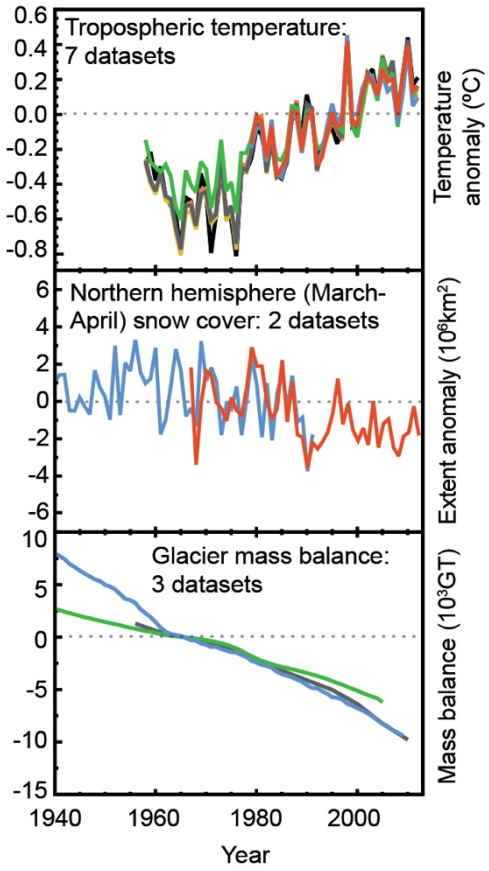

Figure 1.2. Independent indicators from the IPCC AR5 of a changing global climate. Each line represents an independently derived estimate of change in the climate element.

Adapted from: Hartmann et al., 2013, FAQ 2.1, Figure 2.

that glaciers in Western Canada and the United States will lose 85 ± 11% of their current volume on average for the IPCC greenhouse gas concentration trajectory, Representative Concentration Pathway (RCP), of 4.5 by 2100, and more than 90% of their current volume on average by 2100 for RCP of 8.5. According to simulations employed by Clarke et al. (2015), there will be few glaciers that will remain in interior Canada and the Rockies, whereas maritime glaciers such as those in British Columbia will remain, but in a diminished state, by 2100. Regions throughout the world that are predicted to lose glacier volume relatively rapidly include Western Canada, the United States, Scandinavia, North Asia, Central Europe, the Caucasus, and low latitudes for an initial 2K (one unit of Kelvin (K) is equivalent to one unit of degree Celsius) of warming (Radić et al., 2014).

1.2.2.1 Past Reports on Glacier Change in Western Canada

In the region of western Canada, past studies have reported on the changes in glacier extent of British Columbia, Yukon, Alberta, and Northwest Territories where these studies have reported glaciers to be retreating. Bolch et al. (2010) analysed the changes in glacier extents in British Columbia and Alberta over the period of 1985 – 2005. The glaciated terrain was found to have decreased from 30 063.0 km^2 in 1985 to 26 728.3 ± 962 km^2 (-11.1 ± 3.8%) in 2005. Bolch et al. (2010) state that the change in glacier area represents a greater relative loss for smaller glaciers across the study area than for larger ones, but a lower absolute loss for the smaller glaciers. The authors also noted that maritime glaciers lost less relative ice cover than glaciers farther inland, in which the northern Interior Ranges of British Columbia had the greatest reduction (-24.0 ± 4.9%). DeBeer and Sharp (2007) also analysed glaciers in British Columbia in the Canadian Cordillera, where they found that glacial ice coverage decreased by 146 ± 10 km^2 (5.2% of the

initial area) from 1951/52 to 2001/02. Glaciers with an initial area of 1-5 km^2 accounted for a considerable amount of the total area lost.

Barrand and Sharp (2010) provided an assessment of area changes of all glaciers in Yukon during the period from 1958-2008. The findings of this study that Yukon glaciers have experienced large losses in surface area indicated that Yukon glaciers are sensitive to climate perturbations. The total ice area in Yukon was found to have reduced in extent from 11 622 km^2 in 1958-60 to 9 081 km^2 in 2006-08, representing a loss of 2 541 ± 189 km^2 in which glaciers of all sizes experienced substantial losses. Foy et al. (2011) looked specifically at the Kaskawulsh glacier in Yukon, which retreated by an average of 655 m, with a decrease in terminus area of 8.20 km^2. The glacier reductions reported by Barrand and Sharp (2010) and Foy et al (2011) are in accordance with observed decadal warming trends in northwestern Canada.

In the Ragged Range of the Mackenzie Mountains, located approximately 400 km from the study area, Demuth et al. (2014) examined the glaciated area of the Greater Nahanni Ecosystem in Northwest Territories. The authors found that these glaciers contracted by approximately 30% from an area of 262 km^2 in 1982 to an area of 184 km^2 in 2008. The majority of these glaciers studied (48%) occupied a size of 0.1-1.0 km^2 in 2008 but represented only approximately 20% of the total glaciated area. The greatest relative area loss that occurred was in the glaciers with a size of 1-10 km^2, while the largest number of disappearances of glaciers had an area size of 0.1-1 km^2. It was found overall that the smaller glaciers had a greater relative loss in area than larger glaciers. However, Demuth et al. (2014) noted that several glaciers of a smaller size showed modest growth or relatively little contraction, which were located at higher elevations and were provided with consistent drift snow to support growth.

1.2.2.2 Effects of Retreating Glaciers

As glaciers retreat in response to fluctuations in climate, they have been found to contribute to changing conditions of nearby ecosystems. Ecosystems have been impacted by changes in the water level of lakes (Shugar et al., 2017), changing alpine river habitats (Khamis et al., 2016), and changing river dynamics (Naz et al., 2014). As glaciers retreat or advance, this can change what rivers or lakes receive a glacier's meltwater, sometimes resulting in river piracy. For example, the water levels of Kluane Lake in Yukon have been lowering due to re-routing of meltwater from the Kaskawulsh Glacier (Shugar et al., 2017; Clague et al., 2006). According to Shugar et al. (2017), there may be substantial long-term hydrological and ecological impacts as a result.

Changes in the meltwater from retreating glaciers can also result in losses of water resources for nearby ecosystems. Alpine glaciers are stores of freshwater available to these ecosystems, which can moderate interannual variability of the flow of streams helping maintain stream volume during extreme dry periods (DeBeer and Sharp, 2007). Rivers influenced by glaciers support various aquatic species that depend on the physical and chemical properties of the river habitat. Meltwater runoff in glacier basins contribute to the amount of discharge, temperature of the rivers, suspended sediment content, water chemistry, and channel dynamics, which all serve an important role in the structuring of meltwater-fed rivers and their macroinvertebrate communities (Brown et al., 2010). Aquatic species inhabiting such rivers face population change from future meltwater reduction and habitat alteration.

Shrinking glaciers are contributing to the rise in sea level throughout the world. The mass loss of glaciers and ice sheets are one of the largest contributors to eustatic change (Arendt et al., 2006). Using climate models of IPCC emission and climate scenarios, Radić et al. (2014) predicted that

sea levels will rise by 155 ± 41 mm (RCP 4.5) and 216 ± 44 mm (RCP 8.5) over the period of 2006–2100, thereby reducing global glacier volumes by 29 or 41%, respectively. In western Canada, Clarke et al. (2016) projected that the maximum rate of ice volume loss from the peak input of meltwater to rivers will occur around 2020–2040. Documenting the change in glacier size and how different size glaciers respond to change is important in understanding how climate change and glacier variations may be connected.

1.2.3 Glacier Mapping Techniques

Glacier mapping is a technique used to monitor the changes of glacier extent. Typically, glacier monitoring involves ground-based measurements, aerial reconnaissance, and satellite imaging (Chand and Sharma, 2015). Out of all methods of glacier mapping employed, the remote sensing technique of using aerial photography is the longest established with a long history of application to the study of glaciers (Rees and Pellikka, 2010). There are various techniques, which are often used in conjunction to map the extents of glaciers.

Some examples of these common techniques used to map glaciers are summarised by Pellikka and Rees (2010) including elevation models, airborne laser scanners, photogrammetry, and satellite data. Elevation models can be used for studying the change in slope angle or microtopography between the slope and debris-covered glaciers, to distinguish debris-covered and dead ice areas from valley slopes, and to identify moving glaciers. Glacier area can be mapped using airborne laser scanners producing very high resolution digital elevation models. When using satellite imagery, automated and semi-automated glacier delineation methods can be employed by using various masks created with indices and threshold values. Some studies have used a combination of field and remote sensing techniques to map the change in glacier extent.

For example, Way et al. (2015) used in-situ ground-truthing of moraines and debris fields, in-situ lichen measurements to date former ice margins, as well as aerial photography and optical satellite imagery to map the change in glacier extent of the Torngat glaciers in Labrador.

The change in mass, volume, area, and length of glaciers are monitored and studied worldwide by the World Glacier Monitoring Service, but monitoring is generally focused on large and easily accessed glaciers (Liu et al., 2013). The use of satellite imagery has been increasingly widely applied to glacier mapping. Satellite imagery has been used more frequently, notably after the Landsat archives were made available to the public in late 2008 by the United States Geological Survey (USGS) offering orthorectified products (Paul et al., 2016). Many studies have contributed to the Global Land Ice Measurements from Space database, which is a project designed to monitor glaciers of the world by primarily using optical satellite instruments (e.g., Chand and Sharma, 2015; Demuth et al., 2014; Bolch et al., 2010; Racoviteanu et al., 2008; Andreassen et al., 2008). Glaciers that are smaller than 0.01 km^2, however, are typically omitted from these glacier inventories (Pellikka and Rees, 2010).

1.2.3.1 Remote Sensing Techniques for Studying Glaciers

To quantify glacier changes in mountainous regions, multi-temporal satellite imagery and older aerial photography have been extensively used (e.g., Bolch et al., 2010; Arendt et al., 2006). Remote sensing methods for mapping glaciers include manual delineation based on visual interpretation, qualitative digital thresholding based on spectral reflectance, as well as automated techniques such as unsupervised/supervised pixel-based classification algorithms or object-oriented classification (Pellikka and Rees, 2010). Optical satellite images are more useful for

recent decades, but aerial photographs are especially useful for mapping glaciers at a time before sensors were in orbit.

There are many advantages to using optical satellite imagery for delineating glacier outlines. The entire USGS Landsat Archive is available at no charge, whereas many other images from other satellites, such as the Advanced Spaceborne Thermal Emission and Reflection Radiometer (ASTER) sensor, are available at a low cost. ASTER is a suitable sensor that is commonly used, sometimes in conjunction with Landsat imagery, for monitoring glacier parameters including velocity fields (Recoviteanu et al., 2009). Satellite imagery can also be combined with digital elevation models to derive a topographic glacier inventory, as well as allow for calculations of glacier thickness and volume (Pellikka and Rees, 2010). Automated methods that have been developed and tested are advantageous to use because they are simple, robust, and accurate for the detection of debris-free to slightly debris-covered glaciers (Recoviteanu et al., 2009).

One major limitation of using satellite imagery is the availability of suitable cloud-free images at the end of an ablation season without having remaining seasonal snow in the image (Andreassen et al., 2008). Overall, optical satellite imagery is an effective method for delineating glacier outlines, as shown in various studies mapping glacier change. Barrand and Sharp (2010), for example, made use of both Landsat 7 ETM+ imagery and aerial photographs to delineate glaciers and to provide an assessment of area and volume changes in Yukon. Aerial photographs, however, need to be digitally scanned and spatially referenced to satellite imagery, unlike Landsat imagery provided by the USGS that is already orthorectified.

Often when automated methods are used, manual digitisation is required to edit glacier polygons produced. Bolch et al. (2010) found that manual editing of glacier polygons to exclude misclassified water bodies was superior to any automated method, but that thresholded ratio imagery was an overall more time-effective approach than manual digitisation of areas of extensive ice cover. Wheate et al. (2014) made use of Landsat images as well as ASTER images to produce three-dimensional views to better visualise glacier area and volume changes. Other studies have not used automated methods at all, and instead manually digitised the glaciers. For example, DeBeer and Sharp (2009) defined glaciers by manually digitising a series of points along ice margins to construct a shapefile of individual glacier polygons of Landsat imagery and aerial photographs. Burns and Nolin (2014) considered manual delineation of remotely sensed images to be the most accurate method for mapping glaciers, but that this method is very time-consuming for a change analysis of a large area.

Since debris-free glacier ice is highly reflective in the visible spectrum and essentially not visible in the short-wave infrared part of the electromagnetic spectrum, this contrast enables automated and semi-automated mapping techniques of the debris-free glacier ice (Burns and Nolin, 2014). Glacier ice and other land surface features are more reflective in different parts of the electromagnetic spectrum. Since the surface of a glacier is not entirely composed of ice, but also of firn, snow, water, and debris, these different materials will be more reflective in different wavelengths. With a high variable fraction of each component per glacier, optical properties of the glacier are impacted in which there is a high spectral reflectance of snow in the visible spectrum (Paul and Hendriks, 2010a).

A time-effective semi-automated method for delineating glacial ice is by thresholding single band ratio images or normalised images (Durán-Alarcón et al., 2015). Many glacier mapping studies (e.g., Chand and Sharma, 2015) have preferred manual digitisation to map debris-covered glacier areas because the spectral signature on satellite images does not differentiate debris-covered ice with the surrounding bare terrain. Whether automated techniques by thresholding band ratios or manual digitising glacier outlines are employed, producing glacier outlines allows for the detection of area or volume changes over time. The monitoring of change is a natural progression from mapping area and volume of a glacier (Pellikka and Rees, 2010).

1.2.3.2 Landsat Satellites

There have been eight Landsat satellites in orbit, with Landsat 1 first in operation in 1972 (USGS, 2017). The spectral characteristics of the Landsat Thematic Mapper (TM) sensor, Enhanced Thematic Mapper (ETM+) sensor, and Operational Land Imager (OLI) sensor bands are summarised in Table 1.1. Since glaciers are usually classified from spectral band ratios, the thermal infrared bands (band 6 for TM and ETM+, and bands 10 and 11 for OLI) were not summarised in Table 1.1. For many glaciological studies, the main data are derived from the Landsat TM sensor. This sensor provides relatively continuous and calibrated data at a 30-m spatial resolution with time-series data that have been collected for more than 30 years (Paul and Hendriks, 2010a). This long-term image availability begins in 1982 with Landsat 4, which are available for free on the USGS Earth Explorer website (earthexplorer.usgs.gov). Although Landsat 5 TM may be the sensor used primarily in studies (e.g., Bolch et al., 2010 and Demuth et al., 2014)., many studies also use the Landsat 7 ETM+ sensor (e.g., Barrand and Sharp, 2010 and Arendt et al., 2006) and more recently, the Landsat 8 OLI sensor.

Table 1.1. Spectral bandwidths of reflective bands from different Landsat sensors.

Band Name	Band Number			Band Wavelength Range (μm)		
	TM	ETM+	OLI	TM	ETM+	OLI
Blue	1	1	2	0.45-0.52	0.45-0.52	0.45-0.51
Green	2	2	3	0.52-0.60	0.53-0.61	0.53-0.60
Red	3	3	4	0.63-0.69	0.63-0.69	0.63-0.68
NIR	4	4	5	0.76-0.90	0.75-0.90	0.85-0.89
SWIR	5	5	6	1.55-1.75	1.55-1.75	1.56-1.66
SWIR	7	7	7	2.08-2.35	2.09-2.35	2.10-2.30
Panchromatic	---	8	8	---	0.52-0.90	0.50-0.68

Information derived from: Paul et al., 2016, Table 2.

Each band of the Landsat sensors represent a certain wavelength range (Table 1.1). The spectral ranges from sensor to sensor are fairly similar because the exact position of each band is related to the atmospheric windows where there is little adsorption by trace gases (Paul and Hendriks, 2010a). The TM, ETM+, and OLI Landsat sensors have relatively large swath zones (185 km) with a moderate spatial resolution of 30 m. These sensors have been particularly useful because of their extensive spatial and temporal coverage and moderate spatial resolution (Liu et al., 2013).

1.2.3.3 Thresholded Ratio Images

Many studies have come to a conclusion that a thresholded band ratio or normalised image applied to raw data is an efficient method for glacier mapping in terms of accuracy and effort (e.g., Durán-Alarcón et al., 2015; Burns and Nolin 2014; Bolch et al., 2010; Racoviteanu et al., 2008; Andreassen et al., 2008). By dividing the raw digital numbers, such as those of near infrared radiation (NIR) by those of short-wave infrared radiation (SWIR), glaciers stand out among a dark land surface (Paul et al., 2009). The Red/SWIR band ratio in particular has been widely applied in glacier mapping studies (e.g., Chand and Sharma, 2015; Liu et al., 2013; Bolch et al.,

2010; Andreassen et al., 2008). The SWIR band used in this thresholded band ratio is TM band 5 for Landsat 5 and OLI band 6 for Landsat 8 (Table 1.1).

The thresholding of ratio images enables the identification of snow and ice in shadow, with certain band ratios to have been proved to be more successful than others. Bolch et al. (2010) found the Red/SWIR ratio (e.g., TM3/TM5 for Landsat 5) to work better in shadows and with thin debris-cover than the NIR/SWIR ratio (e.g., TM4/TM5 for Landsat 5). Chand and Sharma (2015) also preferred the Red/SWIR ratio and effectively mapped debris-free glacial ice. The Red/SWIR ratio, however, suffers from two important limitations. One of these limitations is that this ratio also maps clear and turbid water bodies as glaciers (Paul et al., 2007). Another limitation is that areas of debris-covered ice were found to not be well distinguished due to the spectral similarity between adjacent bedrock (Bolch et al., 2010).

The NIR/SWIR ratio is less commonly used but is another effective method for delineating glacier outlines (Schmidt and Nüsser, 2012). Although Andreassen et al. (2008) utilised the Red/SWIR ratio, which yielded satisfactory results where most glacier ice is debris-free, they found both the Red/SWIR and NIR/SWIR ratios would give good results by adjusting the threshold value. Andreassen et al. (2008) chose the Red/SWIR ratio because it was better suited for ice in shadowed areas and debris-covered ice than the NIR/SWIR ratio.

The Normalised Difference Snow Index (NDSI), NDSI = (Green − SWIR)/(Green + SWIR), is the normalised difference of two bands (one in the visible and one in the near infrared or short-wave infrared parts of the spectrum) and had been applied successfully for mapping glaciers (e.g., Durán-Alarcón et al., 2015; Burns and Nolin, 2014; Racoviteanu et al., 2008). The NDSI is more

effective at distinguishing glacier ice from non-ice areas, especially areas in shadow. Paul and Hendriks (2010a) found that the NDSI performs somewhat better than the Red/SWIR ratio because it maps more debris-covered regions and less of the shadowed regions. There are limitations to this method as well because although the NDSI may map more debris-covered areas than other band ratios, it does not map them all or it may map debris areas not distinguishable as glaciers (Racoviteanu et al., 2008).

1.3 Structure of Thesis

The next chapter of this thesis, Chapter 2, provides a geographical and climatic context of the study area, including a description of historical glaciation in the Mackenzie Mountains. Chapter 3 covers the satellite image data that was utilised in this study and outlines the methods followed for glacier mapping, deriving glacier areas, assessing the change in glacier areas between image dates, estimating the error in glacier area and perimeter length values, statistical analyses, and visualisation. Chapter 4 presents the glacier area and perimeter length results determined for the time period of 1987 to 2013/2017. In Chapter 5, the results of this study are discussed in context of the band ratio chosen for image thresholding, confusion in the mapping of glaciers caused by snow cover, error estimation, and glacier change focused on the study area as well as compared to glacier studies elsewhere in the world. The remainder of this thesis concludes in Chapter 6 by considering the findings in relation to the objectives of this study and recommendations for further work.

CHAPTER 2

Study Area

2.1 Description of Study Area

2.1.1 Geographical Context

The glaciers examined in this study are located in northwestern Canada, in the northern section of the Mackenzie Mountains, on both sides of the Yukon–Northwest Territories border (Figure 2.1). The study area also covers a small portion of the Selwyn Mountains (Figure 2.2). The Mackenzie Mountains are the northward continuation of the Rocky Mountains and are a part of the Mackenzie Mountains Ecoregion located within the Taiga Cordillera Ecozone (Yukon Ecoregions Working Group, 2004). The study area comprises the region between 131°14'07" W, 64°38'39" N and 130°46'52" W, 64°9'50" N (Figure 2.1).

The Mackenzie Mountains extend in an arc from the northwest in Yukon at approximately 65°N to the southeast in Northwest Territories. Within the Mackenzie Mountains range, the study area glaciers are found in the Backbone Range to the east in Northwest Territories and cross over into the northeastern Selwyn Mountains to the west in Yukon (Figure 2.2). The Mackenzie Mountains and the Selwyn Mountains form a broad expanse of unbroken and rugged block of peaks ranging in elevation from 2000 – 3000 m above sea level (ASL) along the Yukon–Northwest Territories border (Klock et al., 2001). The Backbone Ranges are the highest part of the Mackenzie Mountains with an average elevation of 2000 m (Horvath, 1975).

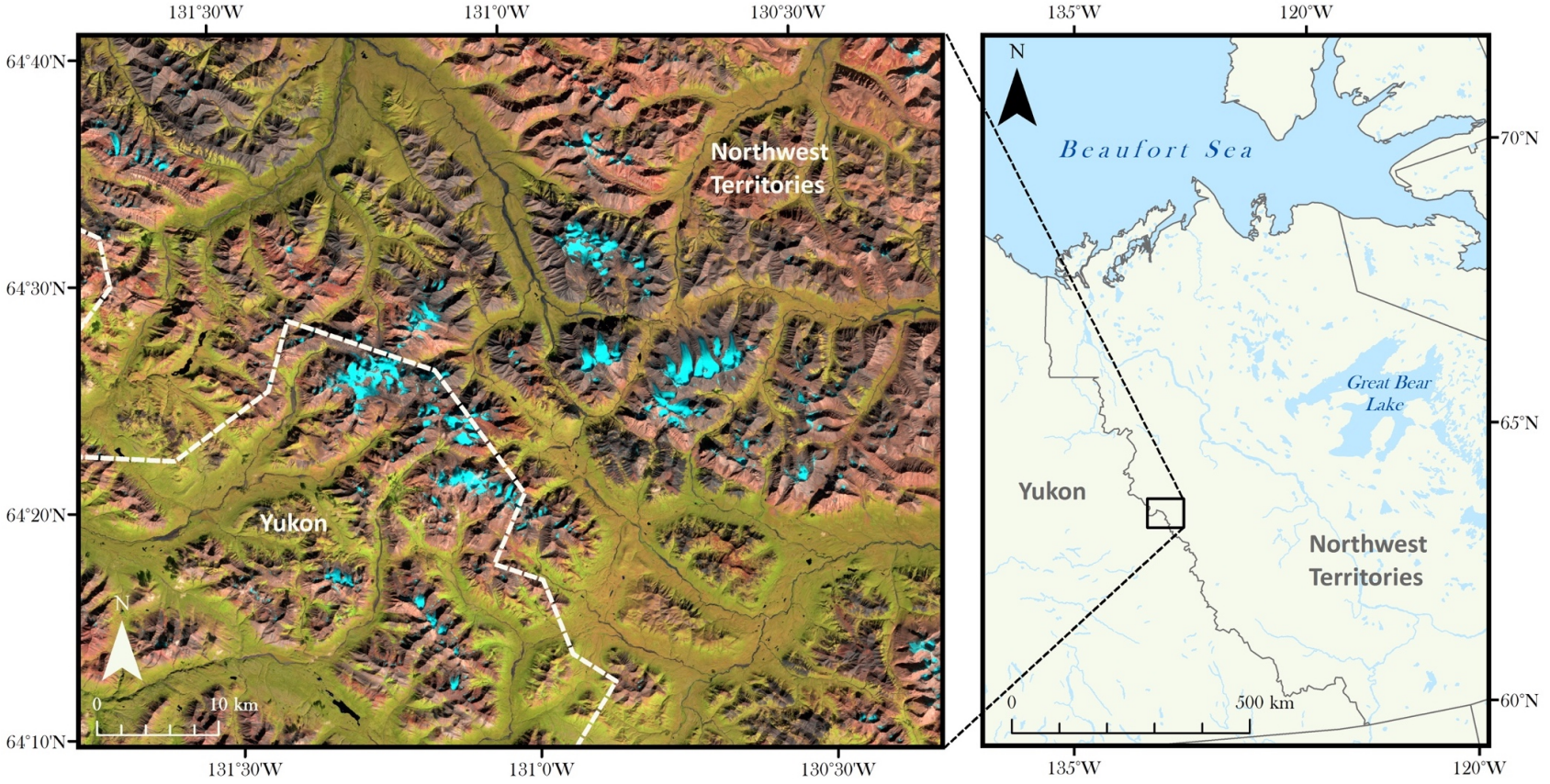

Figure 2.1. Study area location. Study area represented by inset map, which is a false-colour image display of Landsat TM bands SWIR, NIR, and Red, 1987. Glaciers appear in a light blue colour in the inset map.

Map data: WGS 1984, UTM Zone 8W. Sources: North America Water Polygons: ESRI, 2017. Canada Boundary: ESRI Canada Education Team, 2013.

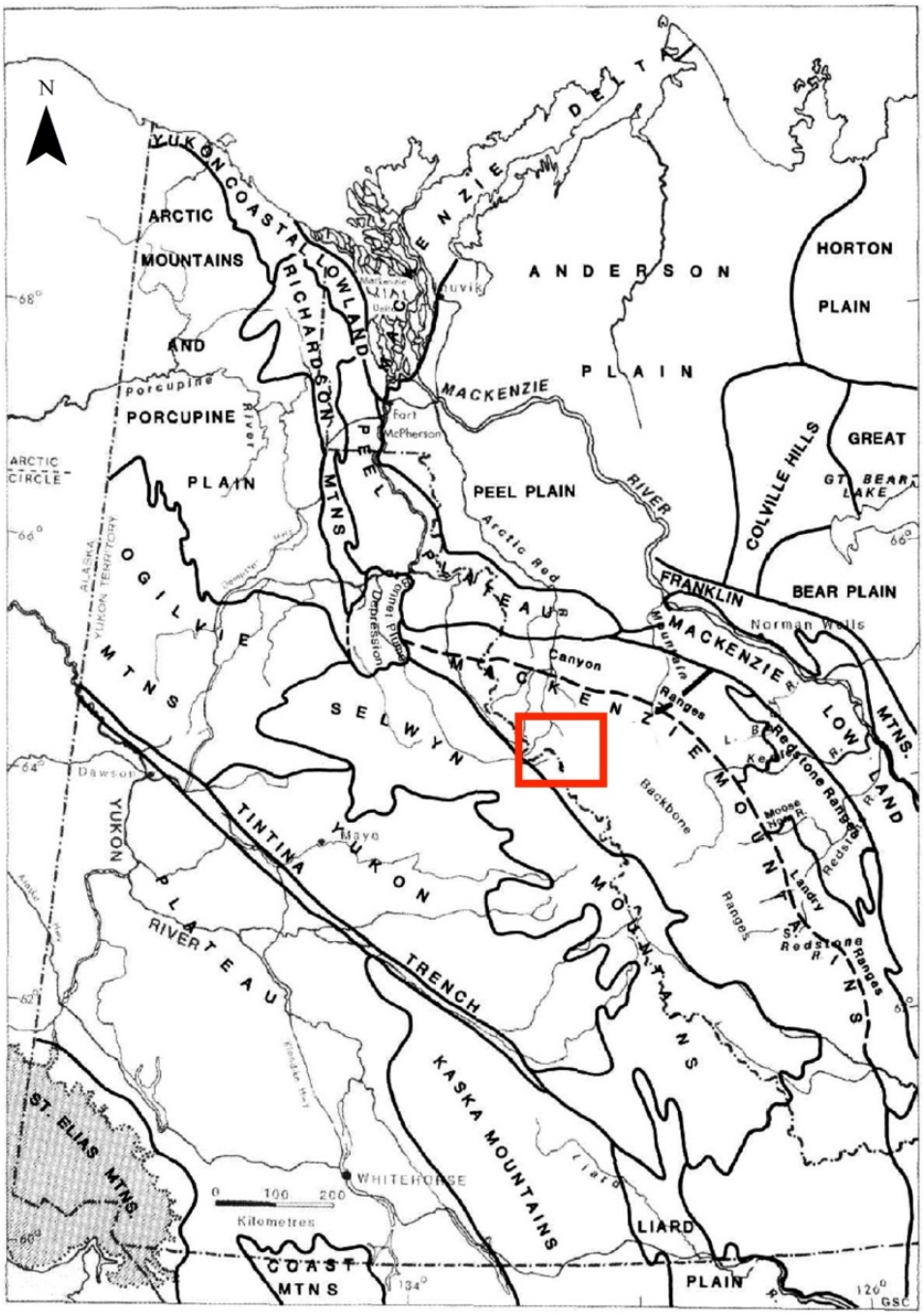

Figure 2.2. Physiography of the Mackenzie Mountains in Yukon and Northwest Territories. Study area represented by red rectangle.

Adapted from: Duk-Rodkin and Hughes, 1992, Figure 2.

The geology of the region has undergone a diverse tectonic evolution. The Mackenzie Mountains and eastern Selwyn Mountains are the northern extent of the Canadian Rocky Mountains and lie

within the Cordilleran Foreland Belt (Ootes et al., 2013), with the Tintina Trench to the southwest of the mountains (Figure 2.2). The oldest sedimentary rocks in the Mackenzie Mountains region range from Early Proterozoic to Middle Jurassic, a 1.6-billion-year sedimentary record (Yukon Ecoregions Working Group, 2004). Older rocks are overlain in the northern part of the mountains by thick-bedded Paleozoic carbonate in the west and sandstone in the east. It is this renewed continental shelf setting that is called the Mackenzie Platform.

As observed throughout the northern Cordillera, the extents of glaciers during older glaciations was greater than during more recent ones. The Mackenzie Mountains, as Duk-Rodkin and Hughes (1992) noted, have been glaciated several times by montane valley glaciers during the Pleistocene. It is the arcuate shape of the mountains that allowed the formation of a radial system of valleys during pre-glacial times from the large montane valley glaciers. Evidence of the youngest two glaciations, the Reid (ca. 200 ka) and the McConnell (ca. 23 ka), is found in most valleys throughout the Mackenzie Mountains (Yukon Ecoregions Working Group, 2004). The McConnell glaciation of Late Wisconsinan age reached the study area of the Mackenzie Mountains.

In more recent decades, Horvath (1975) described the glacial environment of northwestern interior Canada. Most of the glaciers in this area of Canada are located in the Selwyn and Mackenzie Mountains north of 60°N. Small icefields and glaciers covered the summits of high peaks (over 2000 m ASL) near and to the south of the divide between the Yukon and Mackenzie rivers (Figure 2.2). There have been very few mentions of the existence of glaciers in the Mackenzie and Selwyn Mountains appearing in the literature (Barrand and Sharp, 2010, Demuth et al., 2014, Horvath, 1975). Horvath (1975) noted how there were a few scattered and

little-known glaciers in western Canada north of 60°N. These glaciers are found in the higher parts of the Selwyn, Mackenzie, and Ogilvie mountains, as well as the Yukon Plateau (Figure 2.2).

2.2.1 Climatic Context

The Canadian Cordillera act as a major barrier to air masses moving inland from the Gulf of Alaska. These mountains are large enough to stop shallow layers of cold arctic air from reaching central and southern Yukon (Yukon Ecoregions Working Group, 2004). With a cold continental subarctic climate, snowfall accounts for a large portion of the total annual precipitation of the Mackenzie Mountain region. In the far northern and high-elevation areas of the Rocky Mountains, more than 60% of total annual precipitation is snowfall (DeBeer et al., 2016). In the Mackenzie Mountains, the heaviest precipitation occurs in July and August with monthly amounts of up to 50 to 70 mm, whereas December to May have the least amount of precipitation with monthly amounts of 20 to 30 mm (Yukon Ecoregions Working Group, 2004).

Across the interior of western Canada, mean annual air temperature (for the period of 1981–2010) varies considerably, ranging from 5 to 10°C in the southwest to -5 to -10°C in the northwest (DeBeer et al., 2016). During the summer months, temperatures are relatively warm, with average temperatures ranging between 10 and 20°C, whereas average temperatures range from -30 to -5°C during winter months (DeBeer et al., 2016). These climatic conditions of low precipitation and relatively warm summers prevent the growth of glaciers in the mountains of eastern Yukon and western Mackenzie Mountains. According to Horvath (1975), there have been only small glaciers in the Mackenzie Mountains region due to insufficient moisture from only low amounts of precipitation falling in the northern part of the Backbone Ranges.

CHAPTER 3

Methods and Data

3.1 Data Acquisition

Images for use in this study were acquired as Landsat 5 and 8 orthorectified imagery from the USGS Earth Explorer online database (earthexplorer.usgs.gov), with two Landsat scenes – Row 15, Paths 58 and 59 – covering the study area. The Landsat orthorectified imagery was obtained with spatial reference to the Universal Transverse Mercator (UTM) projection on the World Geodetic System 1984 (WGS84) datum and ellipsoid. This imagery is derived from Landsat 5 and 8 raw images of radiometrically and systematically corrected (Collection Level-1, Tier 1) processed data, which is reported to have a horizontal positional accuracy of 30 m or less with a 90% level of confidence.

When conducting a preliminary assessment of the imagery in the Earth Explorer database to ensure that sufficient suitable imagery would be available, images from only July or August were considered. This was done because glaciers were at their minimal annual extent during the ablation season with minimal chances of seasonal snow coverage. Images from 1987 to 2004 were acquired by the Landsat 5 TM satellite and the images from 2013 and 2017 were acquired by the Landsat 8 OLI satellite, with a total of six images utilised (Table 3.1). The 1994 image was re-projected from UTM Zone 9 to Zone 8 to compare with the other images. The images and years chosen for this study were decided on to provide as much temporal spread as possible. Of the total available Landsat imagery in the Earth Explorer database, there were restrictions on which images would be useful for this research due to cloud cover limiting the number of suitable

Table 3.1. Utilised Landsat scenes applied in this study.

Acquisition Date	Sensor	Original Projection	Datum/ Ellipsoid	Path/Row	Scene Size (km)
1987-08-24	Landsat 5 TM	UTM Zone 8	WGS84	059/015	170 x 185
1994-07-10	Landsat 5 TM	UTM Zone 8	WGS84	059/015	170 x 185
1999-08-02	Landsat 5 TM	UTM Zone 9	WGS84	058/015	170 x 185
2004-08-22	Landsat 5 TM	UTM Zone 8	WGS84	059/015	170 x 185
2013-07-14	Landsat 8 OLI	UTM Zone 8	WGS84	059/015	170 x 185
2017-08-10	Landsat 8 OLI	UTM Zone 8	WGS84	059/015	170 x 185

Source: USGS online database.

images. The 1994 images were not of the same extent as the other image years, resulting in some areas of the image not present. Therefore, only 108 of 117 glaciers were able to be compared between each image from 1987 to 2013. Cloud coverage limited the visibility of glaciers in the 2017 image, resulting in fewer glaciers that could be mapped and compared (74) to the other images (108).

3.2 Glacier Mapping

Prior to image processing, a single PIX file was created from the input individual Landsat bands in PCI Geomatica™ 2016 for each image. Processing of the Landsat images follows a sequence of glacier mapping, deriving glacier areas, assessing the change in glacier areas between image dates, and visualisation. Initial processing of comparing band ratio images, applying filters, and creating binary images was conducted using PCI Geomatica™. A semi-automated approach of thresholding ratio images was used for mapping the glacier outlines. Ratio images enhance the image contrast for certain surface types, while reducing the bias in illumination from the terrain at the same time (Paul and Hendriks, 2010b). By using a threshold value for the ratio images, glaciers could be distinguished from the surrounding terrain. The common band ratios used in

glacier studies of Red/SWIR, NIR/SWIR, and NDSI were compared to determine which would be the most effective approach for the study area (Figure 3.1).

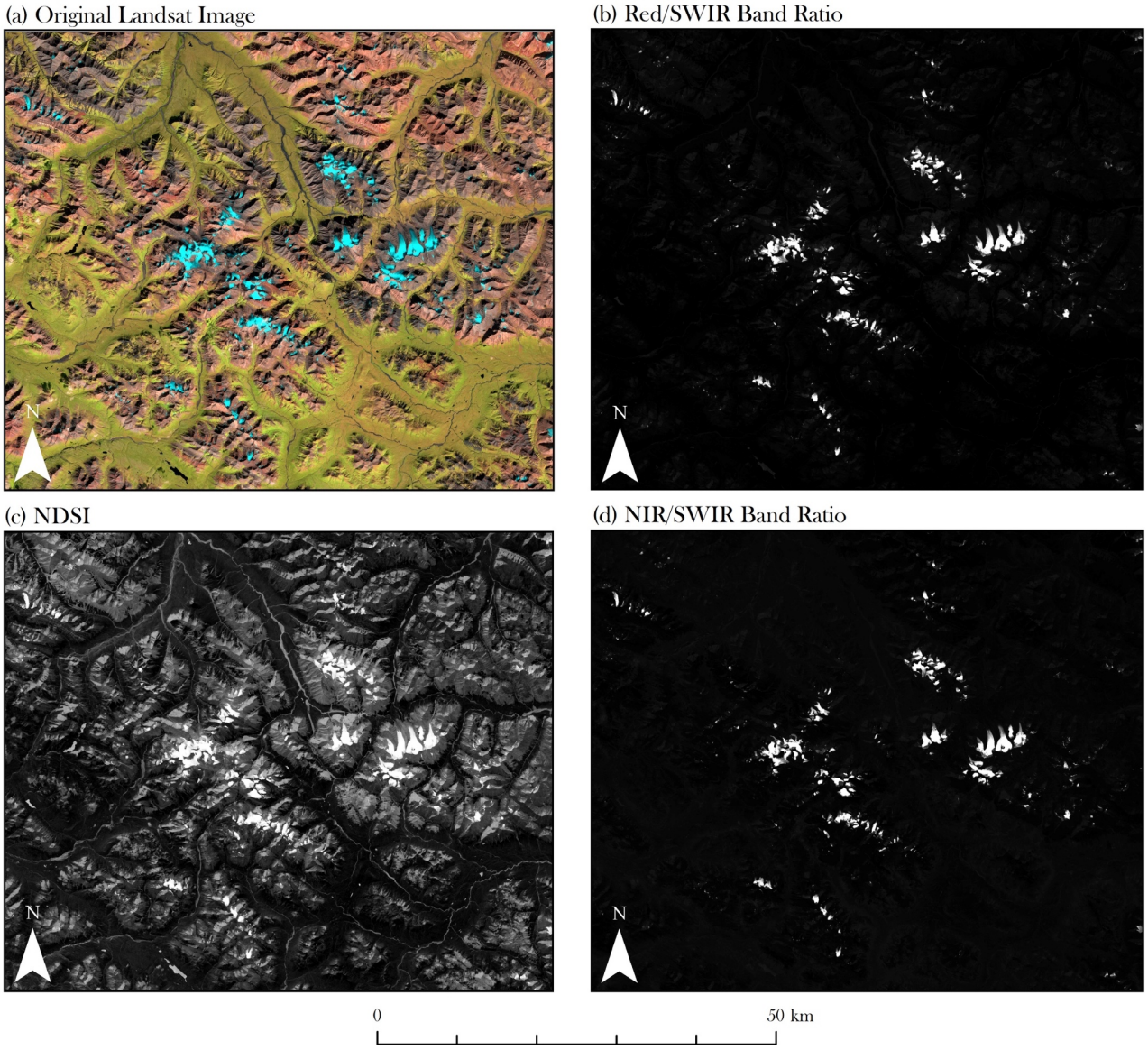

Figure 3.1. Comparison of band ratios from the 1987 image with median 3 x 3 filter applied. (a) False-colour image (SWIR, NIR, and Red bands). (b) Red/SWIR band ratio. (c) NDSI image (Green and SWIR bands). (d) NIR/SWIR band ratio.

For the reduction of noise, a 3x3 median spatial filter was applied prior to further processing. Although applying such a filter can remove isolated snow pixels and close gaps due to noise in shadow, it also reduces the size of very small glaciers (Paul and Hendriks, 2010a). It is this reason and because of the pixel size of the satellite sensor, that glaciers no smaller than 0.02 km^2 can be mapped with Landsat TM and OLI sensors (Paul and Hendriks, 2010a). Without a filter, the binary images created of the glacier outlines would produce too many single-pixel outlines that could not be separated out simply by adjusting the threshold value.

Binary images were generated using threshold values chosen between 1.4 and 7 for Red/SWIR, 1.6 and 7 for NIR/SWIR, and 0.4 and 0.8 for the NDSI to discriminate ice from the surrounding terrain. Initially, threshold values used in the literature (0.35 to 0.55 for NDSI and ~2 for both Red/SWIR and NIR/SWIR) were tested first, but then had to be adjusted. Each individual Landsat image required a unique threshold value. There were small differences in thresholds associated with particular band ratio images, which can have significant effects on the estimation of debris-free glacier area (Burns and Nolin, 2014). Based on comparisons between threshold values and binary images, a thresholded band ratio of Red/SWIR was chosen for this study. The Red/SWIR ratio was chosen because it mapped debris-covered ice better than the NIR/SWIR ratio and the NDSI. The NIR/SWIR did not map as much debris-covered ice, whereas the NDSI mapped debris-covered areas not distinguishable as glaciers. Choosing the Red/SWIR ratio allowed for less manual digitisation of new outlines for debris-covered ice. How and why these values were chosen for this band ratio will be further discussed in Chapter 5, Section 5.1.

Once the glacier areas represented as raster data were generated from the Landsat satellite data as binary images, the glaciers were converted to polygon outlines as vector data for further

analysis. The raster polygon glacier map was exported as a vector shapefile from PCI Geomatica™ and imported to ESRI ArcMap™ v10.5. A separate vector layer was created for removing misclassified pixels, such as snow patches or lakes, and to assign identification codes to the glaciers and other information in the attribute table.

A selection criterion was applied to remove outlines smaller than 0.02 km^2. A smaller threshold would include many features that were most likely snow patches (Bolch et al., 2010). Manual corrections needed to be applied to the resultant outlines. Two primary limitations that thresholded ratio image methods have are that water bodies cannot be completely identified, and that debris-covered ice is not easily distinguished from the surrounding rocks because of their spectral similarity (Liu et al., 2013). To identify the glaciers and delineate their outlines accurately, all images were thoroughly inspected by distinguishing small glaciers from snow patches by confirming the presence of visible crevasses and/or exposed ice.

Manual corrections were required for misclassified polygons as water bodies and snow patches in the study area, and for including debris-covered glacial areas, which were carried out by deleting polygons and editing the vertices of larger polygons for all images. For each image, debris-covered glacier polygons were merged with debris-free glacier polygons for an estimate of total glacier area. Glaciers that had common boundaries in the accumulation zone were separated if they drained into different basins. Manual digitisation was preferred to map debris-covered glacier areas because the spectral signature on satellite images does not differentiate the thick debris-covered glacier with the surrounding terrain (Paul et al., 2009). Single pixel holes in the glacier polygons needed to be deleted as these were most likely misclassified pixels due to glacier debris. Deciding on what to include as glacier surface proved to be one of the most challenging

tasks, especially for determining whether smaller polygons were seasonal or perennial snow, or if they were small glaciers that were disintegrating.

3.3 Glacier Area Derivations and Change Assessments

After glacier outlines were completed for each image in the years of 1987, 1994, 1999, 2004, 2013, and 2017, area and perimeter measurements were determined for each individual glacier attribute derived directly from the ArcView™ shapefiles. Each glacier used in the study was assigned an individual identification. Where a glacier had split into several distinct ice masses, the net area change was based on the total area of the individual glacier parts compared to the area of the single glacier in the earlier image. Glacier mapping was conducted independently for each image date in which change values were calculated separately. The change in glacier area and perimeter length was determined by comparing the tabulated area and perimeter length of all the glaciers for the time periods of 1987-1994, 1994-1999, 1999-2004, 2004-2013, 2013-2017, as well as for 1987-2013 and 1987-2017. To study whether glacier size was important in how they changed, the glaciers were divided into size classes of $A < 0.05$ km^2, 0.05 km^2 $< A <$ 0.1 km^2, 0.1 km^2 $< A <$ 0.5 km^2, 0.5 km^2 $< A <$ 1.0 km^2 and $A >$ 1.0 km^2.

3.4 Error Estimation

Sources of potential error in area estimates from mapping glaciers boundaries from satellite images are derived from scene quality, clouds, seasonal snow, and shadow, methods of glacier delineation, and pixel size. Potential error of glacier area measurements depends on how accurately individual glaciers can be identified and digitised, especially when estimating where glacier margins are of joined glaciers. This also depends on the snow conditions and the contrast

between the ice and adjacent surfaces. To account for uncertainty in glacier outline delineation, the error was estimated for glacier area and perimeter length values.

Previous studies using Landsat satellite images with the Red/SWIR band ratio method to map glaciers indicated an error of ±2-5% for debris-free glaciers (Paul et al., 2013). Bolch et al. (2010) estimated a mapping error of ±2.5% for Landsat TM scenes of glaciers in British Columbia and Alaska, where 0.5% of this error was added to account for the more difficult delineation of debris-covered glacier tongues. The authors also estimated an error of ±3% for scenes that have late-lying snow. Bhambri et al. (2013) estimated similar errors of Landsat TM scenes of the Karakoram mountains of Asia to be 2.1% and 2.2%, as well as an error of 3.2% for a Landsat ETM+ scene. Another study using Landsat TM scenes estimated an error of ±2.4% for glaciers in the Himalayas (Chand and Sharma, 2015).

To apply an error to the present study of glaciers in the Mackenzie Mountains, a similar error value was used as the previous studied mentioned. An average of these error estimates equalling ±2.5% was applied to the area and perimeter length values for accounting for the uncertainty of mapping boundaries of the glaciers. Such error estimates were not found to have been applied to perimeter values in the literature, but these values are applied in the present study as a guideline. Since the 1994 image had considerable seasonal snow cover compared to the other image years, an error estimation of ±3% was added as proposed by Bolch et al. (2010). Thus, the 1994 area values were assigned an error estimation of ±5.5%, whereas other images were assigned ±2.5%. For the area change values, an accumulated error of both individual images was assigned, with ±8% for comparisons with 1994 and ±5% for all other comparisons.

3.5 Statistical Analysis

The sign of the trend estimated for the glacier area (increase or decrease) over time and its strength were obtained by simple linear regression. Linear regression was used to test the significance of the slope of the regression line of glacier area over time and of glacier perimeter over time for both total and mean values, which was conducted using IBM SPSS v24 statistical software. Each of the sample units for linear regression represent either the mean or sum of all individual glacier area and perimeter values for each image year. A one-tailed hypothesis test was used for linear regression, based on an assumption of a decreasing trend in both area and perimeter length over time. To assess the relationship of perimeter and area, perimeter was analysed for correlation with area for both total and mean values of each year using Pearson's Product-Moment Correlation. Assuming that the existing linear trend of total glacier area would continue, the data values were extrapolated to predict when the study area would become glacier-free.

CHAPTER 4

Results

4.1 Thresholded Band Ratio Selection

Binary images created from thresholded single band ratio images (Red/SWIR and NIR/SWIR) and normalised images (NDSI) were compared for the study area to determine which would be most effective for the images. Based on effectiveness of mapping debris-covered glaciers and the misclassification of water bodies as ice, the Red/SWIR ratio was preferred for the study area. Although the NIR/SWIR ratio and NDSI may have been more effective for some of the images, the Red/SWIR ratio proved to be most appropriate for all images requiring the least amount of manual effort. An example of the resultant glacier outlines for 1987 produced using the thresholded Red/SWIR band ratio is presented in Figure 4.1. The thresholded Red/SWIR band ratio images produced similar results as this example in all subsequent image dates.

4.2 Glacier Size Distribution

The 117 glacier units that existed in the 1987 image covered a total area of 72.4 ± 1.8 km^2 (complete glacier area and perimeter data in Appendix: Individual Glacier Area and Perimeter Values). Not all of the 117 glaciers appeared in all of the images, therefore a sample of 108 glaciers was analysed for each image from 1987 to 2013 for comparison purposes. When the 2017 image was included for comparison, a sample of 74 glaciers was used to account for the glaciers not visible in the image. Figure 4.2 presents the distribution of glacier population, according to glacier size class ranging in area from less than 0.05 km^2 to greater than 1.0 km^2 (Figure 4.2a) and

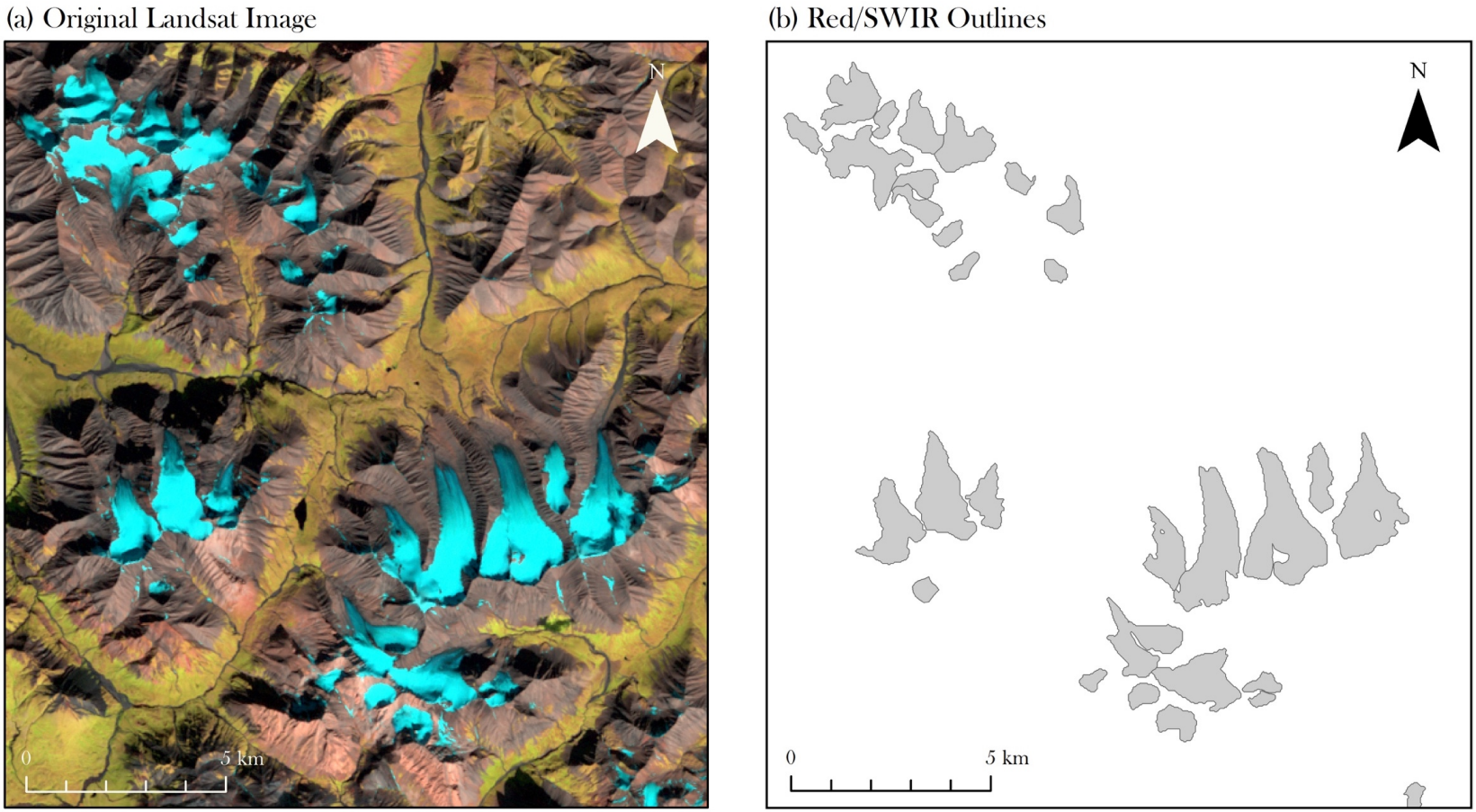

Figure 4.1. A sample of glaciated area from the 1987 image. a) False-colour display of the Landsat satellite image using bands SWIR, NIR, and Red. b) Final glacier outline result derived from thresholded Red/SWIR band ratio image with manual corrections.

according to year (Figure 4.2b). The 2017 glacier data are not included in Figure 4.2a because the absolute values are not comparable among years.

In 1987, the majority of glaciers (54.5%) occupy a size class of 0.1 $km^2 < A < 0.5$ km^2 but represent only 22% of the total glacier area. The second most populous size class is 0.5 $km^2 < A <$ 0.1 km^2 in which 24 glaciers (22%) provide another 22% of the total glacier area. Glaciers that occupy the largest size class of $A > 1.0$ km^2 (18.5%) represent 55% of the total glacier area, with the largest glacier having an area of 3.67 ± 0.09 km^2. The remaining 1% is made up of five glaciers in the 0.05 $km^2 < A < 0.1$ km^2 size class. There were no glaciers in the $A < 0.05$ km^2 size class for the 1987 image.

Glaciers with an area between 0.1 and 0.5 km^2 represent the most frequent size class for all image years (Figure 4.2b). The glacier population of smaller size classes ($A < 0.05$ km^2 and 0.05 $km^2 < A < 0.1$ km^2) increased from 1987 to 2017. There was also a shift in the total area of each size class that occurred in 2004 in contrast to 1999. The smaller size classes ($A < 0.05$ km^2, 0.05 $km^2 < A <$ 0.1 km^2, and 0.1 $km^2 < A < 0.5$ km^2) increased and the larger size classes (0.5 $km^2 < A < 1.0$ km^2 and $A > 1.0$ km^2) decreased, in which the size class of 0.1 $km^2 < A < 0.5$ km^2 remained the most populous (Figure 4.2).

4.3 Glacier Change from 1987 to 2013

The change in area is summarised for 1987-2013, 1987-1994, 1994-1999, 1999-2004, and 2004-2013 (Table 4.1). The sample of 108 glacier units from the 1987 image covers a total area of 69.9 ± 1.75 km^2, with a mean glacier area of 0.65 ± 0.02 km^2. Glacier area decreased from 69.9 ± 1.75 km^2 in 1987 to 41.0 ± 1.03 km^2 in 2013, a loss of 41.5 ± 2.08% or 29.0 ± 1.45 km^2, with an

area reduction rate of 1.59% · a^{-1} and an absolute area reduction rate of 1.12 km^2 · a^{-1}. For the initial 108 glaciers in the study area, three glaciers had retreated to such a small extent that they were unrecognisable.

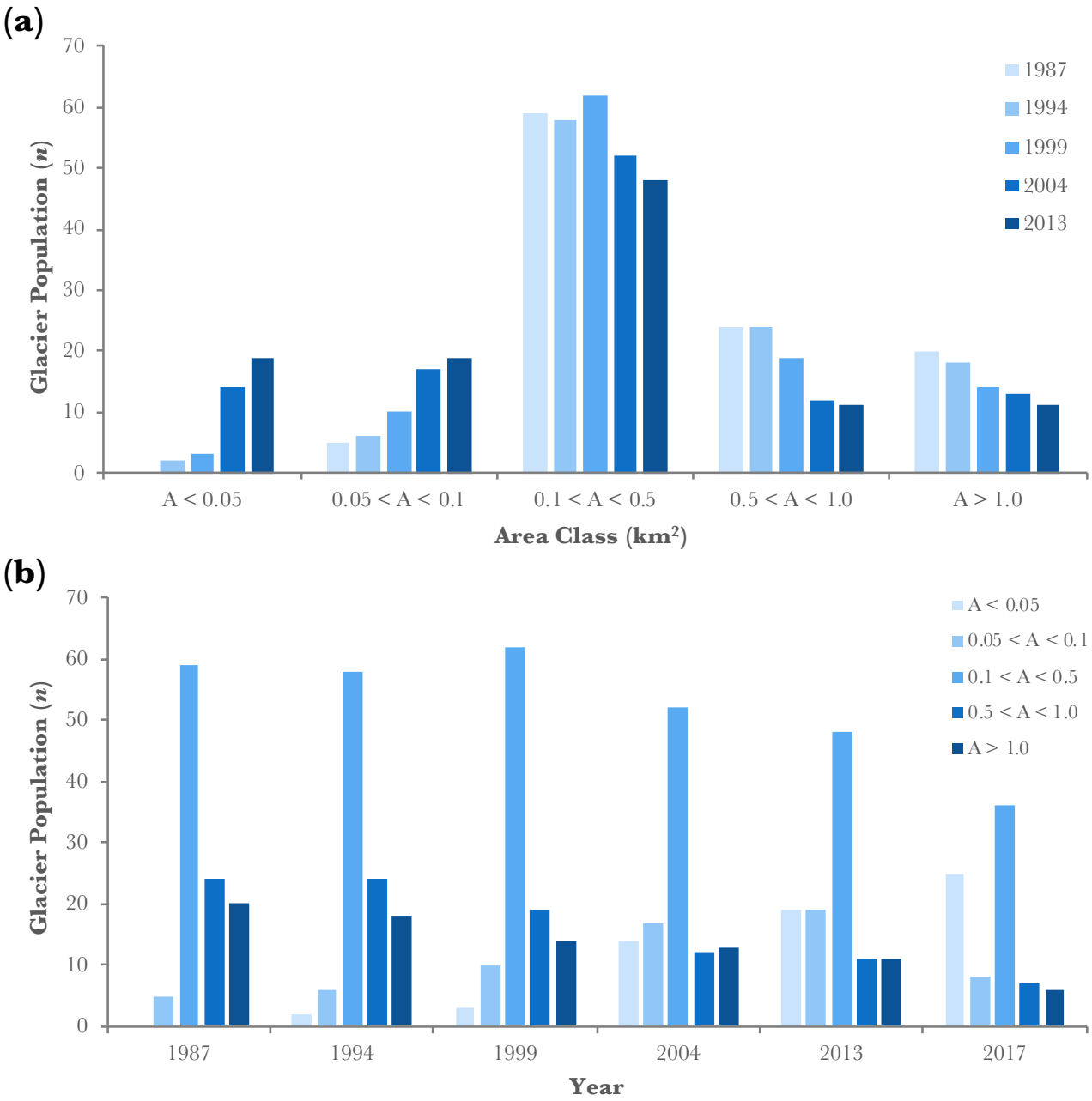

Figure 4.2. Distribution of glacier sizes within the study area. (a) Population of glaciers per area size class for each year from 1987-2013 (n=108). (b) Population of glaciers per year organised by area size class; n=108 for 1987-2013 and n=74 for 2017 to observe glaciers visible in all images.

Glacier area decreased during each of the other time periods; -4.47 ± 0.36% from 1987 to 1994, -15.1 ± 1.21% from 1994 to 1999, -16.2 ± 0.81% from 1999 to 2004, and -13.9 ± 0.70% from 2004 to 2013. Although there were no glaciers in the smaller size classes ($A < 0.05$ km^2, 0.05 km^2 $< A <$ 0.1 km^2, 0.1 km^2 $< A <$ 0.5 km^2) that increased in area over the 1987-2013 period, there were some glaciers that increased in area within the periods of 1987-1994, 1994-1999, 1999-2004, and 2004-2013.

Total area changes from 1987 to 2013 relative to the initial area of 1987 is shown in Figure 4.3. While smaller glaciers underwent greater relative losses than larger glaciers generally, scatter in the relative change data increases as area increases. From 1987 to 2013, there was a greater percentage loss for smaller glaciers across the study area than for the larger ones, although the absolute loss is much lower than for the larger glaciers (Table 4.1 and Figure 4.3). The largest total absolute loss in area is for glaciers in the $A > 1.0$ km^2 area size class.

The relative area changes for individual glaciers from 1987 to 2013 ranged from -9.50 ± 0.48% to -100 ± 5.00%, with a mean area change of -53.3 ± 2.67% and a median of -50.7 ± 2.54% (Figure 4.4). The retreat of glaciers with an initial area greater than 0.1 km^2 accounted for a considerable fraction of the total area change. Figure 4.5 shows the temporal evolution of glacier area from 1987 to 2013 over the study area. The results of the hypothesis testing of the slope of the line show a statistically significant linear relationship (p=0.003) of decreasing mean glacier area over time. Decreasing total glacier area over time was also found to have a statistically significant linear relationship (p=0.002).

Table 4.1. Change in area (A) of glaciers from 1987 to 2013 (n=108).

Area Size Class (km²)	**1987**			**1994**			**1999**			**2004**			**2013**		
	n	A Sum	A Mean	n	A Sum	A Mean	n	A Sum	A Mean	n	A Sum	A Mean	n	A Sum	A Mean
$A < 0.05$	0	0	0	2	0.04	0.04	3	0.08	0.03	14	0.74	0.03	19	0.47	0.03
$0.05 < A < 0.1$	5	0.38	0.08	6	0.49	0.08	10	0.72	0.07	17	1.34	0.07	19	1.37	0.07
$0.1 < A < 0.5$	59	15.6	0.26	58	15.3	0.26	62	14.9	0.24	52	13.2	0.25	48	11.7	0.24
$0.5 < A < 1.0$	24	16.0	0.66	24	16.6	0.69	19	13.3	0.70	12	8.39	0.70	11	7.96	0.72
$A > 1.0$	20	38.1	1.90	18	34.4	1.91	14	27.7	1.98	13	24.4	1.87	11	19.4	1.77
Total	108	69.9±1.75	0.65±0.02	108	66.8±3.67	0.62±0.03	108	56.8±1.41	0.53±0.01	108	47.6±1.19	0.44±0.01	108	41.0±1.03	0.38±0.01
Area Size Class (km²)	**1987-2013**			**1987-1994**			**1994-1999**			**1999-2004**			**2004-2013**		
	n	A (km²)	A (%)	n	A (km²)	A (%)	n	A (km²)	A (%)	n	A (km²)	A (%)	n	A (km²)	A (%)
$A < 0.05$	0	*n/a*	*n/a*	0	*n/a*	*n/a*	2	-0.01	-23.4	3	-0.05	-100	14	-0.04	-12.6
$0.05 < A < 0.1$	5	-0.24	-65.0	5	-0.00	-0.94	6	-0.05	-9.52	10	-0.31	-42.5	17	-0.28	-22.5
$0.1 < A < 0.5$	59	-9.42	-60.6	59	-0.93	-5.98	58	-3.69	-24.2	62	-3.97	-26.6	52	-2.15	-16.3
$0.5 < A < 1.0$	24	-7.03	-44.1	24	-0.32	-2.02	24	-3.21	-19.4	19	-2.50	-18.8	12	-1.05	-12.5
$A > 1.0$	20	-12.3	-32.3	20	-1.87	-4.92	18	-3.10	-9.00	14	-2.37	-8.57	13	-3.08	-12.6
Total	108	-29.0±1.45	-41.5±2.08	108	-3.13±0.25	-4.47±0.36	108	-10.7±0.86	-15.1±1.21	108	-9.20±0.46	-16.2±0.81	108	-6.61±0.33	-13.9±0.70

Table 4.2. Change in perimeter (*P*) of glaciers from 1987 to 2013 (*n*=108).

Area Size Class (km²)	**1987**			**1994**			**1999**			**2004**			**2013**		
	n	*P* Sum	*P* Mean	*n*	*P* Sum	*P* Mean	*n*	*P* Sum	*P* Mean	*n*	*P* Sum	*P* Mean	*n*	*P* Sum	*P* Mean
$A < 0.05$	0	0	0	2	0.85	0.43	3	1.67	0.56	14	9.45	0.67	19	13.3	0.70
$0.05 < A < 0.1$	5	5.74	1.15	6	7.41	1.24	10	12.9	1.29	17	21.8	1.28	19	25.6	1.35
$0.1 < A < 0.5$	59	148	2.52	58	149	2.56	62	168	2.71	52	144	2.76	48	135	2.81
$0.5 < A < 1.0$	24	104	4.33	24	109	4.52	19	97.1	5.11	12	59.7	4.98	11	59.3	5.39
$A > 1.0$	20	151	7.55	18	139	7.73	14	126	9.01	13	109	8.37	11	88.8	8.07
Total	108	409±10.2	3.79±0.09	108	405±22.3	3.75±0.21	108	406±10.2	3.76±0.09	108	343±8.58	3.18±0.08	108	322±8.05	2.98±0.075
Area Size Class (km²)	**1987-2013**			**1987-1994**			**1994-1999**			**1999-2004**			**2004-2013**		
	n	*P* (km²)	*P* (%)	*n*	*P* (km²)	*P* (%)	*n*	*P* (km²)	*P* (%)	*n*	*P* (km²)	*P* (%)	*n*	*P* (km²)	*P* (%)
$A < 0.05$	0	*n/a*	*n/a*	0	*n/a*	*n/a*	2	-0.15	-17.07	3	-0.93	-55.69	14	-1.85	-18.06
$0.05 < A < 0.1$	5	-2.45	-42.7	5	-0.11	-1.99	6	-0.13	-1.75	10	-4.37	-33.86	17	-2.33	-10.60
$0.1 < A < 0.5$	59	-48.9	-31.5	59	-11.37	-7.32	58	-8.91	-5.99	62	-33.3	-19.85	52	-12.16	-8.29
$0.5 < A < 1.0$	24	-15.2	-14.6	24	1.73	1.67	24	-1.80	-1.66	19	-12.5	-12.84	12	-1.78	-3.19
$A > 1.0$	20	-14.0	-9.25	20	-1.42	-0.94	18	11.90	8.56	14	-11.0	-8.72	13	-3.41	-3.13
Total	108	-73.7±3.69	-18.0±0.90	108	-4.32±0.22	-1.06±0.05	108	0.91±0.73	0.23±0.02	108	-62.1±3.11	-15.3±0.77	108	-21.5±1.08	-6.27±0.31

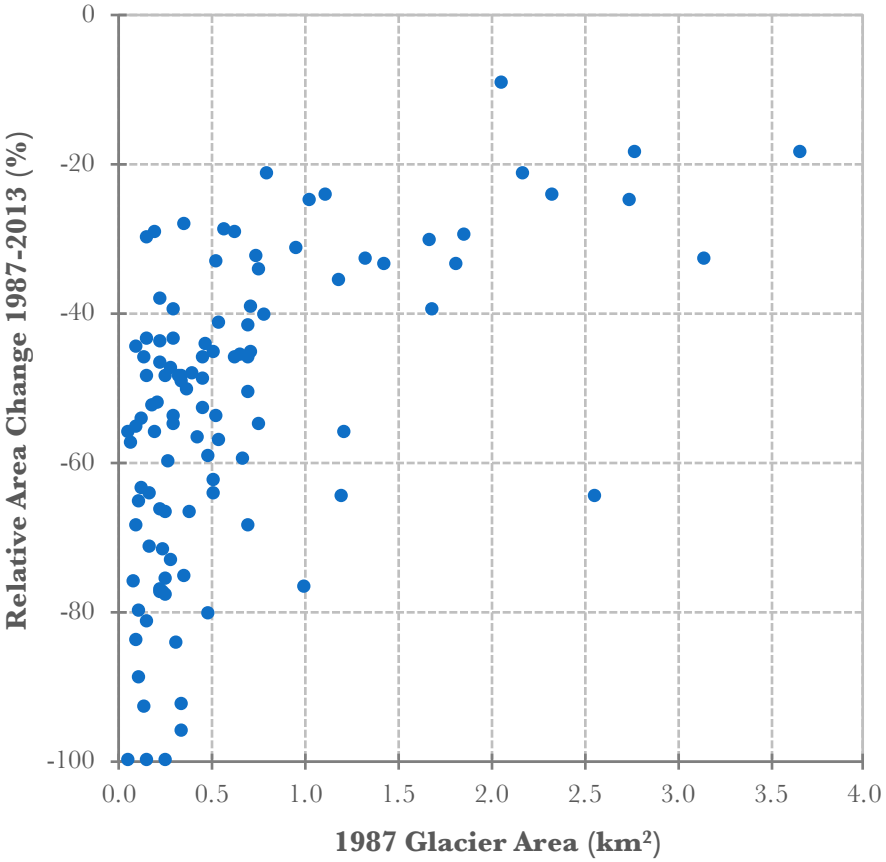

Figure 4.3. Relative change in glacier area from 1987–2013 versus initial glacier area (*n*=108).

The results of extrapolating the total area values per year for the 1987-2013 sample period imply that the study area glaciers will lose all area by 2045. The results of the linear extrapolation should be treated with caution because this method only estimates the value of glacier area based on its relationship with time beyond the original observation period. As glacier area reduces in size, there may also be an acceleration in the decrease in area over time, resulting in the glacier-free study area prediction to occur sooner than the linear extrapolation suggests. If more data points had been used, a type of non-linear extrapolation method may have been more suitable in predicting the future trend in glacier area.

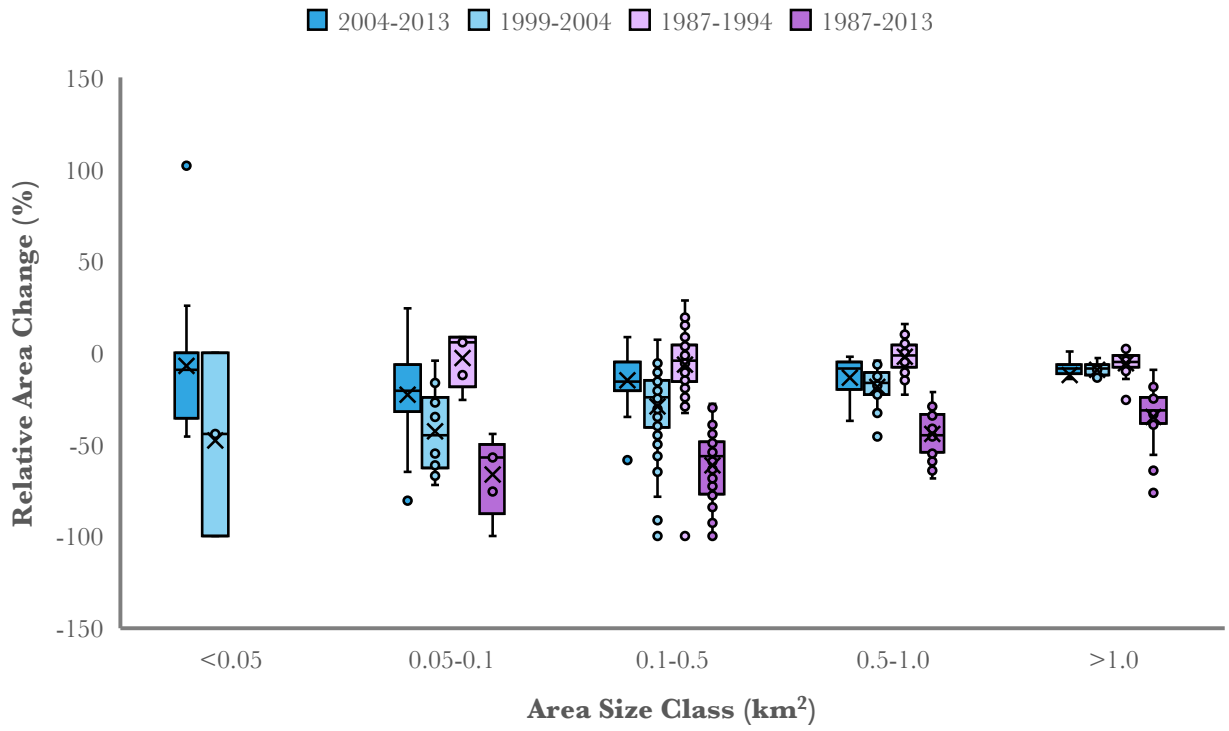

Figure 4.4. Glacier area change from 1987–2013 for different size classes (size in 1987). Centre line of box represents median, x represents mean, and box width defined by interquartile range (25 and 75 percentiles). Whiskers represent minimum and maximum data points.

The change in perimeter is summarised for 1987-2013, 1987-1994, 1994-1999, 1999-2004, and 2004-2013 (Table 4.2). For the sample of 108 glaciers, perimeter length decreased by 73.7 ± 3.69 km (409 ± 10.2 km in 1987 and 322 ± 8.05 km in 2013) from 1987 to 2013, a loss of 30.1 ± 1.51 km or 18.0 ± 0.90%. Glacier perimeter length decreased during each of the time periods, except from 1994 to 1999 in which total perimeter increased by 0.91 ± 0.07 km due to the large increase in perimeter for the glaciers within the area size class $A > 1.0$ km^2. Glacier perimeter length decreased during each of the other time periods; -18.0 ± 0.90% from 1987 to 1994, -1.06 ± 0.05% from 1994 to 1999, and -6.27 ± 0.31% from 2004 to 2013.

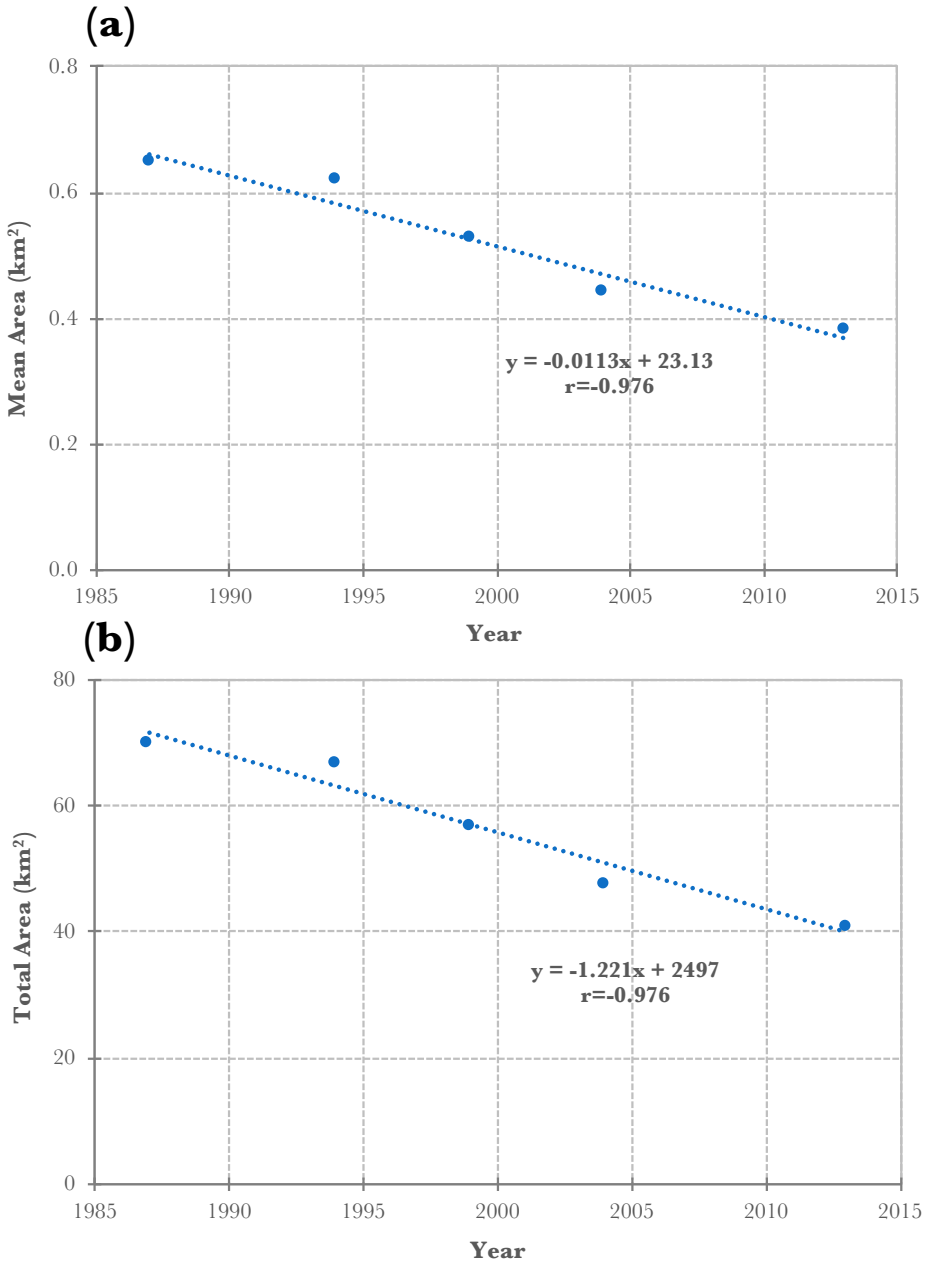

Figure 4.5. Trend of mean (a) and total (b) glacier area from 1987 to 2013 (n=108).

Figure 4.6 shows the temporal evolution of glacier perimeter length from 1987 to 2013 over the study area. The results of the hypothesis testing of the slope of the line show a statistically significant linear relationship (p=0.019) of decreasing mean glacier perimeter length over time.

For decreasing total perimeter length over time, the results also present a statistically significant linear relationship (p=0.019).

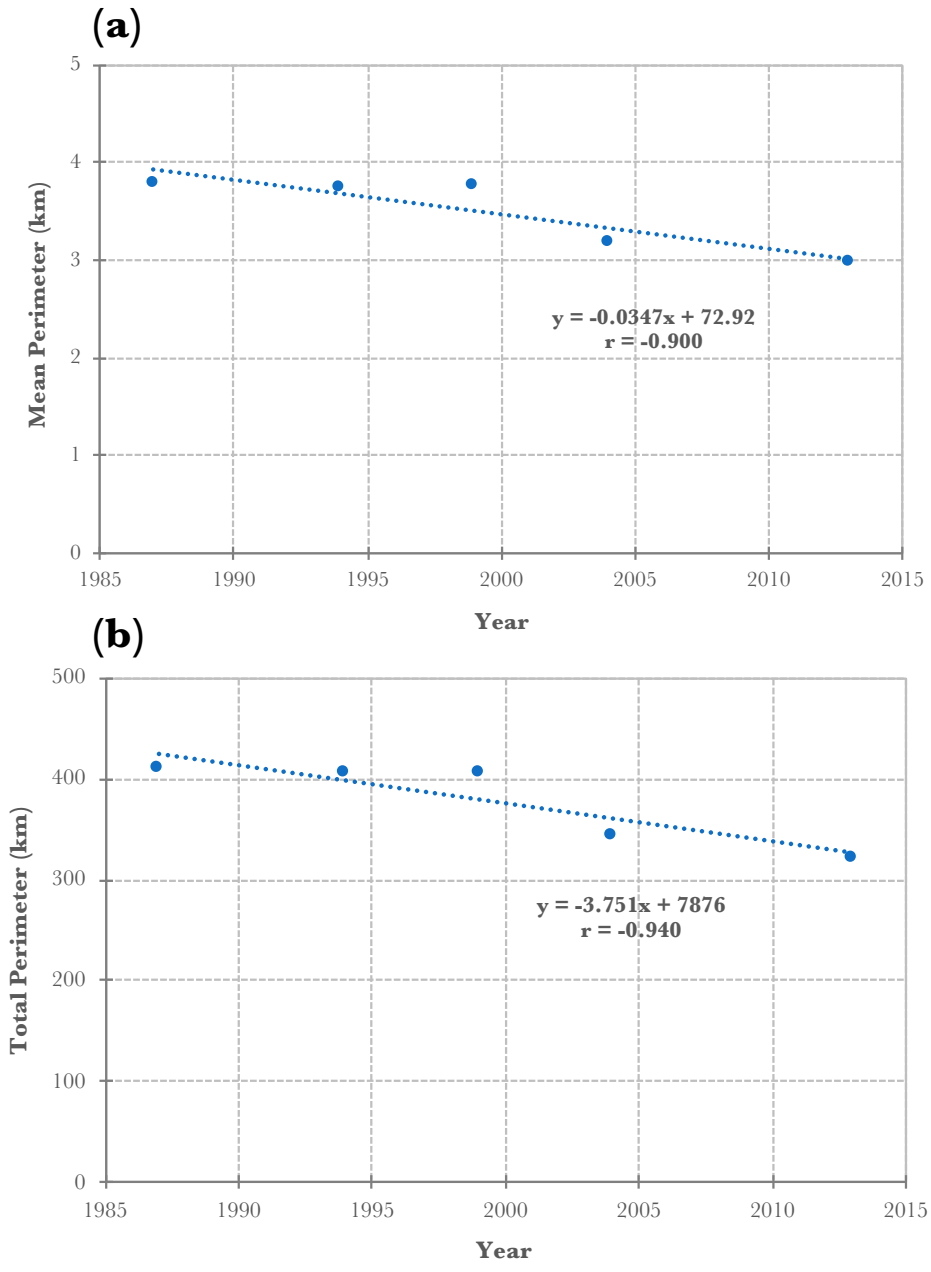

Figure 4.6. Trend of mean (a) and total (b) glacier perimeter from 1987 to 2013 (n=108).

4.4 Glacier Change from 1987 to 2017

Area changes are summarised for 1987-2017, 1987-1994, 1994-1999, 1999-2004, 2004-2013, and 2013-2017 (Table 4.3). The sample of 74 glacier units from the 1987 image covers a total area of 52.8 ± 1.32 km^2 with a mean glacier area of 0.70 ± 0.02 km^2. The sample of glaciers for 1987-2017 have a similar trend over the time periods as the 1987-2013 glacier sample. Glacier area decreased by 4.73 ± 0.38% from 1987 to 1994, 14.6 ± 1.17% from 1994 to 1999, 16.3 ± 0.82% from 1999 to 2004, 12.2 ± 0.61% from 2004 to 2013, and 21.2 ± 1.05% from 2013 to 2017. Over the total period of 1987 to 2017, glacier area decreased from 52.8 ± 1.32 km^2 to 24.9 ± 0.62 km^2, representing a loss of 52.9 ± 2.65% or 27.9 ± 1.40 km^2, with an area reduction rate of 1.76% · a^{-1} and an absolute area reduction rate of 0.93 $km^2 \cdot a^{-1}$.

The period from 2013 to 2017 had the greatest relative change in area (-21.2 ± 1.05%), even though it was the shortest period. However, it did not have the largest absolute change compared to other time periods (Table 4.3). The 1999-2004 and 1994-1999 periods had the next greatest change. Similar to the 1987-2013 period, the 0.1 $km^2 < A < 0.5$ km^2 size class for the 1987-2017 period had the greatest relative change in area, but the absolute change was lower than the $A >$ 1.0 km^2 size class that had the greatest absolute loss. Figure 4.7 shows the temporal evolution of glacier area from 1987 to 2017 over the study area. In comparison with the 1987-2013 sample period, the results of the hypothesis testing of the slope of the line show a statistically significant linear relationship (p=0.001) of decreasing mean glacier area over time. Decreasing total glacier area over time was also found to have a statistically significant linear relationship (p=0.000). Similar to the 1987-2013 sample period, the results of extrapolating total area per year for the 1987-2017 sample period predict that the study area glaciers will lose all area by 2044.

Table 4.3. Change in area (A) of glaciers from 1987 to 2017 (n=74).

Area Size Class (km^2)	**1987**			**1994**			**1999**			**2004**			**2013**			**2017**		
	n	A Sum	A Mean	n	A Sum	A Mean	n	A Sum	A Mean	n	A Sum	A Mean	n	A Sum	A Mean	n	A Sum	A Mean
$A < 0.05$	0	0	0	2	0.04	0.04	3	0.08	0.03	8	0.18	0.02	10	0.23	0.02	21	0.44	0.02
$0.05 < A < 0.1$	1	0.06	0.06	2	0.18	0.08	3	0.21	0.07	7	0.54	0.08	11	0.82	0.07	7	0.54	0.08
$0.1 < A < 0.5$	38	10.4	0.27	37	10.3	0.21	41	10.4	0.25	39	10.0	0.26	36	9.22	0.26	33	7.85	0.24
$0.5 < A < 1.0$	20	13.5	0.67	19	13.1	0.69	16	10.9	0.68	10	18.5	0.69	8	5.52	0.69	7	5.37	0.77
$A > 1.0$	15	28.9	1.92	14	26.6	1.90	11	21.4	1.94	10	18.5	1.85	9	15.8	1.76	6	10.7	1.78
Total	74	52.8±1.32	0.70±0.02	74	50.3±2.77	0.68±0.04	74	42.7±1.07	0.58±0.01	74	36.0±0.90	0.49±0.01	74	31.6±0.79	0.43±0.01	74	24.9±0.62	0.34±0.01
Area Size Class (km^2)	**1987-2017**			**1987-1994**			**1994-1999**			**1999-2004**			**2004-2013**			**2013-2017**		
	n	A (km^2)	A (%)	n	A (km^2)	A (%)	n	A (km^2)	A (%)	n	A (km^2)	A (%)	n	A (km^2)	A (%)	n	A (km^2)	A (%)
$A < 0.05$	0	*n/a*	*n/a*	0	*n/a*	*n/a*	2	-0.01	-23.4	3	-0.05	-100	8	-0.01	-7.27	10	-0.14	-60.6
$0.05 < A < 0.1$	1	-0.06	-100	1	-0.01	-25.7	2	-0.07	-39.7	3	-0.09	-425	7	-0.13	-25.0	11	-0.42	-51.7
$0.1 < A < 0.5$	38	-7.67	-73.9	38	-0.82	-7.89	37	-2.33	-22.6	41	-2.72	-26.2	39	-1.56	-15.5	36	-2.48	-26.9
$0.5 < A < 1.0$	20	-7.61	-56.5	20	-0.14	-1.06	19	-2.42	-18.4	16	-2.18	-20.0	10	-0.98	-14.4	8	-1.20	-21.9
$A > 1.0$	15	-12.6	-43.5	15	-1.52	-5.26	14	-2.49	-9.4	11	-1.94	-9.08	10	-1.70	-9.23	9	-2.45	-15.5
Total	74	-27.9±1.40	-52.9±2.65	74	-2.49±0.20	-4.73±0.38	74	-7.33±0.59	-14.6±1.17	74	-6.98±0.35	-16.3±0.82	74	-4.39±0.22	-12.2±0.61	74	-6.71±0.34	-21.2±1.06

Table 4.4. Change in perimeter (*P*) of glaciers from 1987 to 2017 (*n*=74).

Area Size Class (km²)	**1987**			**1994**			**1999**			**2004**			**2013**			**2017**		
	n	*P* Sum	*P* Mean	*n*	*P* Sum	*P* Mean	*n*	*P* Sum	*P* Mean	*n*	*P* Sum	*P* Mean	*n*	*P* Sum	*P* Mean	*n*	*P* Sum	*P* Mean
$A < 0.05$	0	0	0	2	0.85	0.43	3	1.67	0.56	8	5.40	0.67	10	7.21	0.72	21	14.7	0.73
$0.05 < A < 0.1$	1	1.00	1.00	2	2.83	1.42	3	4.29	1.43	7	9.47	1.35	11	14.4	1.31	7	13.9	1.98
$0.1 < A < 0.5$	38	99.8	2.63	37	101	2.74	41	114	2.78	39	107	2.75	36	103	2.87	33	92.1	2.79
$0.5 < A < 1.0$	20	85.4	4.27	19	84.8	4.46	16	81.5	5.09	10	49.9	4.99	8	39.2	4.90	7	39.1	5.59
$A > 1.0$	15	110	7.36	14	104	7.43	11	92.8	8.44	10	79.0	7.89	9	69.8	7.75	6	48.1	8.01
Total	74	297±7.43	4.01±0.10	74	294±14.7	3.97±0.20	74	294±7.35	3.98±0.10	74	251±6.28	3.39±0.08	74	234±5.85	3.16±0.08	74	208±5.20	2.81±0.07
Area Size Class (km²)	**1987-2017**			**1987-1994**			**1994-1999**			**1999-2004**			**2004-2013**			**2013-2017**		
	n	*P* (km²)	*P* (%)	*n*	*P* (km²)	*P* (%)	*n*	*P* (km²)	*P* (%)	*n*	*P* (km²)	*P* (%)	*n*	*P* (km²)	*P* (%)	*n*	*P* (km²)	*P* (%)
$A < 0.05$	0	*n/a*	*n/a*	0	*n/a*	*n/a*	2	-0.15	-17.1	3	-0.93	-55.7	8	-0.24	-4.36	10	-2.84	-39.4
$0.05 < A < 0.1$	1	-1.00	-100	1	-0.15	-14.9	2	-0.73	-25.6	3	-1.62	-37.8	7	-1.45	-15.34	11	-4.23	-29.5
$0.1 < A < 0.5$	38	-42.5	-42.6	38	-3.00	-3.01	37	-6.47	-6.39	41	-21.6	-18.9	39	-7.04	-6.55	36	-14.5	-14.0
$0.5 < A < 1.0$	20	-18.8	-22.0	20	1.55	1.81	19	-0.81	-0.96	16	-11.62	-14.3	10	-5.53	-11.09	8	-2.61	-6.66
$A > 1.0$	15	-16.9	-15.3	15	-1.29	-1.17	14	8.94	8.60	11	-7.60	-8.19	10	-3.02	-3.82	9	-1.83	-2.62
Total	74	-79.2±3.96	-26.7±1.34	74	-2.90±0.23	-0.98±0.08	74	0.79±0.06	0.27±0.02	74	-43.4±2.17	-14.7±0.74	74	-17.3±0.87	-6.88±0.34	74	-16.4±0.82	-7.03±0.35

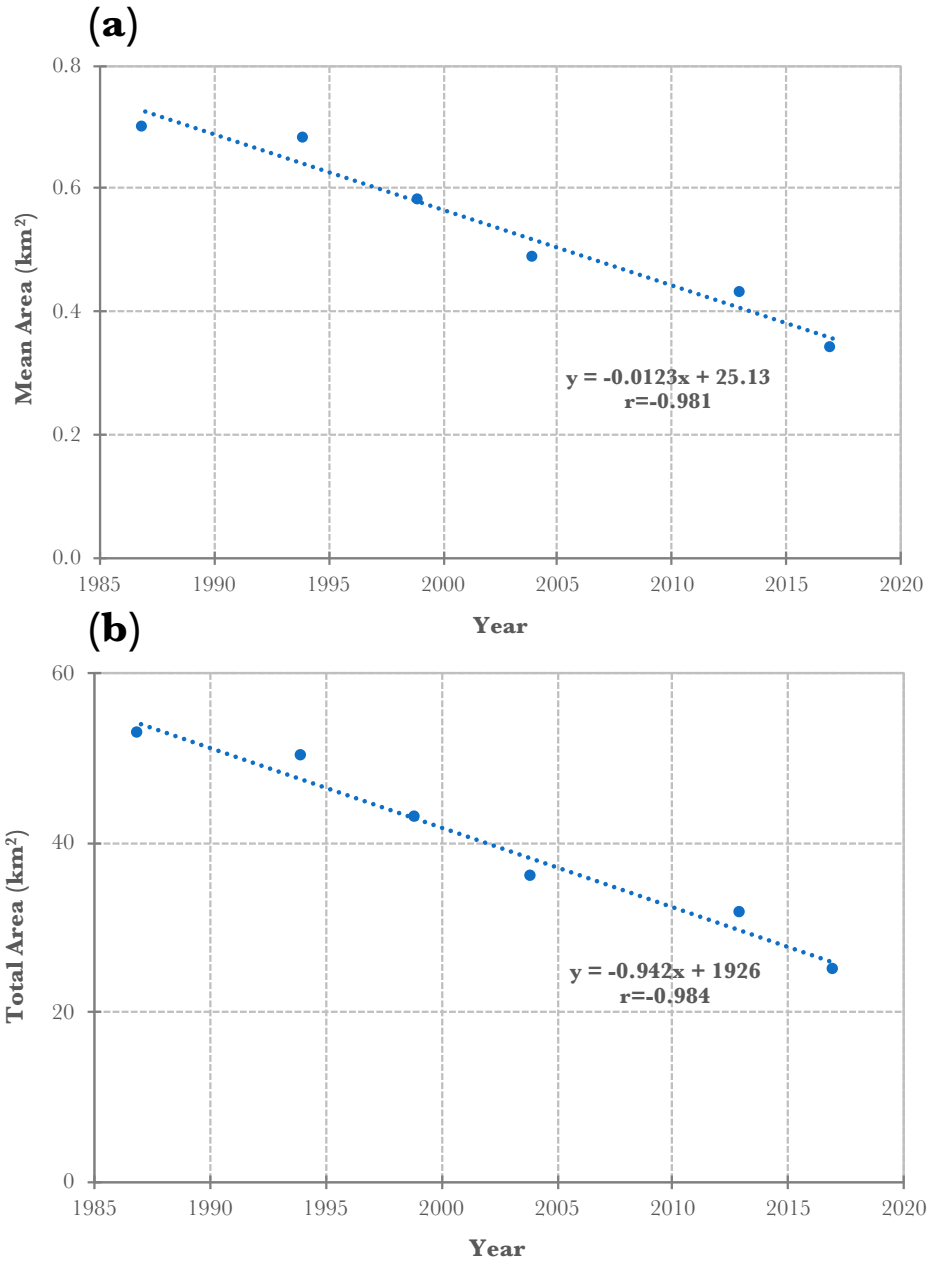

Figure 4.7. Trend of mean (a) and total (b) glacier area from 1987 to 2017 (*n*=74).

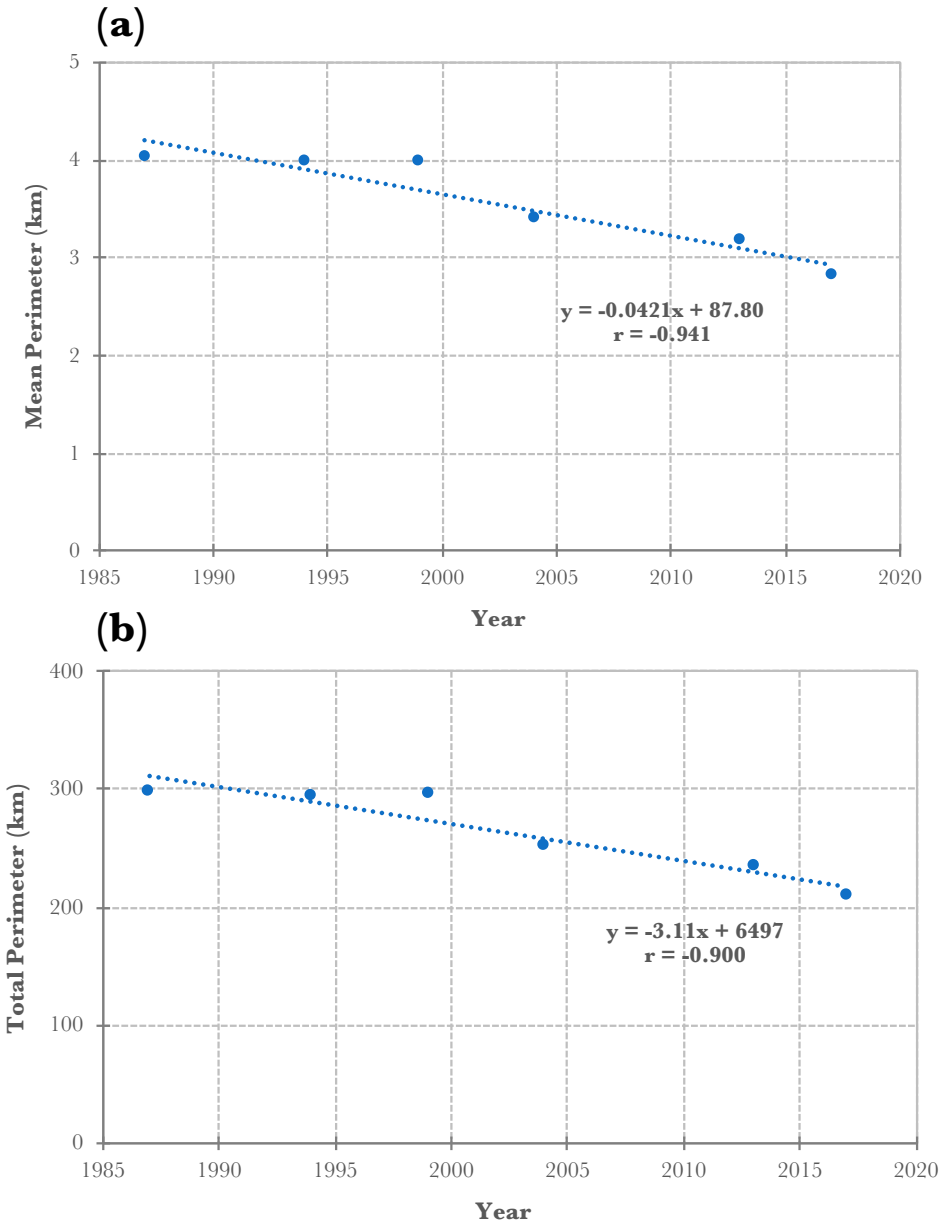

Figure 4.8. Trend of mean (a) and total (b) glacier perimeter from 1987 to 2017 (*n*=74).

The change in perimeter length is summarised for 1987-2013, 1987-1994, 1994-1999, 1999-2004, 2004-2013, and 2013-2017 (Table 4.4). For the sample of 74 glaciers, the total change in perimeter length was 297 ± 7.43 km in 1987 to 208 ± 5.20 km in 2017, which represents a loss of

79.2 ± 3.96 km or 26.7 ± 1.34%. Perimeter length decreased for all time periods except for 1994 to 1999, where glacier perimeter length increased by 0.27 ± 0.02%. The time period with the greatest loss in perimeter was from 1999 to 2004. Glacier perimeter length decreased by 0.98 ± 0.08% from 1987 to 1994, 14.7±0.74% from 1999 to 2004, 6.88 ± 0.34% from 2004 to 2013, and 7.03 ± 0.35% from 2013 to 2017. Figure 4.8 shows the temporal evolution of glacier perimeter length from 1987 to 2017 over the study area. The results of the hypothesis testing of the slope of the line show a statistically significant linear relationship (p=0.003) of decreasing mean glacier perimeter length over time. The results also show a statistically significant linear relationship (p=0.003) of decreasing total glacier perimeter length over time.

Overall, each of the trend analyses (Figures 4.5-4.8), total and mean area and total and mean perimeter have a consistently decreasing trend. The trend of total glacier area for 1987-2017 have the most well-fitted data points to the regression line with r=-0.984 (Figure 4.7b). The data points of the other trends are also well-fitted to the regression line with a high r no less than 0.900.

4.5 Perimeter – Area Relationship

The time period with the greatest loss of perimeter length was from 1999 to 2004, which was also the time period with the greatest relative change in area. In general, as the area decreased, the perimeter length also decreased (Figure 4.9) from 1987 to 2013 with a strong correlation for mean perimeter and area per year (r=0.930) and total perimeter and area per year (r=0.926). There was also a general decrease in area and perimeter from 1987 to 2017, in which there was a strong correlation for mean perimeter and area per year (r=0.961), as well as total perimeter and area per year (r=0.958). Figure 4.10 displays the relationship of the perimeter-area ratio and the size of the glacier for the initial year of 1987. Glaciers of a smaller area size have a larger perimeter-area

ratio, with the largest perimeter-area ratio of glaciers with an area less than 0.5 km^2. The perimeter-area ratio of glaciers becomes consistent in value with an area greater than 1.0 km^2.

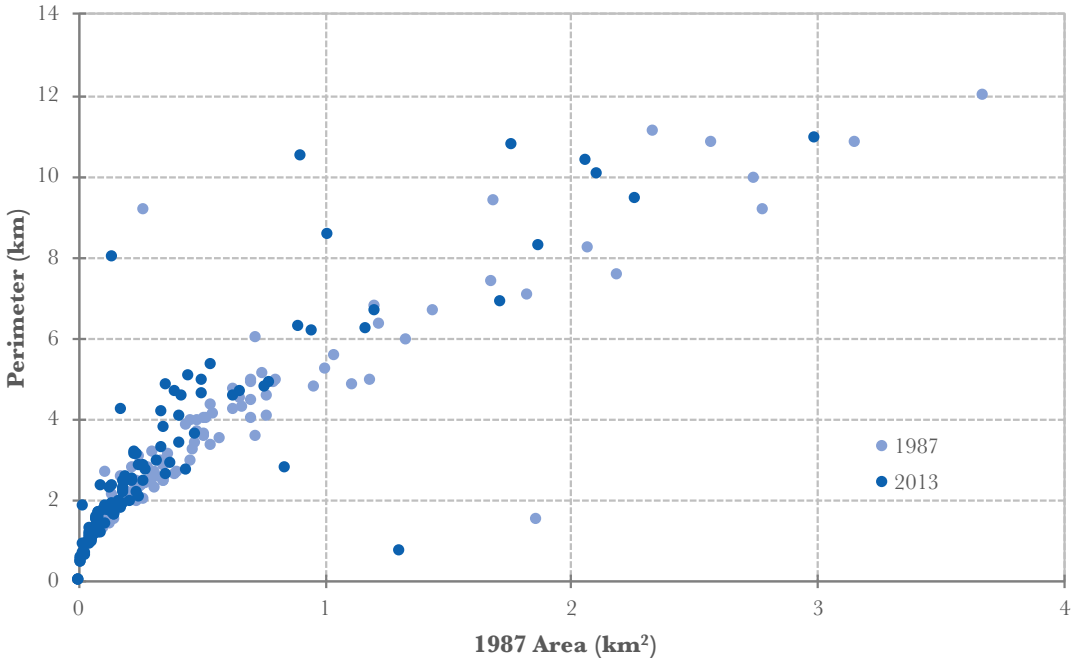

Figure 4.9. Glacier area and perimeter relationship, 1987 and 2013 (*n*=108).

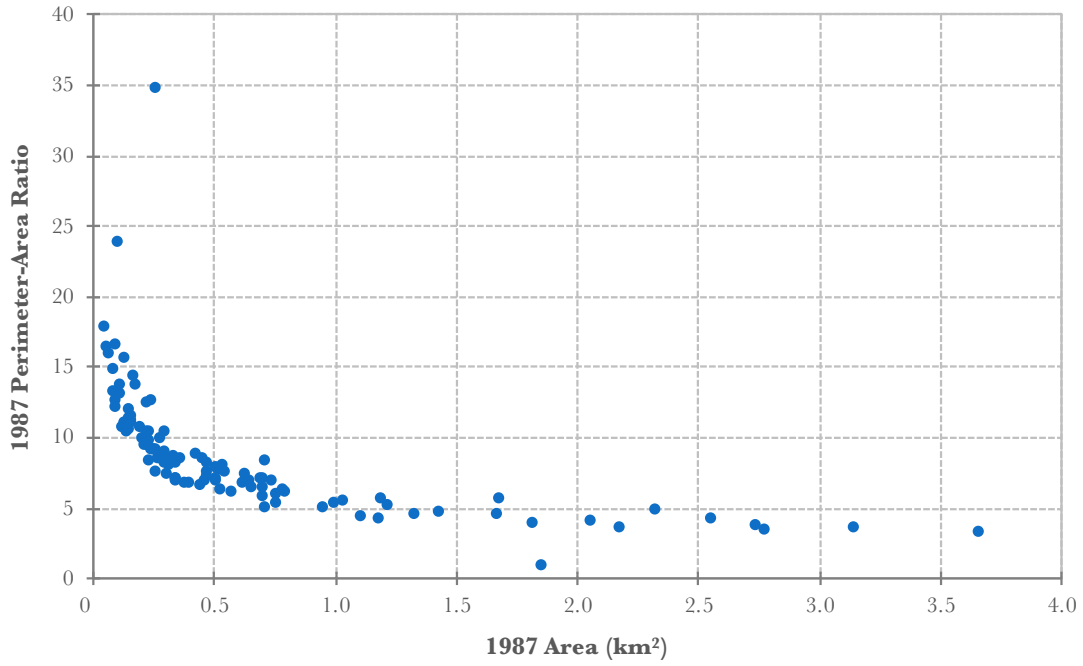

Figure 4.10. 1987 perimeter-area ratio versus glacier area (*n*=108).

CHAPTER 5

Discussion

The goal of this thesis was to map the changes in extent of glaciers in the northern Mackenzie Mountains of Yukon and Northwest Territories by analysing Landsat satellite images, to determine whether there is a trend in glacier extents from 1987 to 2013/2017. This discussion illustrates how and why the Red/SWIR band ratio was chosen for this study area in preference over the NIR/SWIR band ratio and the NDSI to derive glacier outlines. The discussion also focuses on confusion that arose in mapping glaciers caused by snow cover and other issues of uncertainty that were considered when estimating the error of area and perimeter length values. The glacier change results are considered in relation to area size classes as to whether glacier size was important in how they changed. Finally, the glacier change reduction rates were compared to values reported for other glaciers located near the study area such as in Yukon, Alaska, and Northwest Territories, and were compared to values reported by glacier studies elsewhere in the world.

5.1 Selection of Band Ratio for Image Thresholding

In comparing the Red/SWIR and NIR/SWIR ratio binary images (Figure 5.1a), the NIR/SWIR ratio did not map debris-covered glaciers well because debris-covered ice areas are not distinguished well from the surrounding bedrock due to the spectral similarity of these surfaces. The Red/SWIR was more suitable for distinguishing debris-covered ice than the NIR/SWIR ratio and better at mapping glaciers in shadowed areas. In regions with deep shadows, the

Red/SWIR ratio has been applied successfully at the expense of misclassification of most water bodies because the recorded ratio of reflection of water bodies is similar to snow and ice (Paul and Hendriks, 2010a; Bolch et al., 2010). The NIR/SWIR ratio was also found to be problematic for the 2017 image. The glaciers could not be fully mapped without all the clouds mapped as well, whereas the Red/SWIR ratio mapped considerably smaller areas of clouds while sufficiently mapping the glacier outlines. Although the Red/SWIR ratio misclassifies water bodies as ice, these can be easily deleted whereas debris-covered areas not included by the NIR/SWIR ratio would require manual digitisation. Therefore, the Red/SWIR ratio was found to be more effective at mapping the glaciers for the study area than the NIR/SWIR ratio.

The NDSI mapped more debris-covered areas than the other band ratios (Figure 5.1b). In general, both the NDSI and Red/SWIR ratio produced reasonable results, and by adjusting the threshold value, the glacier outlines could have been derived from either. The study area glaciers had little debris-covered glaciers, mostly in the later years, making it easier to apply such thresholded images to the Landsat scenes. The NDSI, however, mapped areas that could not be distinguished as a debris-covered glacier or as simply dirty snow patches or other surfaces. As with the Red/SWIR ratio, the NDSI cannot discern water bodies from clean ice because of the similar NDSI values between the two surfaces (Durán-Alarcón et al., 2015).

Each image required a unique threshold value ranging from 1.4 to 7 for Red/SWIR, 1.6 and 7 for NIR/SWIR, and 0.4 to 0.8 for the NDSI. Although a range of thresholds are commonly used in the literature (0.35 to 0.55 for NDSI and ~2 for both Red/SWIR and NIR/SWIR), different threshold values required for this study area for each scene varied for each image when tested.

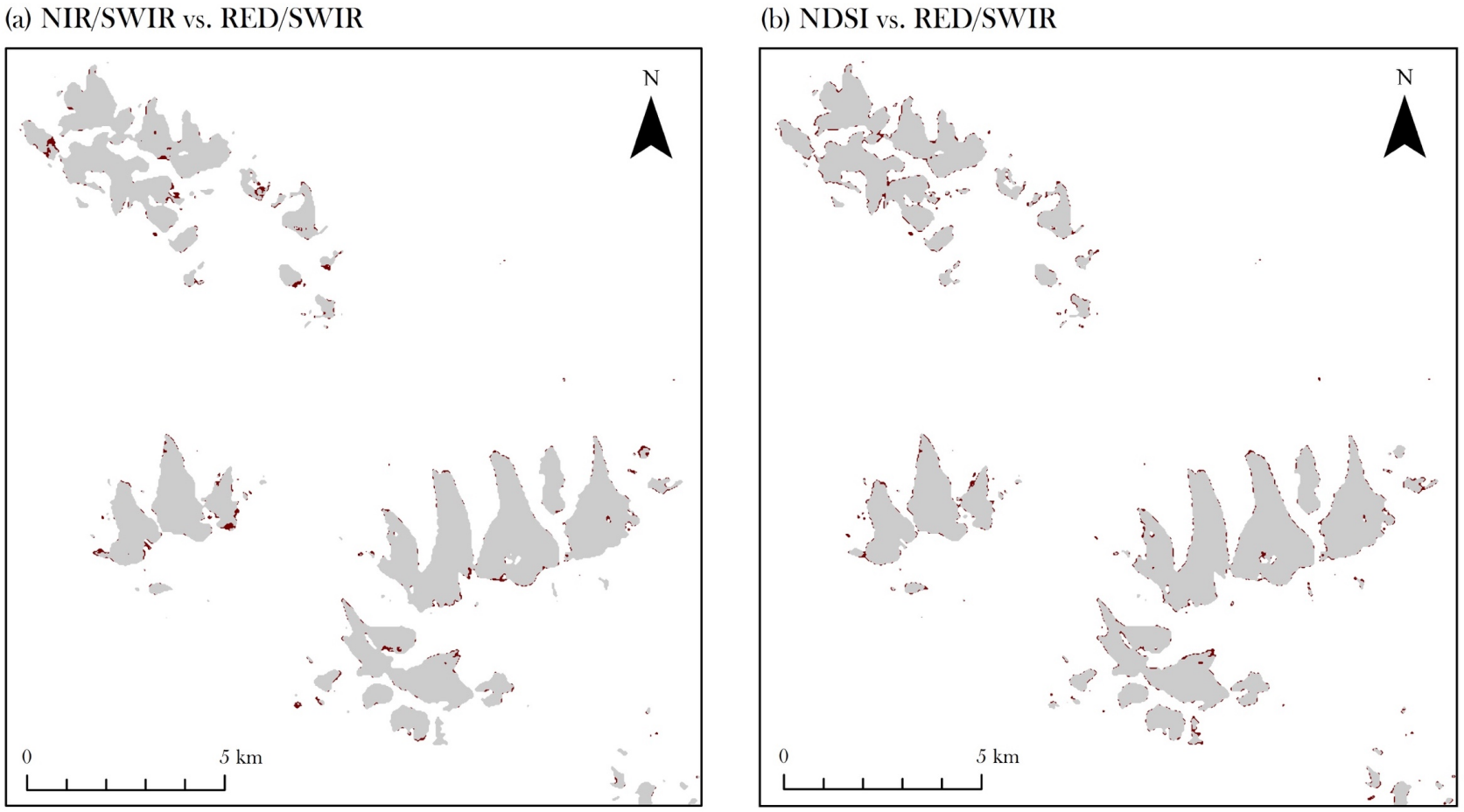

Figure 5.1. Comparison of a sample of glacier polygons from the 1987 image prior to manual editing. a) Polygons derived from NIR/SWIR (grey) overlying Red/SWIR (red). b) Polygons derived from Red/SWIR (grey) overlying NDSI (grey).

Similar semi-automated methods were employed by Bolch et al. (2010) using the Red/SWIR to map the glaciers of British Columbia and Alberta, as well as by Racoviteanu et al. (2008) illustrating the use of the NDSI in the Cordillera Blanca, Peru. These studies emphasised the necessity of choosing a threshold value manually depending on each Landsat scene characteristics (e.g., haze, clouds, topography, and snow cover).

Unlike a threshold value of ~2 for the Red/SWIR ratio that has been used in previous studies (e.g., Chand and Sharma, 2015, Bolch et al., 2010, Andreassen et al., 2008), the threshold values varied for each image in the present study. For instance, while a threshold value of 1.7 was used for one image, a value of 7 was used for another. In a study by Liu et al. (2013), the authors found that when a Red/SWIR threshold value was defined as greater than 5 for Landsat 4 and 5 images, the glacier boundaries could be appropriately identified and delineated. As shown in Figure 5.2, in comparison with a threshold value of 2 and 7, the threshold value of 2 overestimated the area of glacier ice. A threshold value of 2 also mapped more water bodies, which is represented by dot line-circled areas in Figure 5.2a. Although the higher threshold of 7 did not map water bodies and more closely matched the glacier perimeter, it also did not map as much darker or shadowed areas (full line-circled area in Figure 5.2a, which corresponds to the full line-circled area in Figure 5.2b).

Although the semi-automated approach of the thresholded Red/SWIR band ratio is an efficient method to delineate glacier outlines, manual corrections were still required for lakes, shadows, and seasonal snow patches. There was no threshold value for either band ratio that would map outlines well enough for corrections to not be required. If values were higher than that chosen for an image, there would be more areas mapped that were not glaciers (i.e., water bodies and snow

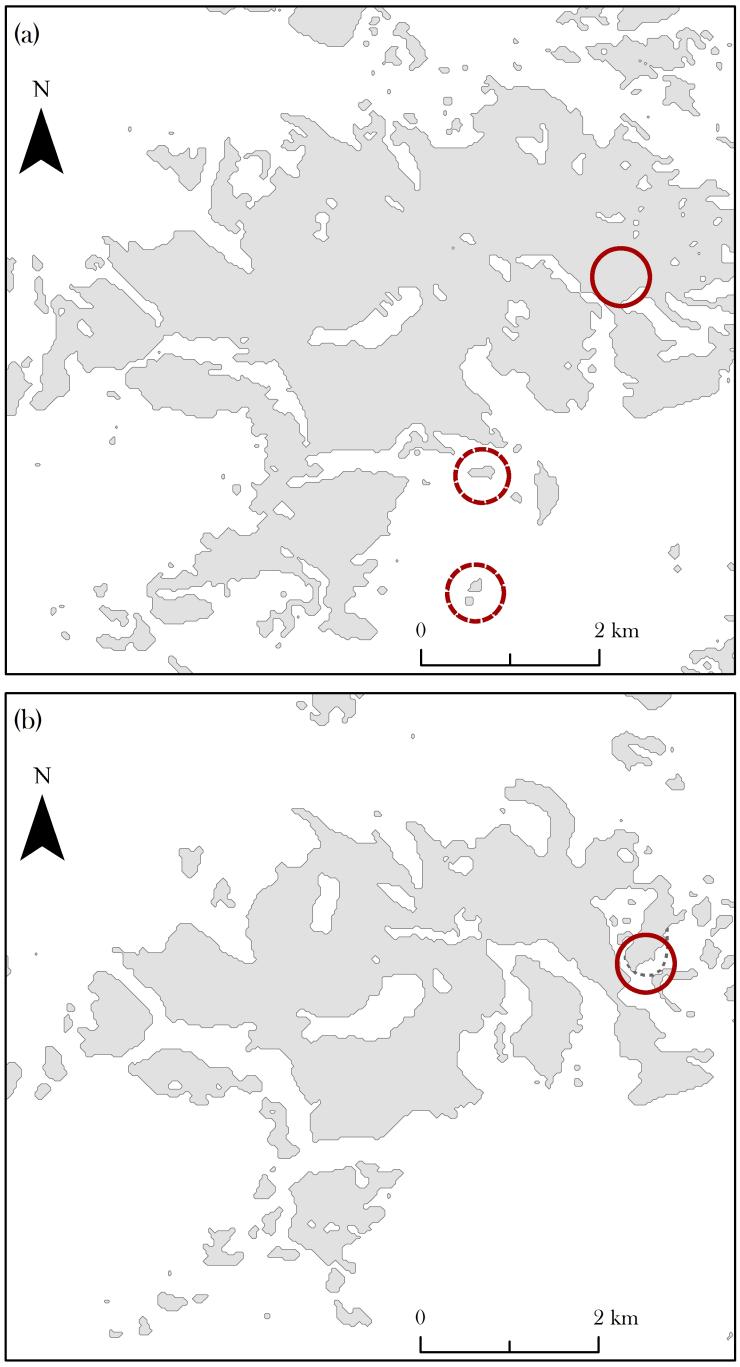

Figure 5.2. Example glacier outlines of binary images from a portion of the unedited 1994 Landsat scene. (a) Glacier outlines derived using a threshold value of 2 suggested by previous studies mentioned in the text. (b) Glacier outlines derived using a threshold value of 7 in this study. Red dot line-circles encompassing mapped water bodies. Red full line-circles showing mapped (a) and unmapped (b) glacier in shadowed area.

patches) or if values were lower, there would not be enough of the glacier boundary mapped. A compromise had to be made so that there was enough glacier area mapped to limit corrections on the glacier boundary and that there were not too many misclassified polygons to delete. In Figure 5.3, a section of a non-altered binary image is overlain by a binary image with corrections made for comparison. All polygons were inspected to see how well the outlines matched the glacier perimeter, with some polygons needing to be deleted and outlines edited, such as splitting polygons.

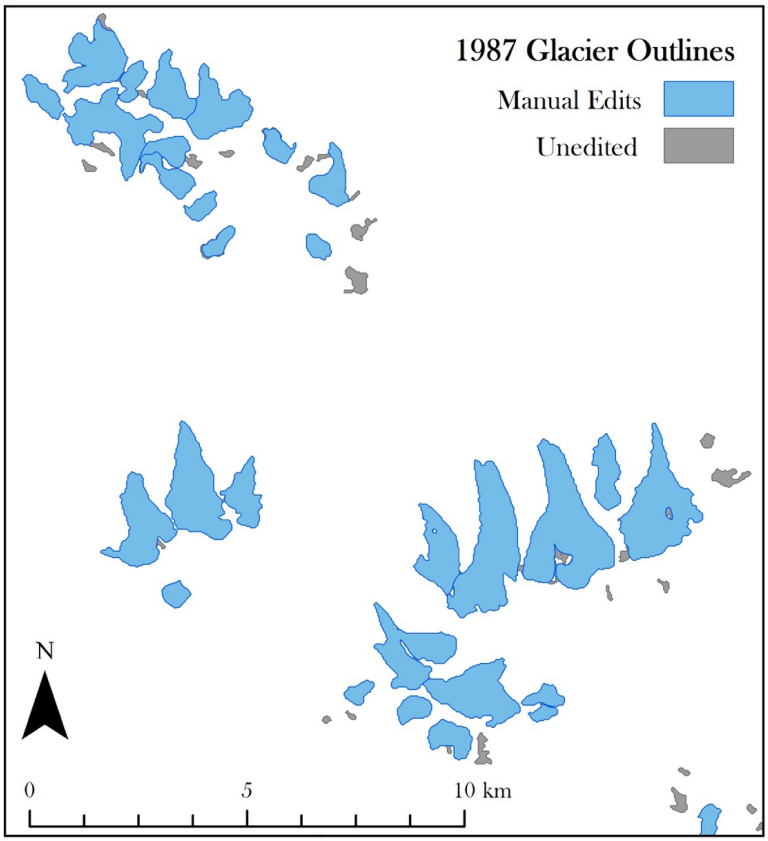

Figure 5.3. Example glacier outlines of a manually edited binary image overlying an unedited binary image.

5.2 Confusion in Glacier Mapping due to Snow Cover

In each of the individual images, there were many glaciers that underwent increases in area change (refer to Appendix: Individual Glacier Area and Perimeter Values). This was particularly the case between 1987 and 1994 and between 1994 and 1999, but as well for other time intervals. This was generally the case for smaller glaciers ($A < 0.1$ km^2), but there were also a few occurrences in larger area size classes. In some cases, this may have been due to the misclassification of snowfields as glaciers, especially in the 1994 image (Figure 5.4) in which there were numerous small patches of snow present. Even though the Landsat images were selected from the summer season to limit the possibility of snow cover, there was a greater amount of snow cover in 1994 than all the other years studied.

The presence of snowfields made it difficult to distinguish the glacier area from snow, possibly resulting in larger areas than the previous image of 1987. Comparing the 1987 image, as well as the other images, to the 1994 image, aided in distinguishing snow patches from actual glaciers that were not present in these other images. As well, further inspection of the changing geometry of the snow patches versus glaciers between image years helped with estimating the glacial boundaries (Figure 5.5). Even though using the Red/SWIR ratio assisted in distinguishing some snow cover from glacier ice, the outlines created from the Red/SWIR ratio image required further visual inspection for manual corrections because snow was sometimes outlined as glaciers (Figure 5.6). However, the positive area changes did not alter the overall negative trend in glacier area change over either of the time periods, and also did not result in any overall increases in area observed per size class.

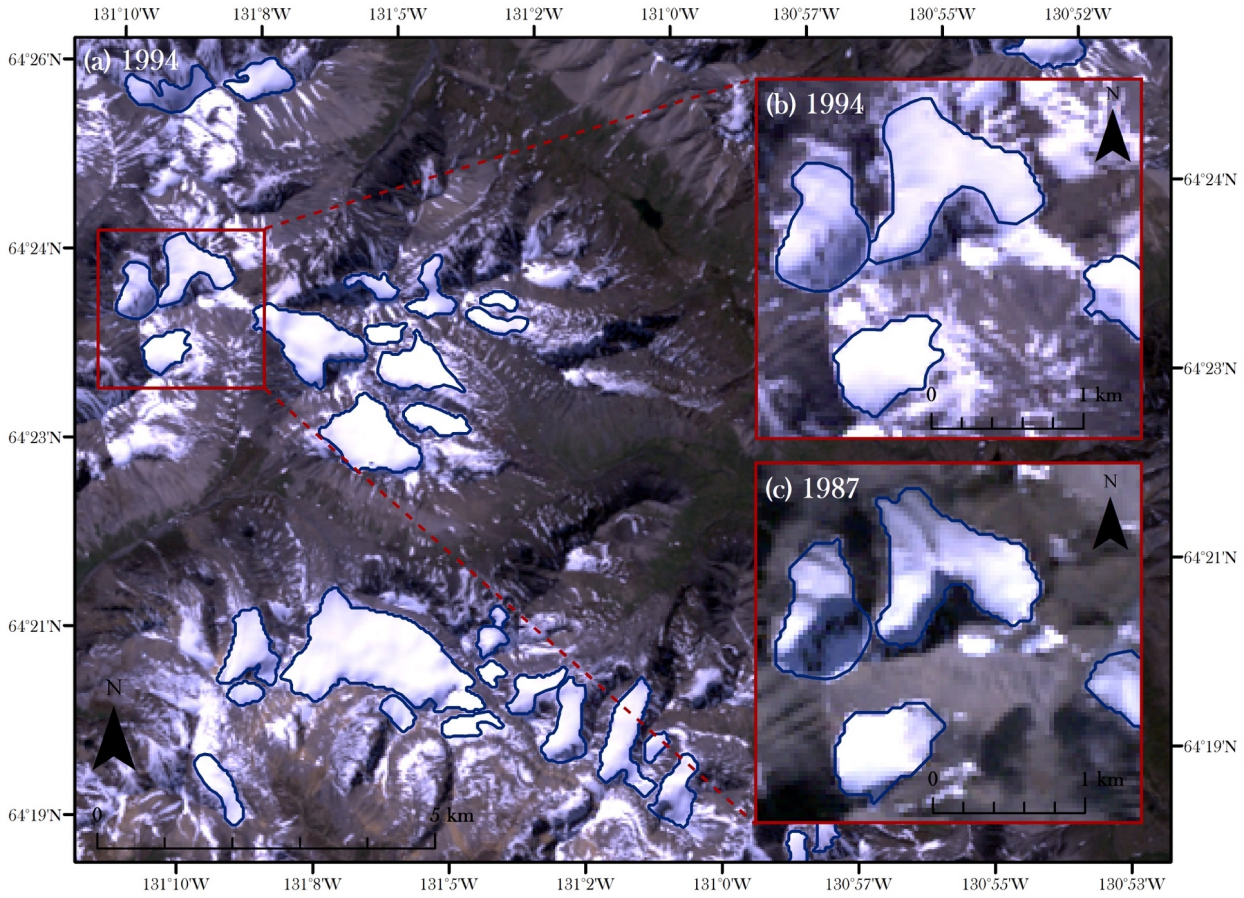

Figure 5.4. Example of a problematic case of distinguishing glacier area from snowfields. (a) A portion of the 1994 Landsat scene. (b) Close up of glaciers in the 1994 Landsat scene. (c) Close up of glaciers in the 1987 Landsat scene. Areas mapped as glaciers are outlined.

5.3 Error Estimation

Seasonal snow, as described earlier, introduced errors in the area determination of small glaciers, but there were negligible errors from clouds and shadows. Errors in the glacier outlines occurred in all images, but glacier extent was estimated to have a greater error in the 1994 image due to seasonal snow. The uncertainty is greatest where late-lying seasonal snow obscures the location of the ice margin or may have been misinterpreted as glacier ice. To avoid misclassification of snow patches, measures were taken to compare the images from each of the years to visualise how the geometry of the glacier changes and to detect crevasses or bare ice if visible (Figure 5.5). Images

were also selected to avoid seasonal snow when possible and was only an issue with the 1994 image.

Small calculated glacier area changes may in part be due to differences in methods and interpretation instead of actual area changes. There are various human interpretations that can influence the calculated area, by overestimating or underestimating the values, including decisions of what polygons are actually water bodies, distinguishing seasonal snow cover from

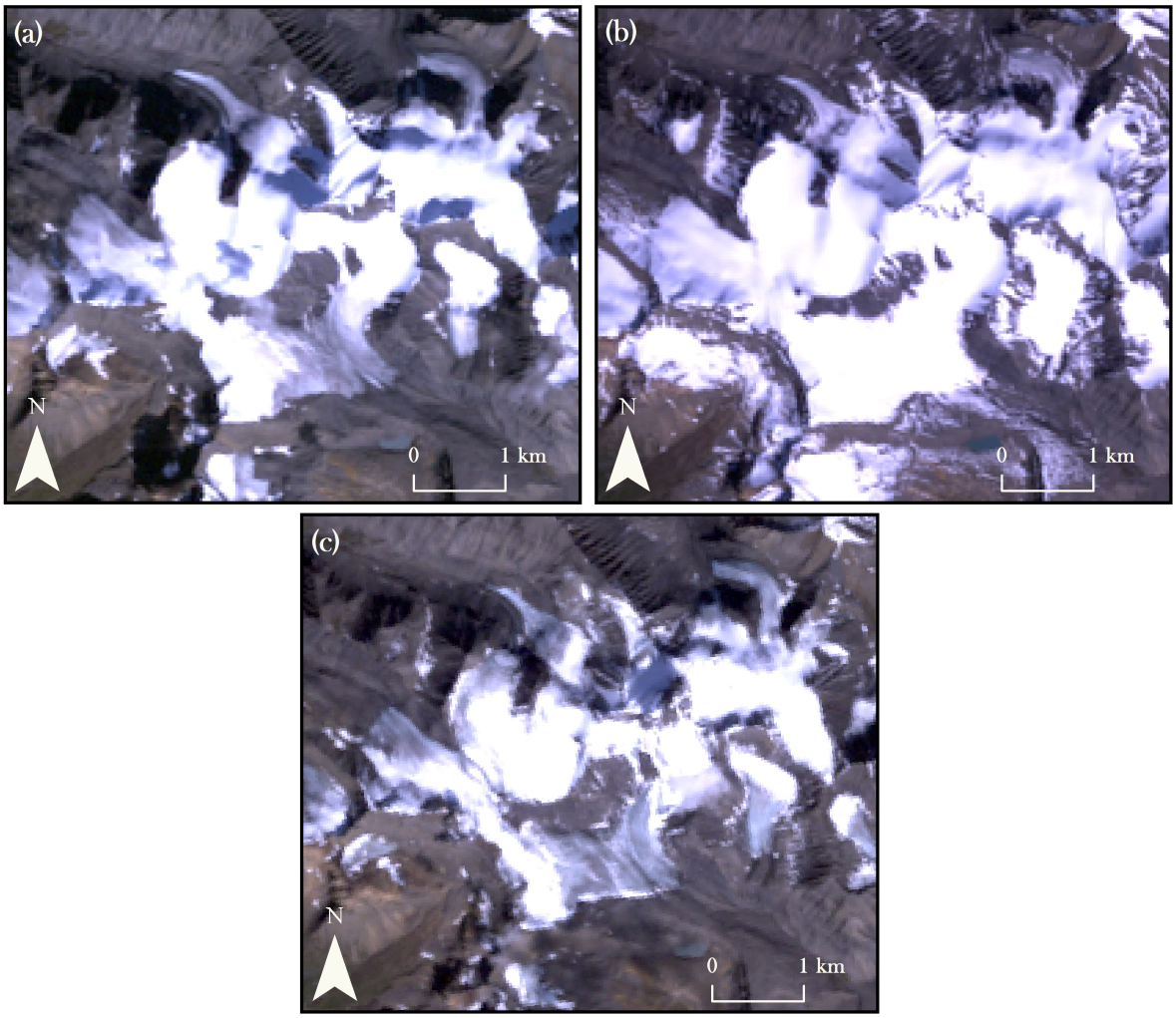

Figure 5.5. Change in snow and ice geometry of a small cluster of glaciers for 1987 (a), 1994 (b), and 1999 (c).

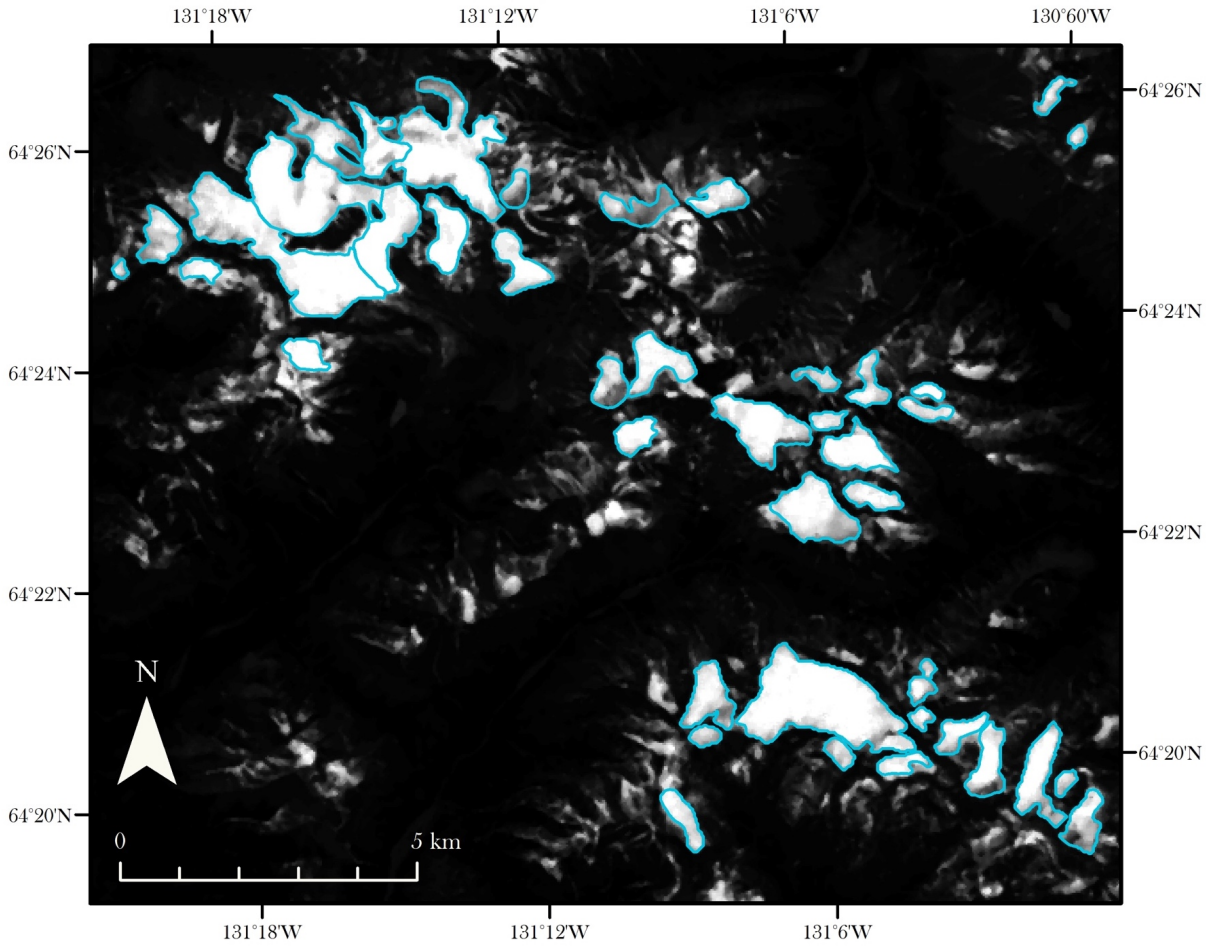

Figure 5.6. Example of glacier outlines overlying a thresholded Red/SWIR band ratio image from the 1994 Landsat image. Glaciers outlined in blue.

perennial snow cover, and identifying the margins of debris-covered glaciers. This results in a subjective selection process of recognising area as a glacier, which influences the absolute and relative change values calculated, producing uncertainty in the mapped glacier outlines (Andreassen et al., 2008).

The pixel size of the image can have an important influence on the digitisation of glacier outlines. With a pixel size of only 30m, the small details in Landsat images may have been more difficult to interpret than in higher resolution images. Gardent et al. (2014), who mapped the extent of

glaciers in the French Alps, found that uncertainty relative to glacier size is mainly linked with differences in spatial resolution. The lower resolution of Landsat satellite images creates difficulty in identifying ice flow or separating perennial snow from seasonal ice, glaciers, or ice remnants (Andreassen et al., 2008). Identifying ice flow margins of glaciers in the present study was difficult for certain glaciers, especially when there was greater seasonal snow (note Figure 5.5b compared to 5.5a and 5.5c). Aerial images, for example, generally have a higher resolution at a decametric level than satellite images at a metric level. However, the price for aerial images may be high and there may be poor availability of these images. It is for this reason that satellite images, such as Landsat images, are more commonly used for analysing glacier change (Liu et al., 2013).

With such small glaciers, the pixel size limits the ability to map the glaciers under a certain size. Glaciers under 0.02 km^2 were difficult to be distinguished as a glacier unless compared with the other image years. A smaller pixel size has been reported to improve the accuracy of mapping glacier outlines. When mapping recent glacier change in the Cordillera Real, Liu et al. (2013) found that Landsat images with a 30-m resolution produced unclear glacier boundaries from thresholding ratio images. As compared to the Landsat images, Advanced Land Observing Satellite images with a 10-m resolution, which were used as a reference for defining glacier boundaries derived from Landsat images, provided more well-defined boundaries. Chand and Sharma (2015) noted that the higher resolution images from the Corona satellite provided more consistent results than topographic maps and coarse resolution satellite datasets.

The pixel size determines the amount of glacier ice that is mapped within a pixel using a thresholded band ratio method. Since glaciers may have slight debris-covered surfaces along their

perimeter, this area could be excluded from the mapped glacier outlines. According to Paul et al. (2017) who found this to be true, mapping with a higher resolution will exclude such areas because the proportion of non-ice cover within a smaller pixel is higher. As explained by Paul et al. (2017), a 30-m pixel as compared to a 10-m pixel may be mapped as clean glacier ice if more than half of its area is ice, which results in larger glacier extents mapped by lower resolution satellite sensors.

Area changes may also be detected mistakenly by the formation or ablation of ice around the glacier perimeter, resulting in area variations between years (Hoffmann et al., 2007). As noted by Schmidt and Nüsser (2012), these effects can increase with an increasing perimeter-area ratio. Thus, this may have resulted in greater uncertainty of mapping smaller glaciers where there were greater perimeter-area ratios for the smaller glaciers. Although the area of these small glaciers may have greater uncertainty than larger glaciers, they are important to analyse because of their assumed direct response to climate change (Paul et al., 2009).

5.4 Glacier Change

The present study observed significant loss in glacier area since 1987 in the northern Mackenzie Mountain Range. A comparison of the calculated relative changes in area for the study area revealed that the glacier area has declined over the periods analysed (Tables 4.1, 4.3 and Figure 5.7). The sample of 108 glaciers from 1987-2013 shows decreasing rates for each of the four periods and the sample of 74 glaciers from 1987-2017 shows decreasing rates for the five periods. The relative change in area for the 2013-2017 time period had almost halved from the 2004-2013 time period, which also represented the largest change in area for the time periods. Although there were many glaciers that were not mapped due to cloud cover, the relative change of the

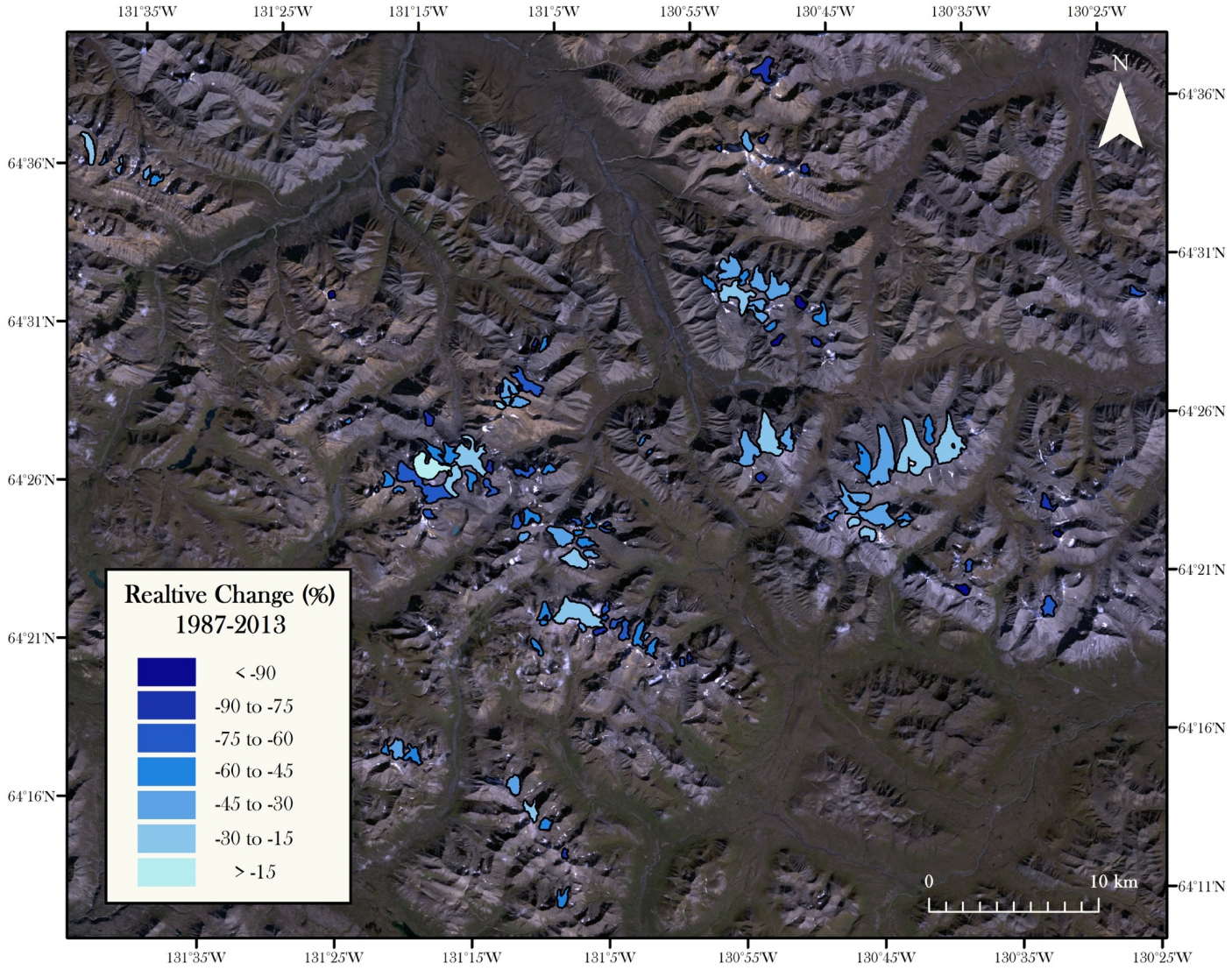

Figure 5.7. Relative area change (%) per glacier from 1987 to 2013.

other intervals during the 1987-2013 period are similar to the change of the time periods for 1987-2017 (Tables 4.1-4.4), which may indicate that the 1987-2017 results are representative of the entire study area glaciers.

Of all the glaciers mapped in 1987, four glaciers disintegrated, while other glaciers split apart and later disintegrated. There were 24 glaciers mapped that split apart over the period from 1987 to

2017 (Figure 5.8). Even though perimeter generally decreases with decreasing area (Figure 4.9), the splitting of these glaciers increased the perimeter, accounting for some of the glaciers that did not follow the trend of decreasing perimeter over time. The change in perimeter represents a large portion of the area lost by the glaciers, as these alpine glaciers retreat within the valleys (Figure 5.8).

Figure 5.9 provides a clear example of a glacier that has almost disappeared in 2017, which is indicated as 'a'. As can be seen in this image, this small glacier has undergone a greater relative change in area than the larger glaciers although it has lost less absolute area (glacier a: -94.8 ± 4.7%, glacier b: -78.9 ± 3.9%, glacier c: -72.4 ± 3.6%, and glacier d: -37.1 ± 1.9%). From 2013 to 2017, such small glaciers ($A < 0.05$ km^2) lost the largest percentage of area in total as compared to the other area size classes (Table 4.3; -60.6 ± 3.0%). Overall, the study area is predicted to become glacier-free by 2045 (1987-2013 sample period) or 2044 (1987-2017 sample period) based on the results of extrapolation.

5.4.1 Glacier Change in Relation to Past Glacier Studies

Reductions in glacier area reported in this study, as well as in recent studies in Canada, are in accordance with observed warming trends in interior Alaska and northwestern Canada (ECCC, 2016). Recent studies have reported on the changes in glacier area, volume, and thickness with patterns of changes in precipitation and increasing surface air temperature throughout Canada, including Yukon (Barrand and Sharp, 2010), British Columbia (Bolch et al., 2010), Northwest Territories (Demuth et al., 2014), and Labrador (Way et al., 2015). There has been a winter warming trend since the 1950s, as well as a summer warming trend since the 1970s in northwestern Canada (DeBeer et al., 2016, Vincent et al., 2015, Barrand and Sharp, 2010).

Reductions in precipitation and winter accumulation as well as summer warming result in increasingly negative mass balances of glaciers, leading to increasing reductions in glacier area.

The area reduction rates of 1.59% · a^{-1} (1987-2013) and 1.76% · a^{-1} (1987-2017) are much higher than changes in area reported by other studies in western Canada. In the Canadian Cordillera stretching across British Columbia and Alberta, Bolch et al. (2010) reported a reduction rate of 0.55% · a^{-1} from 1985 to 2005. However, the initial glacierised area of ~30 000 km^2 analysed by

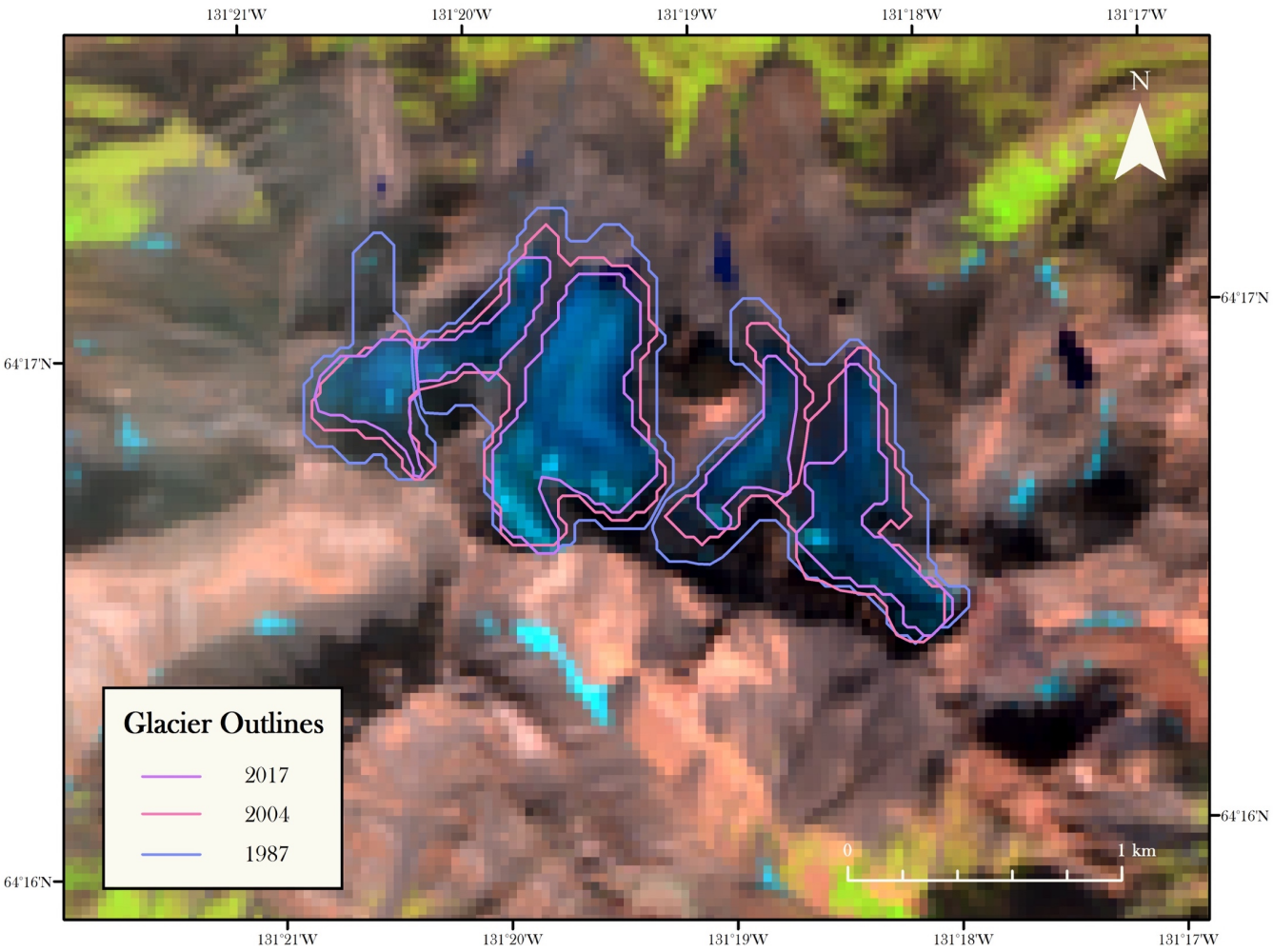

Figure 5.8. Example of glacier recession, 1987-2017.

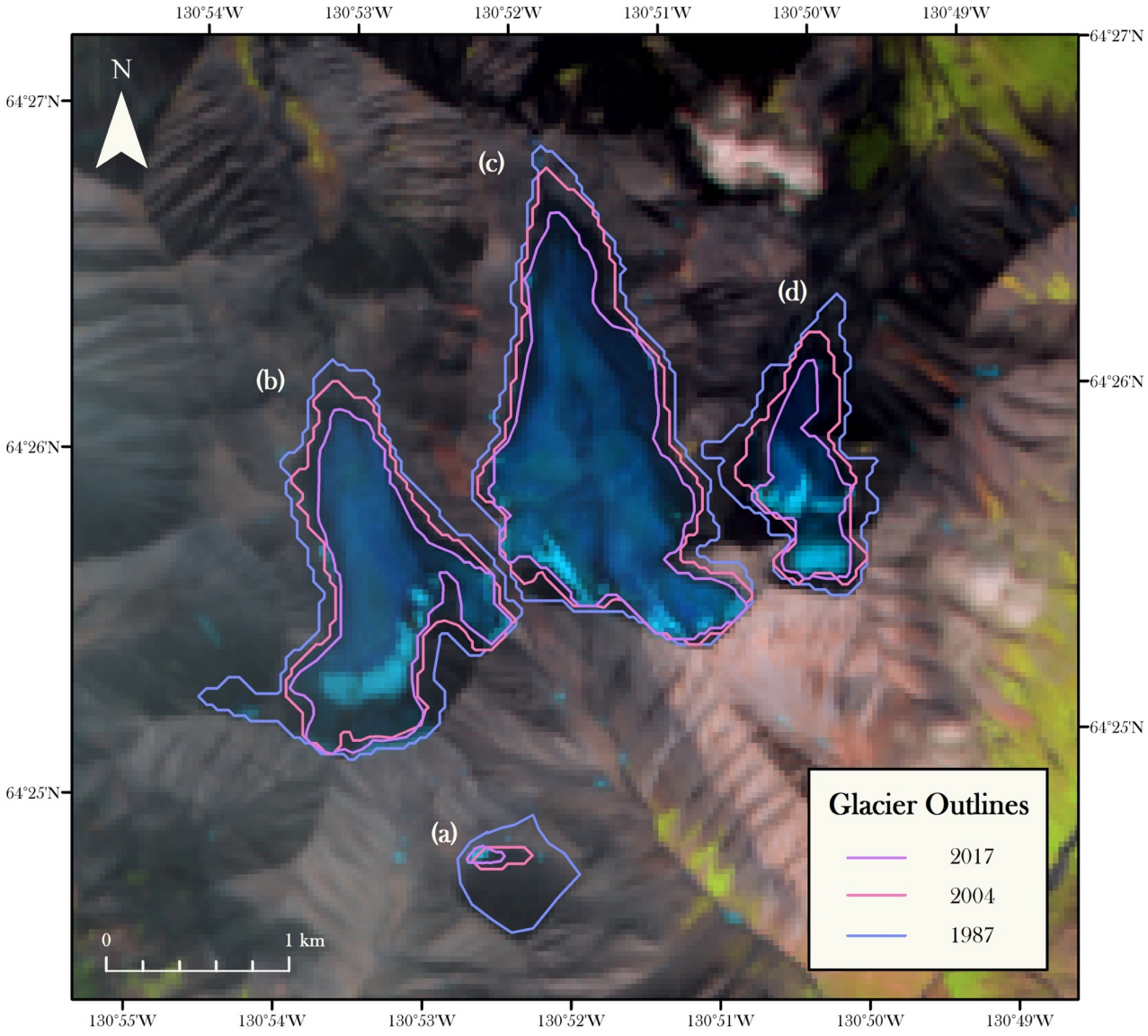

Figure 5.9. Example of glacier recession, 1987-2017. (a) Smallest glacier with an area loss of -94.8 ± 4.7%. (b) Glacier with an area loss of -78.9 ± 3.9%. (c) Glacier with an area loss of -72.4 ± 3.6%. (d) Glacier with an area loss of -37.1 ± 1.9%.

Bolch et al. (2010) was much larger than the area analysed for this study (69.9 ± 1.7 km^2 for n=108 and 52.8 ± 1.3 km^2 for n=74). Nearby in the Canadian Rockies, Tennant and Menounos (2013) reported an area reduction of the Columbia Icefield to be ~0.25% · a^{-1} from 1919–2009. DeBeer and Sharp (2007) reported area changes that have a reduction of only 0.30% · a^{-1} from

1951/52 to 2001 of interior British Columbia, but with a smaller initial area in comparison (40 ± 3 km^2).

In a similar study conducted within the Ragged Range of the Mackenzie Mountains approximately 400 km south of the study area, the rate of glacier area reduction is more comparable. Between 1982 and 2008, the glaciated area contracted by approximately 30% from 262 km^2 to 184 km^2 (Demuth et al., 2014). To compare with the reduction rates of the present study, a reduction rate of the Ragged Range study was calculated to be ~1.15% · a^{-1}. Interestingly though, Demuth et al. (2014) reported that small glaciers (0.01-1.0 km^2) located in topographic niches, provided with drift snow and protected from solar radiation, have been found to show limited to modest growth. Although a few glaciers in the present study were also revealed to have increased in area, the overall trend in area for the present study from 1987 to 2013/2017 for glaciers is negative, in which most of these glaciers are within the same size class reported by Demuth et al. (2014) of small glacier area (0.01-1.0 km^2).

There are various glacier studies of area change within western North America that present conflicting evidence of how smaller glaciers are impacted by recent climate changes of increasing surface air temperature and reduced winter precipitation. Some studies found smaller area glaciers to be more susceptible to climate change (e.g., Way et al., 2015; Racoviteanu et al., 2008; Granshaw and Fountain, 2006). This may hold true for the glaciers of the Mackenzie Mountains in this study that have shown an increase in the rate of area reduction since 1987. Although such studies suggest that the smaller glaciers (<~0.5 km^2) are affected more by recent climate variations, other studies report very limited changes in the area of smaller glaciers because they were sheltered from direct solar radiation or were insensitive to recent decline in winter

precipitation (DeBeer and Sharp, 2009). For example, DeBeer and Sharp (2007) found little to no change of smaller glaciers (<0.5 km^2) in the southern Canadian Cordillera between 1951/1962 and 2001/2002.

Of the glaciers mapped in this study, glaciers within an area size class less than ~1.0 km^2 lost the greatest percentage of their area. This finding is compatible with other previous studies of glaciers in Canada and the United States (e.g., Schmidt and Nüsser, 2012; Tennant et al., 2012; Bolch et al., 2010; Granshaw and Fountain, 2006; Demuth et al., 2008). In contrast to the large relative area change of A < 1.0 km^2, the greatest absolute area loss was in the area size class of A > 1.0 km^2. DeBeer and Sharp (2007) also found there to be a greater absolute loss of area for glaciers within this size class in which they describe as being the result of a large number of glaciers of this size and the large losses per individual glaciers. As glaciers reduce in size, they may also become more susceptible to an accelerated retreat. Racoviteanu et al. (2008) and Xiang et al. (2014) found that small low-lying glaciers, with the majority of their area in the ablation zone, to have lost more ice at higher rates than larger glaciers.

A trend in previous published glacier datasets (e.g., Andreassen et al., 2008; DeBeer and Sharp, 2007; Granshaw and Fountain, 2006) is an increase in the relative area change with decreasing glacier area size. This can be observed in the results of the present study as well (Figure 4.2). As noted by Tennant et al. (2012), such a trend presumably arises from factors that are not climate related such as the local topography, elevation, and debris-cover of glaciers, which may result in a stronger influence over glacier change than climate (Andreassen et al., 2008; DeBeer and Sharp, 2007; Granshaw and Fountain, 2006).

The glaciers within the Yukon border of this study were also included in a recent study by Barrand and Sharp (2010). Although the authors of that study analysed the Yukon glaciers, glaciers extending across Yukon and Northwest Territories were cropped along the administrative boundary line. With an initial area of 11 622 km^2 in 1958-60, the total glacier area shrank to 9 081 km^2 in 2006-08 (Barrand and Sharp, 2010). A reduction rate in area was calculated for the Yukon glaciers to compare with the present study, which is ~0.42% · a^{-1}. Although this study includes some of the same glaciers of interior Yukon, the authors reported the area change of all the glaciers in Yukon, encompassing those within the coastal St. Elias Mountains. The coastal environment of these glaciers in the St. Elias Mountains provide more moisture to facilitate growth of glacial area, such as the nearby advancing Hubbard Glacier in Alaska that is acting independently of climate trends (Stearns et al., 2015). Therefore, these contrasting environments restrict the value of comparing the results of this study to.

The observed glacier shrinkage in the study area is in line with the findings of many other glaciated mountain ranges throughout the world. However, compared to glacier recession trends in other mountain ranges in the world, the study area Mackenzie Mountain glaciers have a greater rate of reduction over time. In the Ravi Basin of the Himalayas, the glacier area (initially 121.4 ± 5.4 km^2) had an area reduction rate of only 0.10 ± 0.10%· a^{-1} from 1971–2010/13 (Chand and Sharma, 2015). In comparison, Racoviteanu et al. (2008) found a greater reduction of 0.68% · a^{-1} of glaciers in the Cordillera Blanca of Peru from 1970 to 2003, but still less of a reduction than the Mackenzie Mountain glaciers.

A possible explanation of why glaciers in the present study are losing greater area at a faster rate than other glaciers reported is that small glaciers have a higher perimeter-area ratio. The glaciers

in this study are small in comparison to glaciers of other studies mentioned earlier. A high perimeter-area ratio makes the small glaciers more susceptible to radiation from the surrounding terrain (Tennant et al., 2012; Jiskoot and Mueller, 2012; Demuth et al., 2008). Although not analysed in this study, it is argued by Granshaw and Fountain (2006) that small glaciers have a high area-volume ratio, so for the same ablation rate, small glaciers would reduce in size at a greater rate than larger glaciers. The glaciers that had the largest decrease in area or disappeared may have been impacted more by increasing surface air temperatures or decreasing winter precipitation reported in northwestern Canada. When glacier ice thins, a small reduction in thickness can result in a greater proportional reduction in the area. This may have been due to their location in areas that are marginal for ice preservation.

CHAPTER 6

Conclusions

This study mapped the extents over the past three decades of an assemblage of glaciers not previously reported on in the northern Mackenzie Mountains using satellite imagery. To determine whether there was a trend in the glacier extents over time, Landsat imagery was analysed from 1987 to 2013/2017 by using the method of a thresholded Red/SWIR band ratio for delineating glacier boundaries. This study demonstrated that the semi-automated technical process of thresholding band ratios using Landsat imagery is an effective approach for mapping glaciers in a region with sparse glacial debris cover. The Red/SWIR band ratio was found to have worked well to delineate glacier ice for the entire study area and most effectively for all images. However, manual corrections were still required for misclassified polygons and for areas of shadow and debris-covered glaciers. The most laborious task for glacier mapping was the manual delineation of glaciers when seasonal snow cover was an issue for the 1994 image. The thresholded band ratio was a time-effective and simple method for mapping the glacier outlines of this study with multiple Landsat images, so the time required to make manual corrections may have been negligible if a smaller sample of glaciers had been mapped.

Using Landsat imagery proved to be an effective method for mapping glacier extents for this study area. The availability of free data online and over the past three decades provided sufficient imagery to determine a trend in glacier change over time. The limitation of finding enough suitable images due to cloud cover was an issue, with no cloud-free images available for the most

recent year of 2017. An image for 2017 was chosen, but with only ~70% of the glaciers that were visible in the other images. Thus, to incorporate glacier data from 2017, a sample of the original glaciers from 1987-2013 were analysed separately. Some other glaciers also had to be excluded in the area change analysis because the scene of the 1994 image was not the same. The importance of monitoring small alpine glaciers as the ones in this study is that generally they are located in alpine regions where there are no larger sized glaciers and no climate records. Even though there were limits to what glaciers could be mapped and what years had suitable images, enough images were available for assessing the state of these glaciers over the past three-decade period.

It was hypothesised that glaciers within the study area would be affected by changes in climate by decreasing in spatial extent in accordance with other studies of glaciers throughout the world. The findings of this study support the hypothesis in which there were trends of both decreasing glacier areas and decreasing glacier perimeter lengths, with strong correlation values ($r > 0.900$). Annual area reduction rates (1.59% · a^{-1} from 1987-2013 and 1.76% · a^{-1} from 1987-2017) were also found to be greater than glacier studies in other regions. The glaciers investigated reduced in size since 1987 to 2013 by 43.1 ± 2.1% or 30.1 ± 1.51 km^2 and to 2017 by 46.6 ± 2.3% or 24.6 ± 1.23 km^2. There was also an increase in area change over the time period, which is in line with trends reported in other recent glacier studies. The largest reduction that occurred overall was during the period from 2013-2017, possibly indicating greater susceptibility of the increasingly smaller size glaciers to climate change. The study area is predicted to be glacier-free by 2045 (based on 1987-2013 sample period) or by 2044 (based on 1987-2017 sample period).

Small glaciers have been considered either insensitive or highly sensitive to climatic variations. Glaciers studies within western North America present conflicting evidence of how smaller glaciers are impacted by recent climate changes. This study supports those other recent studies of glaciated areas of northwestern Canada that have found small glaciers to be more responsive to climate change. This study mapped glaciers small in size (all with an area less than 4.0 km^2) in which the smallest glaciers reduced the most in area over the time period of 1987 to 2013/2017. This is in contrast to studies that have reported small glaciers to be located in topographic niches provided with ample snow.

The large reduction rates of the glaciers in comparison with other studies may be due to their small size and their higher perimeter-area ratio than larger glaciers, causing these glaciers to be more susceptible to surface air temperature increases. The reduction rate is influenced largely by glacier size, where smaller glaciers were susceptible to greater area changes. However, the method of interpreting glacier boundaries of small glaciers from the surrounding terrain and seasonal snow may have contributed to uncertainty of mapping, resulting in larger estimated glacier changes. This also highlights the importance of choosing imagery with minimal seasonal snow cover when possible. Careful error evaluation and quantification of each image used for change detection are thus important to assessing the trend in glacier change when using satellite image mapping techniques.

The small assemblage of glaciers has been sufficiently delineated in this study to determine glacier change in the study area. Further data analysis of the level of error associated with mapping using the semi-automated band ratio technique is needed to more accurately define the glacier outlines.

Error values applied to the results were based on values reported by previous glacier mapping studies rather than determined from the results of the present study. Since this study mapped small glaciers using 30-m pixel Landsat images, only glaciers with an area greater than 0.02 km^2 were sufficiently mapped with the thresholded images. At an increasingly smaller glacier area size, it was more difficult to map the outlines possibly resulting in a limitation of the level of mapping accuracy. With increasingly smaller glacier areas, the glaciers of the study area may be more difficult to accurately map in future images. Therefore, to better refine the error estimates, the pixel size of the satellite sensor should be addressed in the error estimation values.

LIST OF REFERENCES

Andreassen, L. M., Paul, F., Kääb, A., and Hausberg, J. E. (2008). Landsat-derived glacier inventory for Jotunheimen, Norway, and deduced glacier changes since the 1930s. *The Cryosphere, 2,* 131-145.

Barrand, N. E., Way, R. G., Bell, T., and Sharp, M. J. (2017). Recent changes in area and thickness of Torngat Mountain glaciers (northern Labrador, Canada). *The Cryosphere, 11,* 157-168. doi: 10.5194/tc-11-157-2017.

Barrand, N. E. and Sharp, M. J. (2010). Sustained rapid shrinkage of Yukon glaciers since the 1957–1958 international geophysical year. *Geophysical Research Letters, 37*(7), L07501. doi: 10.1029/2009GL042030.

Bhambri, R., Bolch, T., Kawishwar, P., Dobha, D. P., Srivastava, D., and Pratap, B. (2013). Heterogeneity in glacier response in the upper Shyok valley, northeast Karakoram. *The Cryosphere, 7,* 1385–1398. doi: 10.5194/tc-7-1385-2013.

Bolch, T., Menounos, B., and Wheate, R. (2010). Landsat-based inventory of glaciers in western Canada, 1985-2005. *Remote Sensing of Environment, 114,* 127–137. doi: 10.1016/j.rse.2009.08.015.

Brown, L. E., Milner, A. M., and Hannah, D. M. (2010). Predicting river ecosystem response to glacial meltwater dynamics: a case study of quantitative water sourcing and glaciality index approaches. *Aquatic Sciences, 72,* 325-334. doi: 10.1007/s00027-010-0138-7.

Burns, P. and Nolin, A. (2014). Using atmospherically-corrected Landsat imagery to measure glacier area change in the Cordillera Blanca, Peru from 1987 to 2010. *Remote Sensing of Environment, 140,* 165-178. doi: 10.1016/j.rse.2013.08.026.

Burn, C. R. and Kokelj, S. V. (2009). The environment and permafrost of the Mackenzie Delta area. *Permafrost and Periglacial Processes, 20,* 83-105. doi: 10.1002/ppp.655.

Chand, P. and Sharma, M. C. (2015). Glacier changes in the Ravi basin, North-Western Himalaya (India) during the last four decades (1971–2010/13). *Global and Planetary Change, 135,* 133-147. doi: 10.1016/j.gloplacha.2015.10.013.

Clague, J. J., Luckman, B. H., Van Dorp, R. D., Gilbert, R., Froese, D., Jensen, B. J. L., and Reyes, A. V. (2006). Rapid changes in the level of Kluane Lake in Yukon Territory over the last millennium. *Quaternary Research, 66,* 342-355. doi: 10.1016/j.yqres.2006.06.005.

Clarke, G. K. C., Jarosch, A. H., Anslow, F. S., Radić, V., and Menounos, B. (2015). Projected deglaciation of western Canada in the twenty-first century. *Nature Geoscience, 8*(5), 372-377. doi: 10.1038/NGEO2407.

DeBeer, C. M., Wheater, H. S., Carey, S. K., and Chun, K. P. (2016). Recent climatic, cryospheric, and hydrological changes over the interior of western Canada: a review and synthesis. *Hydrology and Earth System Sciences, 20,* 1573–1598. doi: 10.5194/hess-20-1573-2016.

DeBeer, C. M. and Sharp, M. J. (2009). Topographic influences on recent changes of very small glaciers in the Monashee Mountains, British Columbia, Canada. *Journal of Glaciology, 55*(192), 691-700.

DeBeer, C. M. and Sharp, M. J. (2007). Recent changes in glacier area and volume within the southern Canadian Cordillera. *Annals of Glaciology, 46,* 215-221.

Demuth, M. N., Wilson, P., and Haggarty, D. (2014). Glaciers of the Ragged Range, Nahanni National Park Reserve, Northwest Territories, Canada. In J. S. Kargel, G. J. Leonard, M. P. Bishop, A. Kääb, and B. H. Raup (Eds.), *Global land ice measurements from space* (Ch. 16, pp. 375-383). Berlin, Germany: Springer.

Demuth, M., Pinard, V., Pietroniro, A., Luckman, B., Hopkinson, C., Dornes, P., and Comeau, L. (2008). Recent and past-century variations in the glacier resources of the Canadian Rocky Mountains: Nelson River system. *Terra Glacialis, Special Issue: Mountain Glaciers and Climate Changes of the Last Century,* 27-52.

Derksen, C. and Brown, R. (2012). Spring snow cover extent reductions in the 2008-2012 period exceeding climate model projections. *Geophysical Research Letters, 39,* L19504. doi: 10.1029/2012GL053387.

Déry, S. J. and Wood, E. F. (2005). Decreasing river discharge in northern Canada. *Geophysical Research Letters, 32,* L10401. doi: 10.1029/2005GL022845.

Duk-Rodkin, A. and Hughes, O. L. (1992). Pleistocene montane glaciations in the Mackenzie Mountains, Northwest Territories. *Géographie Physique et Quaternaire, 46*(1), 69-83. doi: 10.7202/032889ar.

Durán-Alarcón, C., Gevaert, C. M., Mattar C., Jiménez-Muñoz, J. C., Pasapera-Gonzales, J. J., Sobrino, J. A., Silvia-Vidal, Y., Fashé-Raymundo, O., Chavez-Espiritu, T. W., and Santillan-Portilla, N. (2015). Recent trends on glacier area retreat over the group of Nevados Caullaraju-Pastoruri (Cordillera Blanca, Peru) using Landsat imagery. *Journal of South American Earth Sciences, 59,* 19-26. doi: 10.1016/j.jsames.2015.01.006.

Environment and Climate Change Canada (ECCC). (2016). *Climate indicators.* Retrieved from https://www.canada.ca/en/environment-climate-change/services/environmental-indicators/climate.html. Accessed on September 18, 2017.

Foy, N., Copland, L., Zdanowicz, C., Demuth, M., and Hopkinson, C. (2011). Recent volume and area changes of Kaskawulsh Glacier, Yukon, Canada. *Journal of Glaciology, 57*(203), 515-525.

Gardent, M., Rabatel, A., Dedieu, J. -P., Deline, P. (2014). Multitemporal glacier inventory of the French Alps from the late 1960s to the late 2000s. *Global and Planetary Change, 120,* 24-37. doi: 10.1016/j.gloplacha.2014.05.004.

Granshaw, F. D. and Fountain, A. G. (2006). Glacier change (1958–1998) in the North Cascades National Park Complex, Washington, USA. *Journal of Glaciology, 52*(177), 251-256.

Hartmann, D. L., Tank, A. M. G. K., Rusticucci, M., Alexander, L. V., Brönnimann, S., Charabi, Y., Dentener, F. J., Dlugokencky, E. J., Easterling, D. R., Kaplan, A., Soden, B. J., Thorne, P. W., Wild, M., and Zhai, P. M. (2013). Observations: Atmosphere and Surface. In T. F., Stocker, D. Qin, G. -K. Plattner, M. Tignor, S. K. Allen, J. Boschung, A. Nauels, Y. Xia, V. Bex, and P. M. Midgley (Eds.): *Climate Change 2013: The Physical Science Basis. Contribution of Working Group I to the Fifth Assessment Report of the Intergovernmental Panel on Climate Change* (Ch. 2, pp. 159-254). Cambridge, UK and New York, NY: Cambridge University Press.

Hoffman, M. J., Fountain, A. G., and Achuff, J. M. (2007). 20th-century variations in area of cirque glaciers and glacierets, Rocky Mountain National Park, Rocky Mountains, Colorado, USA. *Annals of Glaciology, 46,* 349-354.

Horvath, E. (1975). Glaciers of the Yukon and Northwest Territories (excluding the Queen Elizabeth Islands and St. Elias Mountains). In: W. O. Field (Ed.), *Mountain Glaciers of the Northern Hemisphere, Vol. 1,* (Ch. 4, 689-698). Hanover, NH: U.S. Army Cold Regions Research and Engineering Laboratory.

Jiskoot, H. and Mueller, M. S. (2012). Glacier fragmentation effects on surface energy balance and runoff: field measurements and distributed modelling. *Hydrological Processes, 26,* 1861-1875. doi: 10.1002/hyp.9288.

Khamis, K., Brown, L. E., Hannah, D. M., and Milner, A. M. (2016). Glacier-groundwater stress gradients control alpine river biodiversity. *Ecohydrology, 9,* 1263-1275. doi: 10.1002/eco.1724.

Kuhn, M. (2010). The formation and dynamics of glaciers. In P. Pellikka and W. G. Rees (Eds.), *Remote sensing of glaciers: techniques for topographic, spatial and thematic mapping of glaciers* (Ch. 2, pp. 21-39). Boca Raton, FL: CRC Press.

Klock, R., Hudson, E., Aihoshi, D., and Mullock, J. (2001). The weather of the Yukon, Northwest Territories and Western Nunavut (Graphic Area Forecast 35). Nav Canada.

Larsen, C. F., Motyka, R. J., Arendt, A. A., Echelmeyer, K. A., and Geissler, P. E. (2007). Glacier changes in southeast Alaska and northwest British Columbia and contribution to sea level rise. *Journal of Geophysical Research: Earth Surface, 112*(F1), F01007. doi: 10.1029/2006JF000586.

Liu T., Kinouchi T., and Ledezma, F. (2013). Characterization of recent glacier decline in the Cordillera Real by LANDSAT, ALOS, and ASTER data. *Remote Sensing of Environment, 137,* 158-172. doi: 10.1016/j.rse.2013.06.010.

Mekis, É. and Vincent, L. A. (2011). An overview of the second generation adjusted daily precipitation dataset for trend analysis in Canada. *Atmosphere-Ocean, 49*(2), 163-177. doi: 10.1080/07055900.2011.583910.

Naz, B. S., Frans, C. D., Clarke, G. K. C., Burns, P., and Lettenmaier, D. P. (2014). Modeling the effect of glacier recession on streamflow response using a coupled glacio-hydrological model. *Hydrology and Earth System Sciences, 18,* 787-802. doi: 10.5194/hess-18-787-2014.

Ootes, L., Gleeson, S. A., Turner, E., Rasmussen, K., Gordey, S., Falck, H., Martel, E., and Pierce, K. (2013). Metallogenic evolution of the Mackenzie and eastern Selwyn Mountains of Canada's Northern Cordillera, Northwest Territories: a compilation and review. *Geoscience Canada, 40*(1), 40-69. doi: http://dx.doi.org/10.12789/geocanj.2013.40.005.

Paul, F., Winsvold, S. H., Kääb, A., Nagler, T., and Schwaizer, G. (2016). Glacier remote sensing using Sentinel-2. Part II: mapping glacier extents and surface facies, and comparison to Landsat 8. *Remote Sensing, 8*(7), 575-587. doi: 10.3390/rs8070575.

Paul, F., Barrand, N. E., Baumann, S., Berthier, E., Bolch, T., Casey, K., Frey, H., Joshi, S. P., Konovalov, V., Le Bris, R., Mölg, N., Nosenko, G., Nuth, C., Pope, A., Racoviteanu, A., Rastner, P., Raup, B., Scharrer, K., Steffen, S., and Winsvold, S. (2013). On the accuracy of glacier outlines derived from remote-sensing data. *Annals of Glaciology, 54*(63), 171-182.

Paul, F. and Hendriks, J. (2010a). Optical remote sensing of glacier extent. In P. Pellikka and W. G. Rees (Eds.), *Remote sensing of glaciers: techniques for topographic, spatial and thematic mapping of glaciers* (Ch. 8, pp. 137-152). Boca Raton, FL: CRC Press.

Paul, F. and Hendriks, J. (2010b). Detection and visualization of glacier area changes. In P. Pellikka and W. G. Rees (Eds.), *Remote sensing of glaciers: techniques for topographic, spatial and thematic mapping of glaciers* (Ch. 12, pp. 231-243). Boca Raton, FL: CRC Press.

Paul, F., Barry, R. G., Cogley, J. G., Frey, H., Haeberli, W., Ohmura, A., Ommanney, C. S. L., Raup, B., Rivera, A., and Zemp, M. (2009). Recommendations for the compilation of glacier inventory data from digital sources. *Annals of Glaciology, 50*(53), 119-126.

Paul, F., Kääb, A., and Haeberli, W. (2007). Recent glacier changes in the Alps observed by satellite: consequences for future monitoring strategies. *Global and Planetary Change, 56,* 111-122. doi: 10.1016/j.gloplacha.2006.07.007.

Pellikka, P. and Rees, W., G. (2010). Glacier parameters monitored using remote sensing. In P. Pellikka and W. G. Rees (Eds.), *Remote sensing of glaciers: techniques for topographic, spatial and thematic mapping of glaciers* (Ch. 3, pp. 41-66). Boca Raton, FL: CRC Press.

Radić, V., Bliss, A., Beedlow, A. C., Hock, R., Miles, E., and Cogley, J. G. (2014). Regional and global projections of twenty-first century glacier mass changes in response to climate scenarios from global climate models. *Climate Dynamics, 42,* 37-58. doi: 10.1007/s00382-013-1719-7.

Rees, W., G. and Pellikka, P. (2010). Principles of remote sensing. In P. Pellikka and W. G. Rees (Eds.), *Remote sensing of glaciers: techniques for topographic, spatial and thematic mapping of glaciers* (Ch. 1, pp. 1-20). Boca Raton, FL: CRC Press.

Racoviteanu, A. E., Paul, F., Raup, B., Khalsa, S. J. S., and Armstrong, R. (2009). Challenges and recommendations in mapping of glacier parameters from space: results of the 2008 Global Land Ice Measurements from Space (GLIMS) workshop, Boulder, Colorado, USA. *Annals of Glaciology, 50*(53), 53-69.

Racoviteanu, A. E., Arnaud, Y., Williams, M. W., and Ordoñez, J. (2008). Decadal changes in glacier parameters in the Cordillera Blanca, Peru, derived from remote sensing. *Journal of Glaciology, 54*(186), 499-510.

Schmidt, S. and Nüsser, M. (2012). Changes of high altitude glaciers from 1969 to 2010 in the Trans-Himalayan Kang Yatze Massif, Ladakh, Northwest India. *Arctic, Antarctic, and Alpine Research, 44*(1), 107-121. doi: 10.1657/1938-4246-44.1.107.

Shugar, D. H., Clague, J. J., Best, J. L., Schoof, C., Willis, M. J., Copland, L., and Roe, G. H. (2017). River piracy and drainage basin reorganization led by climate-driven glacier retreat. *Nature Geoscience, 10,* 370–375. doi: 10.1038/NGEO2932.

Stearns, L. A., Hamilton, G. S., van der Veen, C. J., Finnegan, D. C., O'Neel, S., Scheick, J. B., and Lawson, D. E. (2015). Glaciological and marine geological controls on terminus dynamics of Hubbard Glacier, southeast Alaska. *Journal of Geophysical Research: Earth Surface, 120,* 1065–1081, doi: 10.1002/2014JF003341.

Tennant, C. and Menounos, B. (2013). Glacier change of the Columbia Icefield, Canadian Rocky Mountains, 1919–2009. *Journal of Glaciology, 59*(216), 671-686. doi: 10.3189/2013JoG12J135.

Tennant, C., Menounos, B., Wheate, R., and Clague, J. J. (2012). Area change of glaciers in the Canadian Rocky Mountains, 1919 to 2006. *The Cryosphere, 6,* 1541–1552. doi: 10.5194/tc-6-1541-2012.

United States Geological Survey (USGS). (2017). *Earth Explorer.* https://earthexplorer.usgs.gov/.

USGS. (2017). *Landsat missions timeline.* Retrieved from https://landsat.usgs.gov/landsat-missions-timeline. Accessed on September 28, 2017.

Vincent, L. A., Zhang, X., Brown, R. D., Feng, Y., Mekis, E., Milewska, E. J., Wan, H., and Wang, X. L. (2015). Observed trends in Canada's climate and influence of low-frequency variability modes. *Journal of Climate, 28,* 4545-4560. doi: 10.1175/JCLI-D-14-00697.1.

Wang, L., Wang, F., Li, Z., Wang, W., Li, H., and Wang, P. (2015). Glacier changes in the Sikeshu River basin, Tienshan Mountains. *Quaternary International, 358,* 153-159. doi: 10.1016/j.quaint.2014.12.028.

Way, R. G., Bell, T., and Barrand, N. E. (2015). Glacier change from the early little ice age to 2005 in the Torngat Mountains, northern Labrador, Canada. *Geomorphology, 246,* 558–569. doi: 10.1016/j.geomorph.2015.07.006.

Wheate, R. D., Berthier, E., Bolch, T., Menounos, B. P., Shea, J. M., Clague, J. J., and Schiefer, E. (2014). Remote sensing of glaciers in the Canadian Cordillera, Western Canada. In J. S. Kargel, G. J. Leonard, M. P. Bishop, A. Kääb, and B. H. Raup (Eds.), *Global land ice measurements from space (*Ch. 14, pp. 333-352). Berlin, Germany: Springer.

Xiang, Y., Gao, Y., and Yao, T. (2014). Glacier change in the Poiqu River basin inferred from Landsat data from 1975 to 2010. *Quaternary International, 349,* 392-401. doi: 10.1016/j.quaint.2014.03.017.

Yukon Ecoregions Working Group (2004). Mackenzie Mountains. In: C. A. S. Smith, J. C. Meikle, and C. F. Roots (Eds.), *Ecoregions of the Yukon Territory: biophysical properties of Yukon landscapes* (PARC Technical Bulletin No. 04-01, pp. 139-148). Summerland, BC.

Zhang, X., Vincent, L. A., Hogg, W. D., and Niitsoo, A. (2000). Temperature and precipitation trends in Canada during the 20th century. *Atmosphere-Ocean, 38*(3), 395-429. doi: 10.1080/07055900.2000.9649654.

APPENDIX

Individual Glacier Area and Perimeter Values

Table A.1. Area and perimeter values for each glacier, 1987.

ID	Area (km^2)	Perimeter (km)	ID	Area (km^2)	Perimeter (km)
1	0.8015	4.9092	38	0.2776	2.3570
2	0.1373	2.1231	39	2.0663	8.1940
3	0.2255	2.7801	40	1.0372	5.5590
4	0.2315	2.1780	41	0.7199	5.9965
5	0.3713	3.1019	42	0.7043	4.4356
6	1.0024	5.2288	43	2.3291	11.0585
7	0.1013	1.2715	44	0.2492	2.2645
8	0.5360	3.3068	45	0.5146	3.5215
9	0.2300	2.3734	46	0.4622	3.9140
10	0.4649	3.2116	47	0.5146	3.9872
11	1.4392	6.6374	48	0.3245	2.5546
12	0.3512	2.8289	49	0.3897	2.6054
13	0.9565	4.7412	50	0.6275	4.1939
14	1.3329	5.9427	51	0.3083	2.2679
15	0.3458	2.8433	52	1.1864	4.9084
16	0.6669	4.2379	53	0.2444	3.0625
17	0.2354	1.9534	54	0.1621	1.7836
18	0.2630	2.3684	55	0.3076	3.1661
19	0.2840	2.4098	56	0.0914	1.3461
20	0.5428	4.2896	57	0.1760	2.5225
21	0.4743	3.3927	58	0.4821	3.6368
22	0.2633	2.6352	59	0.3056	2.4904
23	1.8603	9.1243	60	1.1142	4.8155
24	0.1112	1.4661	61	0.3425	2.9322
25	1.1997	6.7569	62	0.5246	4.0053
26	0.0563	1.0005	63	0.1303	1.3952
27	0.7452	5.0886	64	2.7794	9.1553
28	0.1003	1.6510	65	0.1606	1.6857
29	0.7054	4.9178	66	0.1205	1.5621
30	0.2084	2.0382	67	0.2580	2.3447
31	0.1445	1.5012	68	0.2366	2.3027
32	0.3530	2.4617	69	0.2835	2.7900
33	0.1037	1.2488	70	0.5165	3.5975
34	0.0617	1.0064	71	0.7033	4.8759
35	0.4539	2.9250	72	0.0950	1.2484
36	0.2012	2.1304	73	0.4358	3.8054
37	2.5645	10.8322	74	0.1337	1.4618

75	0.1211	1.6461	97	0.3533	2.4231
76	0.2361	2.4348	98	1.8207	7.0531
77	0.7660	4.0171	99	0.5801	3.4649
78	0.6567	4.4951	100	0.2997	2.6574
79	0.7205	3.5468	101	0.1586	1.7921
80	0.6350	4.6807	102	0.4811	3.9286
81	0.4037	2.6704	103	0.1515	1.7976
82	0.1625	1.8158	104	0.2534	2.3031
83	0.5495	4.1116	105	0.3481	2.4507
84	0.1822	2.4817	106	0.7070	3.9989
85	0.0716	1.1340	107	0.3140	2.6563
86	1.6758	7.3806	108	0.1661	1.9079
87	2.1832	7.5538	109	0.6472	4.4378
88	0.7929	4.8912	110	0.3173	2.5752
89	0.2653	1.9704	111	0.2034	2.2383
90	1.2246	6.2983	112	0.2232	2.3364
91	3.1472	10.8236	113	0.1202	1.5085
92	3.6692	11.9926	114	0.1724	1.8758
93	0.7628	4.5286	115	0.2246	2.2752
94	2.7428	9.9452	116	0.2844	2.1693
95	1.6831	9.3431	117	0.2846	2.1507
96	0.2192	2.0455	**Total**	**77.419**	**430.53**

Table A.2. Area and perimeter values for each glacier, 1994.

ID	Area (km²)	Perimeter (km)	ID	Area (km²)	Perimeter (km)
1	0.8222	4.9662	44	0.2117	1.8258
2	0.1396	2.4204	45	0.5626	3.6364
3	0.2759	3.3419	46	0.4996	3.7189
4	0.2398	2.1491	47	0.4344	3.9607
5	0.3542	3.0595	48	0.3734	3.0600
6	0.7424	5.1379	49	0.3644	2.4499
7	0.0813	1.1138	50	0.6011	4.0641
8	0.4543	3.2525	51	0.3024	2.3363
9	0.1864	1.6645	52	1.0173	5.1626
10	0.3827	2.7975	53	0.1634	2.2152
11	1.3157	5.4405	54	0.1415	1.6623
12	0.2648	2.7430	55	0.2957	3.1440
13	0.9270	4.5266	56	0.0991	1.4193
14	1.2257	6.2835	57	0.1927	2.2262
15	0.2900	2.1991	58	0.5800	3.7770
16	0.5638	4.0649	59	0.2938	2.5494
17	0.2506	2.0031	60	1.0036	4.4829
18	0.2647	2.2859	61	0.3244	2.7951
19	0.2660	2.3074	62	0.5957	4.0799
20	0.4916	4.0495	63	0.1355	1.4661
21	0.4762	3.5061	64	2.8347	8.9975
22	0.2738	2.5810	65	0.1599	1.5970
23	1.8274	8.9816	66	0.0977	1.3710
24	0.1015	1.3585	67	0.2023	2.4296
25	1.1211	6.9962	68	0.1991	2.5397
26	0.0419	0.8515	69	0.2766	2.7558
27	0.7181	5.0796	70	0.5002	3.4639
28	0.0847	1.4617	71	0.6863	5.1371
29	0.7269	5.2713	72	0.1004	1.3037
30	0.1748	1.7749	73	0.4228	3.0911
31	0.1385	1.5220	74	0.1238	1.5115
32	0.2813	3.2746	75	0.1553	1.9212
33	0.1227	1.3742	76	0.2583	2.8018
34	0.0540	0.9363	77	0.8025	4.3894
35	0.4338	3.0331	78	0.6500	4.3742
36	0.1802	1.8776	79	0.7762	3.7103
37	2.6177	10.5465	80	0.6313	4.9037
38	0.2747	2.2514	81	0.4802	3.1868
39	2.0405	8.3868	82	0.1859	1.9607
40	0.9959	5.3092	83	0.5778	4.0814
41	0.7106	6.1454	84	0.1611	2.2743
42	0.5431	4.4206	85	0.0772	1.1106
43	2.1582	11.0247	86	1.5991	7.2227

87	2.1686	7.7081	103	0.0000	0.0000
88	0.7925	4.7013	104	0.2759	2.8825
89	0.2048	2.4698	105	0.2651	2.5401
90	1.1253	5.8828	106	0.8168	5.0026
91	2.9316	11.3034	107	0.2213	1.9922
92	3.4979	12.2140	108	0.1625	1.9182
93	0.7223	4.4613	109	N/A	N/A
94	2.6725	10.1029	110	N/A	N/A
95	1.5447	9.0389	111	N/A	N/A
96	0.2066	2.0020	112	N/A	N/A
97	0.3569	2.4304	113	N/A	N/A
98	1.7458	6.9287	114	N/A	N/A
99	0.5180	3.8279	115	N/A	N/A
100	0.3133	2.6434	116	N/A	N/A
101	0.1415	1.6616	117	N/A	N/A
102	0.3425	2.9849	**Total**	**66.812**	**404.64**

Table A.3. Area and perimeter values for each glacier, 1999.

ID	Area (km²)	Perimeter (km)	ID	Area (km²)	Perimeter (km)
1	0.7675	5.3777	44	0.1208	1.5800
2	0.1080	1.9287	45	0.4456	3.4995
3	0.1447	2.5791	46	0.4456	3.4995
4	0.1915	2.2438	47	0.3286	3.9912
5	0.3177	3.2754	48	0.2757	2.5260
6	0.4327	3.6358	49	0.1647	1.8705
7	0.1190	1.5586	50	0.5123	4.4125
8	0.4592	3.2283	51	0.2096	1.8343
9	0.1409	1.6399	52	0.8917	4.8171
10	0.3422	2.7200	53	0.1074	1.5249
11	1.1754	6.5307	54	0.1062	1.3596
12	0.2452	2.7945	55	0.2578	3.2793
13	0.8960	5.2487	56	0.0680	1.3473
14	1.1275	6.5558	57	0.1174	2.1045
15	0.2791	3.1909	58	0.3346	4.1978
16	0.6086	4.1432	59	0.2267	2.3639
17	0.2129	2.1159	60	0.9085	4.7256
18	0.1529	1.9117	61	0.2271	3.0245
19	0.1879	1.8285	62	0.3304	3.6692
20	0.4713	4.4593	63	0.1032	1.5749
21	0.4013	3.1140	64	2.5381	10.4816
22	0.2030	2.2665	65	0.1276	1.5169
23	1.5904	9.0487	66	0.0601	1.1411
24	0.1611	1.8416	67	0.1297	2.3843
25	0.8487	7.7959	68	0.1450	2.2675
26	0.0321	0.7062	69	0.1852	2.6168
27	0.6697	5.2334	70	0.3373	3.4752
28	0.0499	0.9654	71	0.5245	4.7665
29	0.7269	5.2713	72	0.0745	1.2781
30	0.1555	1.7164	73	0.2797	2.8591
31	0.1079	1.3837	74	0.0673	1.1312
32	0.2287	2.2318	75	0.0565	1.1830
33	0.0935	1.3938	76	0.1616	1.7745
34	0.0522	0.9389	77	0.6619	4.7710
35	0.3535	3.0800	78	0.5349	6.0837
36	0.1555	2.5768	79	0.5105	3.1081
37	2.3328	12.2576	80	0.4525	4.3496
38	0.2022	2.6413	81	0.2560	2.6544
39	1.9844	9.3933	82	0.0729	1.7462
40	0.9337	5.6669	83	0.4026	3.7162
41	0.5818	5.0946	84	0.1651	2.5084
42	0.4560	4.1127	85	0.0977	1.3322
43	2.0205	11.6133	86	1.4467	6.2085

87	2.0720	7.6869	103	0.0000	0.0000
88	0.6634	4.2525	104	0.1904	2.3059
89	0.0757	1.4034	105	0.1455	2.0809
90	0.9837	7.5357	106	0.5031	3.4986
91	2.7438	10.9561	107	0.2117	2.0616
92	3.3734	13.2424	108	0.1377	1.8385
93	0.6834	4.5257	109	0.4212	3.0680
94	2.4096	11.8899	110	0.3008	2.5046
95	1.3838	9.8371	111	0.1346	1.7305
96	0.1315	1.7123	112	0.1886	2.3156
97	0.3020	2.4526	113	0.0830	1.1809
98	1.5172	7.6121	114	0.1296	1.7909
99	0.4726	3.8514	115	0.1100	1.7371
100	0.2396	3.0369	116	0.1803	2.0585
101	0.1129	1.4840	117	0.2140	2.8622
102	0.3700	3.2760	**Total**	**58.518**	**424.80**

Table A.4. Area and perimeter values for each glacier, 2004.

ID	Area (km²)	Perimeter (km)	ID	Area (km²)	Perimeter (km)
1	0.6592	4.7840	44	0.0757	1.3447
2	0.0729	1.6447	45	0.3452	2.9498
3	0.1168	2.2067	46	0.3134	3.4180
4	0.1432	1.8699	47	0.2772	3.2766
5	0.2246	2.2679	48	0.1836	2.0337
6	0.2220	3.2955	49	0.1346	1.9110
7	0.0410	0.8018	50	0.4285	3.7608
8	0.3545	2.6865	51	0.1958	1.7837
9	0.0652	1.2194	52	0.8080	4.6420
10	0.2653	2.6713	53	0.0770	1.2788
11	1.0377	6.8741	54	0.0806	1.1794
12	0.1998	2.3776	55	0.1714	2.4274
13	0.7143	4.5412	56	0.0221	0.6643
14	0.9717	6.2914	57	0.0505	1.2418
15	0.0239	0.6043	58	0.3029	3.5819
16	0.3282	3.1661	59	0.2174	2.1942
17	0.0772	1.2168	60	0.8657	4.3667
18	0.0000	0.0000	61	0.2096	2.9879
19	0.1688	1.9255	62	0.3113	3.4774
20	0.3717	3.3920	63	0.0748	1.1580
21	0.3226	2.7794	64	2.4602	8.9063
22	0.1580	1.9885	65	0.1139	1.3885
23	1.4424	8.0245	66	0.0437	0.8515
24	0.0344	0.8374	67	0.0995	1.7061
25	0.6733	7.0322	68	0.0980	1.7947
26	0.0000	0.0000	69	0.1112	1.8479
27	0.5575	4.5759	70	0.2313	2.6259
28	0.0277	0.7408	71	0.4541	4.3318
29	0.4278	3.9377	72	0.0621	1.1067
30	0.1417	1.5724	73	0.2182	2.3122
31	0.0540	1.0369	74	0.0644	1.1370
32	0.1256	1.6212	75	0.0156	0.5900
33	0.0635	0.9715	76	0.1210	1.6668
34	0.0216	0.5672	77	0.5958	4.0994
35	0.3061	3.0950	78	0.4745	5.3022
36	0.1073	1.4837	79	0.4757	2.9279
37	2.1691	10.4456	80	0.4820	4.1262
38	0.1391	1.7837	81	0.2331	2.1195
39	1.8646	8.2680	82	0.0473	1.0564
40	0.8040	5.1781	83	0.3191	3.0376
41	0.4773	4.9098	84	0.1066	1.6833
42	0.4460	3.7589	85	0.0440	0.8252
43	1.8710	11.1495	86	1.2534	6.2431

87	1.8932	7.2827	103	0.0000	0.0000
88	0.5342	3.8613	104	0.1013	1.4515
89	0.0293	0.7594	105	0.0730	1.3648
90	0.6857	6.3829	106	0.3344	2.8722
91	2.4312	9.7282	107	0.1205	1.4515
92	3.1647	11.2354	108	0.0710	1.2023
93	0.5243	3.9565	109	0.2977	2.7250
94	2.2511	10.8836	110	0.2066	2.3601
95	1.1827	9.2147	111	0.1360	1.8189
96	0.1157	1.5437	112	0.1339	2.0312
97	0.2580	2.1791	113	0.0365	0.8018
98	1.3481	7.7442	114	0.0284	0.9043
99	0.4284	3.5170	115	0.0815	1.4134
100	0.1452	2.2822	116	0.0842	1.2861
101	0.0925	1.1948	117	0.1334	1.6547
102	0.2104	2.4122	**Total**	**48.694**	**358.47**

Table A.5. Area and perimeter values for each glacier, 2013.

ID	Area (km²)	Perimeter (km)	ID	Area (km²)	Perimeter (km)
1	0.6286	4.5521	44	0.8434	4.2218
2	0.0740	1.5514	45	0.1730	2.7475
3	0.1264	2.2729	46	0.2406	3.1112
4	0.1431	1.6358	47	0.0594	1.0713
5	0.1837	1.8674	48	2.2583	9.4241
6	0.2311	3.0921	49	0.1122	1.3980
7	0.0319	0.6689	50	0.0418	0.8801
8	0.3578	2.6150	51	0.0623	1.1038
9	0.0515	1.2876	52	0.0795	1.5094
10	0.2184	2.4735	53	0.0757	1.4723
11	0.9520	6.1725	54	0.1924	2.4471
12	0.1806	2.2470	55	0.3451	3.7409
13	0.6562	4.6336	56	0.0527	1.1164
14	0.8915	6.2397	57	0.1877	2.1785
15	0.0129	0.4464	58	0.0486	1.0290
16	0.2688	2.8432	59	0.0132	0.4916
17	0.0532	0.9133	60	0.1252	1.6955
18	0.0000	0.0000	61	0.5033	4.9353
19	0.1491	1.5954	62	0.3560	4.7921
20	0.3183	2.9284	63	0.4372	2.7044
21	0.2637	2.4304	64	0.4492	5.0563
22	0.1351	1.8172	65	0.2084	1.9044
23	1.3060	7.9819	66	0.0303	0.9050
24	0.0220	0.7330	67	0.2351	2.1595
25	0.4227	4.5252	68	0.0866	1.6435
26	0.0000	0.0000	69	0.0305	0.8945
27	0.5010	4.5804	70	1.1673	6.2084
28	0.0159	0.5698	71	1.7113	6.8768
29	0.4100	4.0346	72	0.4731	3.5818
30	0.1472	1.6154	73	0.0590	0.9891
31	0.0102	0.4270	74	0.5389	5.3004
32	0.0871	1.6376	75	2.1043	10.0258
33	0.0463	0.8515	76	2.9858	10.9229
34	0.0270	0.6155	77	0.3436	3.2638
35	0.2450	2.8245	78	2.0550	10.3854
36	0.0882	1.5577	79	1.0134	8.5132
37	0.9015	10.4559	80	0.1049	1.6873
38	0.1106	1.8254	81	0.2532	2.0646
39	1.8699	8.2688	82	1.2072	6.6687
40	0.7779	4.8908	83	0.4111	3.3902
41	0.3928	4.6513	84	0.1377	2.3131
42	0.3792	2.8867	85	0.0895	1.1795
43	1.7599	10.7504	86	0.0932	1.7848

87	0.0555	1.1430	103	0.0000	0.0000
88	0.2804	2.7317	104	0.0842	1.3740
89	0.2349	3.1788	105	0.0254	0.8963
90	0.1842	2.4070	106	0.2204	2.4207
91	0.1670	1.9357	107	0.0493	1.1806
92	0.1285	1.7848	108	0.0471	0.9612
93	0.3371	4.1257	109	0.4203	4.0568
94	0.1741	1.7525	110	0.1648	2.0044
95	0.7608	4.7750	111	0.1309	1.7139
96	0.0689	1.2590	112	0.1118	1.9506
97	0.0830	1.1493	113	N/A	N/A
98	0.1385	1.9005	114	0.0225	0.8193
99	0.0217	0.6590	115	N/A	N/A
100	0.0626	1.2884	116	0.0463	0.9774
101	0.1966	2.5631	117	0.0935	1.7801
102	0.1843	2.1862	**Total**	**41.939**	**334.73**

Table A.6. Area and perimeter values for each glacier, 2017.

ID	Area (km²)	Perimeter (km)	ID	Area (km²)	Perimeter (km)
1	0.6286	4.5521	44	0.0555	1.1430
2	0.0740	1.5514	45	0.2804	2.7317
3	0.1264	2.2729	46	0.2349	3.1788
4	0.1431	1.6358	47	0.1842	2.4070
5	0.1837	1.8674	48	0.1670	1.9357
6	0.2311	3.0921	49	0.1285	1.7848
7	0.0319	0.6689	50	0.3371	4.1257
8	0.3578	2.6150	51	0.1741	1.7525
9	0.0515	1.2876	52	0.7608	4.7750
10	0.2184	2.4735	53	0.0689	1.2590
11	0.9520	6.1725	54	0.0830	1.1493
12	0.1806	2.2470	55	0.1385	1.9005
13	0.6562	4.6336	56	0.0217	0.6590
14	0.8915	6.2397	57	0.0626	1.2884
15	0.0129	0.4464	58	0.1966	2.5631
16	0.2688	2.8432	59	0.1843	2.1862
17	0.0532	0.9133	60	0.8434	4.2218
18	0.0000	0.0000	61	0.1730	2.7475
19	0.1491	1.5954	62	0.2406	3.1112
20	0.3183	2.9284	63	0.0594	1.0713
21	0.2637	2.4304	64	2.2583	9.4241
22	0.1351	1.8172	65	0.1122	1.3980
23	1.3060	7.9819	66	0.0418	0.8801
24	0.0220	0.7330	67	0.0623	1.1038
25	0.4227	4.5252	68	0.0795	1.5094
26	0.0000	0.0000	69	0.0757	1.4723
27	0.5010	4.5804	70	0.1924	2.4471
28	0.0159	0.5698	71	0.3451	3.7409
29	0.4100	4.0346	72	0.0527	1.1164
30	0.1472	1.6154	73	0.1877	2.1785
31	0.0102	0.4270	74	0.0486	1.0290
32	0.0871	1.6376	75	0.0132	0.4916
33	0.0463	0.8515	76	0.1252	1.6955
34	0.0270	0.6155	77	0.5033	4.9353
35	0.2450	2.8245	78	0.3560	4.7921
36	0.0882	1.5577	79	0.4372	2.7044
37	0.9015	10.4559	80	0.4492	5.0563
38	0.1106	1.8254	81	0.2084	1.9044
39	1.8699	8.2688	82	0.0303	0.9050
40	0.7779	4.8908	83	0.2351	2.1595
41	0.3928	4.6513	84	0.0866	1.6435
42	0.3792	2.8867	85	0.0305	0.8945
43	1.7599	10.7504	86	1.1673	6.2084

87	1.7113	6.8768	103	0.0000	0.0000
88	0.4731	3.5818	104	0.0842	1.3740
89	0.0590	0.9891	105	0.0254	0.8963
90	0.5389	5.3004	106	0.2204	2.4207
91	2.1043	10.0258	107	0.0493	1.1806
92	2.9858	10.9229	108	0.0471	0.9612
93	0.3436	3.2638	109	0.4203	4.0568
94	2.0550	10.3854	110	0.1648	2.0044
95	1.0134	8.5132	111	0.1309	1.7139
96	0.1049	1.6873	112	0.1118	1.9506
97	0.2532	2.0646	113	N/A	N/A
98	1.2072	6.6687	114	0.0225	0.8193
99	0.4111	3.3902	115	N/A	N/A
100	0.1377	2.3131	116	0.0463	0.9774
101	0.0895	1.1795	117	0.0935	1.7801
102	0.0932	1.7848	**Total**	**25.732**	**221.31**